EA790-SAR-001

DOCKET NO. 71-9270

UMS®

UNIVERSAL MPC SYSTEM®

SAFETY ANALYSIS REPORT

for the

UMS® Universal Transport Cask

NOVEMBER 2001 UMST-01D

VOLUME 2 OF 2

NAC INTERNATIONAL

List of Effective Pages

Master Table of Contents

Chapter 1

List of Effective Pages (Continued)

List of Effective Pages (Continued)

List of Effective Pages (Continued)

List of Effective Pages (Continued)

List of Effective Pages (Continued)

List of Effective Pages (Continued)

2.6-168...........Revision UMST-01D
2.6-169...........Revision UMST-01D
2.6-170...........Revision UMST-01D
2.6-171...........Revision UMST-01D
2.6-172...........Revision UMST-01D
2.6-173...........Revision UMST-01D
2.6-174...........Revision UMST-01D
2.6-175...........Revision UMST-01D
2.6-176...........Revision UMST-01D
2.6-177...........Revision UMST-01D
2.6-178...........Revision UMST-01D
2.6-179...........Revision UMST-01D
2.6-180...........Revision UMST-01D
2.6-181...........Revision UMST-01D
2.6-182...........Revision UMST-01D
2.6-183...........Revision UMST-01D
2.6-184...........Revision UMST-01D
2.6-185...........Revision UMST-01D
2.6-186...........Revision UMST-01D
2.6-187...........Revision UMST-01D
2.6-188...........Revision UMST-01D
2.6-189...........Revision UMST-01D
2.6-190...........Revision UMST-01D
2.6-191...........Revision UMST-01D
2.6-192...........Revision UMST-01D
2.6-193...........Revision UMST-01D
2.6-194...........Revision UMST-01D
2.6-195...........Revision UMST-01D
2.6-196...........Revision UMST-01D
2.6-197...........Revision UMST-01D
2.6-198...........Revision UMST-01D
2.6-199...........Revision UMST-01D
2.6-200...........Revision UMST-01D
2.6-201...........Revision UMST-01D
2.6-202...........Revision UMST-01D
2.6-203...........Revision UMST-01D
2.6-204...........Revision UMST-01D
2.6-205...........Revision UMST-01D
2.6-206...........Revision UMST-01D
2.6-207...........Revision UMST-01D
2.6-208...........Revision UMST-01D
2.6-209...........Revision UMST-01D
2.6-210...........Revision UMST-01D
2.6-211...........Revision UMST-01D
2.6-212...........Revision UMST-01D
2.6-213...........Revision UMST-01D
2.6-214...........Revision UMST-01D
2.6-215...........Revision UMST-01D
2.6-216...........Revision UMST-01D
2.6-217...........Revision UMST-01D
2.6-218...........Revision UMST-01D
2.6-219...........Revision UMST-01D
2.6-220...........Revision UMST-01D
2.6-221...........Revision UMST-01D
2.6-222...........Revision UMST-01D
2.6-223...........Revision UMST-01D
2.6-224...........Revision UMST-01D
2.6-225...........Revision UMST-01D
2.6-226...........Revision UMST-01D
2.6-227...........Revision UMST-01D
2.6-228...........Revision UMST-01D
2.6-229...........Revision UMST-01D
2.6-230...........Revision UMST-01D
2.6-231...........Revision UMST-01D
2.6-232...........Revision UMST-01D
2.6-233...........Revision UMST-01D

List of Effective Pages (Continued)

List of Effective Pages (Continued)

List of Effective Pages (Continued)

List of Effective Pages (Continued)

List of Effective Pages (Continued)

List of Effective Pages (Continued)

List of Effective Pages (Continued)

List of Effective Pages (Continued)

Chapter 3

List of Effective Pages (Continued)

List of Effective Pages (Continued)

List of Effective Pages (Continued)

Chapter 4

4-i ....Revision UMST-00A
4-ii ....Revision UMST-00A
4-iii ....Revision UMST-00A
4-iv ....Revision UMST-01D
4-1..................Revision UMST-01D
4-2..................Revision UMST-01D
4.1-1...............Revision UMST-00A
4.1-2...............Revision UMST-01D
4.1-3...............Revision UMST-01D
4.1-4...............Revision UMST-01D
4.1-5...............Revision UMST-01D
4.2-1...............Revision UMST-01D
4.2-2...............Revision UMST-01D
4.2-3...............................Revision 0
4.2-4...............Revision UMST-00A
4.2-5...............Revision UMST-01D
4.2-6...............Revision UMST-01D
4.2-7...............Revision UMST-01D
4.2-8...............Revision UMST-01D
4.2-9...............Revision UMST-01D
4.2-10.............Revision UMST-01D
4.2-11.............Revision UMST-00A
4.3-1...............Revision UMST-01D
4.3-2...............Revision UMST-00A
4.3-3...............Revision UMST-00A
4.3-4...............Revision UMST-01D
4.3-5...............Revision UMST-01D
4.4-1...............................Revision 0
4.5-1...............Revision UMST-00A
4.5.1-1............Revision UMST-01D
4.5.2-1............Revision UMST-99A
4.5.2-2............Revision UMST-99A
4.5.2-3............Revision UMST-99A
4.5.2-4............Revision UMST-99A
4.5.2-5............Revision UMST-99A
4.5.2-6............Revision UMST-99A
4.5.2-7............Revision UMST-99A
4.5.2-8............Revision UMST-99A
4.5.2-9............Revision UMST-99A
4.5.2-10..........Revision UMST-99A
4.5.2-11..........Revision UMST-99A
4.5.3-1............Revision UMST-00A
4.5.3-2............Revision UMST-00A
4.5.3-3............Revision UMST-00A
4.5.3-4............Revision UMST-00A
4.5.3-5............Revision UMST-00A
4.5.3-6............Revision UMST-00B
4.5.3-7............Revision UMST-00B
4.5.3-8............Revision UMST-00B
4.5.3-9............Revision UMST-00B
4.5.3-10..........Revision UMST-00A
4.5.3-11..........Revision UMST-00A
4.5.3-12..........Revision UMST-00A
4.5.3-13..........Revision UMST-00A
4.6-1...............Revision UMST-00A

Chapter 5

5-i ....Revision UMST-99A
5-ii ....Revision UMST-00A
5-iii ....Revision UMST-00A
5-iv ....Revision UMST-00A
5-v..................Revision UMST-00A
5-vi ....Revision UMST-97A

List of Effective Pages (Continued)

List of Effective Pages (Continued)

List of Effective Pages (Continued)

Chapter 6

List of Effective Pages (Continued)

List of Effective Pages (Continued)

List of Effective Pages (Continued)

6.6.2-12..........Revision UMST-00A
6.6.2-13..........Revision UMST-00A
6.6.2-14..........Revision UMST-00A
6.6.2-15..........Revision UMST-00A
6.6.2-16..........Revision UMST-00A
6.6.2-17..........Revision UMST-00A
6.6.2-18..........Revision UMST-00A
6.6.2-19..........Revision UMST-00A
6.6.2-20..........Revision UMST-00A
6.6.2-21..........Revision UMST-00A
6.6.2-22..........Revision UMST-00A
6.6.2-23..........Revision UMST-00A
6.6.2-24..........Revision UMST-00A
6.6.2-25..........Revision UMST-00A
6.6.2-26..........Revision UMST-00A
6.6.2-27..........Revision UMST-00A
6.6.2-28..........Revision UMST-00A
6.6.2-29..........Revision UMST-00A
6.6.2-30..........Revision UMST-00A
6.6.2-31..........Revision UMST-00A
6.6.2-32..........Revision UMST-00A
6.6.2-33..........Revision UMST-00A
6.6.2-34..........Revision UMST-00A
6.6.2-35..........Revision UMST-00A
6.6.2-36..........Revision UMST-00A
6.6.2-37..........Revision UMST-00A
6.6.2-38..........Revision UMST-00A
6.6.2-39..........Revision UMST-00A
6.6.2-40..........Revision UMST-00A
6.6.2-41..........Revision UMST-00A
6.6.2-42..........Revision UMST-00A
6.6.2-43..........Revision UMST-00A
6.6.2-44..........Revision UMST-00A
6.6.2-45..........Revision UMST-00A
6.6.2-46..........Revision UMST-00A
6.6.2-47..........Revision UMST-00A
6.6.2-48..........Revision UMST-00A
6.6.2-49..........Revision UMST-00A
6.6.2-50..........Revision UMST-00A
6.6.2-51..........Revision UMST-00A
6.6.2-52..........Revision UMST-00A
6.6.2-53..........Revision UMST-00A
6.6.2-54..........Revision UMST-00A
6.6.2-55..........Revision UMST-00A
6.6.2-56..........Revision UMST-00A
6.6.2-57..........Revision UMST-00A
6.6.2-58..........Revision UMST-00A
6.6.2-59..........Revision UMST-00A
6.6.2-60..........Revision UMST-00A
6.6.2-61..........Revision UMST-00A
6.6.2-62..........Revision UMST-00A
6.6.2-63..........Revision UMST-00A
6.6.2-64..........Revision UMST-00A
6.6.2-65..........Revision UMST-00A
6.6.2-66..........Revision UMST-00A
6.6.2-67..........Revision UMST-00A
6.6.2-68..........Revision UMST-00A
6.6.2-69..........Revision UMST-00A
6.6.2-70..........Revision UMST-00A
6.6.2-71..........Revision UMST-00A
6.6.2-72..........Revision UMST-00A
6.6.2-73..........Revision UMST-00A
6.6.2-74..........Revision UMST-00A
6.6.2-75..........Revision UMST-00A
6.6.2-76..........Revision UMST-00A
6.6.2-77..........Revision UMST-00A

List of Effective Pages (Continued)

Chapter 7

List of Effective Pages (Continued)

Master Table of Contents (Continued)

Master Table of Contents (Continued)

Master Table of Contents (Continued)

Master Table of Contents (Continued)

Master Table of Contents (Continued)

Master Table of Contents (Continued)

Master Table of Contents (Continued)

Master Table of Contents (Continued)

Master Table of Contents (Continued)

Master Table of Contents (Continued)

Master Table of Contents (Continued)

Master Table of Contents (Continued)

Master Table of Contents (Continued)

Master Table of Contents (Continued)

Table of Contents

Table of Contents (Continued)

List of Figures

List of Figures (Continued)

List of Figures (Continued)

List of Figures (Continued)

List of Tables

List of Tables (Continued)

List of Tables (Continued)

THIS PAGE INTENTIONALLY LEFT BLANK

3.0 THERMAL EVALUATION

This chapter presents the thermal design and analyses of the Universal Transport Cask for the 10 CFR 71 normal conditions of transport and hypothetical accident conditions. The analyses include consideration of design basis PWR and BWR fuel. Results of the analyses demonstrate that with the design basis payloads, the Universal Transport Cask meets the thermal performance requirements of 10 CFR 71 [1] and IAEA Safety Series No. 6 [2].

3.1 Discussion

The Universal Transport Cask is designed to transport one of three classes of PWR fuel or one of two classes of BWR fuel, which are already sealed in a Transportable Storage Canister (canister). Only the bounding evaluation for the PWR and BWR classes of fuel is reported herein. The bounding case is represented by a configuration consisting of the shortest canister, shortest fuel tube, and shortest fuel assemblies with the lowest effective thermal conductivity. The fuel assemblies are confined within the fuel basket. The shortest fuel basket contains the fewest support disks and longest space in the bottom of the cask cavity. The result is greater concentration of heat and maximized thermal resistance for rejection of heat through the cavity top and bottom. The shorter fuel tube results in reduced axial conductance.

The design basis heat loads are 20 kW for up to 24 PWR assemblies and 16 kW for up to 56 BWR fuel assemblies. The individual PWR assembly decay heat is limited to 0.83 kW and the individual BWR assembly decay heat load is limited to 0.29 kW. As shown in Section 3.4.6, the thermal analysis considers a range of fuel assembly burnup and cool times for both fuel types to establish the allowable cladding temperatures. These limits are used to establish the allowable decay heat loads for fuel having cooling times of 5 years or more.

The thermal analyses presented in the following sections use helium as the cover gas in the cask cavity and in the canister.

Heat transfer from the Universal Transport Cask to the environment is by passive means only. No forced cooling is necessary. Conduction and radiation are the means by which heat is transferred from the fuel assemblies to the fuel tubes and through the tubes to the support disks and heat transfer disks. Heat is transferred through the support disks and heat transfer disks by conduction and radiation. Radiation and conduction are the means by which heat is transferred from the support disks and heat transfer disks to the canister wall and then to the cask cavity inner wall. From the Universal Transport cask cavity inner shell surface, heat is conducted through the lead (gamma shield) and then through the cask outer shell.

The neutron shield region surrounding the outer shell along most of the cask's length conducts heat to the neutron shield shell, primarily through the Cu/SS fins located within the NS-4-FR radial neutron shield material. The stainless steel shell that encloses the radial neutron shield is exposed to the environmental ambient temperature. Heat is removed from the surface of the neutron shield shell by convection and radiation. Heat transfer through the cask lid at the top of the cask and through the bottom forging and enclosed neutron shield material at the bottom of the cask is by conduction. Because of the insulating characteristics of the impact limiters, essentially no heat is removed from the ends of the cask. The bounding thermal conditions for the analysis required by 10 CFR 71 and IAEA Safety Series No. 6 under normal conditions of transport are presented in Table 3.1-1.

During normal conditions of transport and hypothetical accident conditions, the cask must reject the fuel decay heat to the environment without exceeding the operational temperature ranges of the cask seals or other components important to safety. In addition, to maintain fuel rod integrity for normal conditions of transport the fuel must be maintained at a sufficiently low temperature in an inert atmosphere such that thermally induced fuel rod cladding deterioration is precluded. To preclude fuel degradation, a maximum allowable cladding temperature of 716°F (380°C) is used for normal conditions of transport for 5-year cooled PWR and BWR fuel. Finally, the thermally induced stresses, in combination with pressure and mechanical load stresses, must be below allowable stress levels.

The temperatures for the various components of the fuel, canister, basket, and cask during normal conditions of transport and hypothetical accident condition fire are calculated by using finite element methods. For both normal conditions and the hypothetical accident conditions, the cask

3.2.2.3 Radiation Across Gaps Within the Cask

The gaps represented in the cask model are small compared with the surfaces separated by the gap. These gaps for both the PWR and the BWR casks are provided in Table 3.2-14.

The total heat transfer can be expressed as the sum of the radiation and the conduction processes.

$$Q_t = q_r + q_k$$

where q_r is specified as shown for the radiation heat transfer and q_k, which is the heat transfer by conduction, is expressed as

$$q_k = \frac{KA}{g}(T_i - T_j)$$

where:

g = gap distance (between two surfaces defined by nodes i and j)
K = conductivity of gas in gap
A = cross sectional area for heat conduction

By combining the two expressions (for q_k and q_r) and factoring out the term $A(T_i - T_j)/g$,

$$Q_t = [g\sigma\varepsilon F(T_i^2 + T_j^2)(T_i+T_j) + K][A(T_i - T_j)/g]$$

or

$$Q_t = K_{eff}A(T_i - T_j)/g$$

where $K_{eff} = g\sigma\varepsilon F(T_i^2 + T_j^2)(T_i+T_j) + K$.

The material conductivity used in the analysis for the elements that constitute the gap includes the heat transfer by both conduction and radiation. Because the gap is small compared with the disk thickness, the form factor (F) is taken to be unity.

3.2.2.4 Radiation from the Top of the Canister

The radiation heat transfer from the top of the canister is based on the expression:

$$q_r = \sigma \varepsilon A F (T_i^4 - T_j^4)$$

where the area (A) corresponds to the basket, lids, and spacer areas, and (ε) corresponds to the emissivities.

On the basis of the preceding equation, the radiation heat transfer is modeled by using radiation link elements in the cask three-dimensional model for the following locations:

1. From top of fuel region to bottom surface of canister shield lid;
2. From bottom of fuel region to top surface of canister bottom plate; and,
3. From exterior surfaces of the fuel tubes to the inner surface of the canister shell.

3.2.3 Convective Properties

A convective heat transfer coefficient, h_c, is associated with each surface where convection operates. Several surfaces must be considered. Surfaces vary by shape and orientation. Only the cylindrical surface of the cask takes part in the heat removal process, because the ends of the cask are thermally "insulated" from the environmental ambient thermal sink by the impact limiters.

The cask body surface is represented by a horizontal cylinder in air. From the Standard Handbook for Mechanical Engineers [16, Eq. 4.4.12d, Page 4-88], the heat transfer coefficient, h_c, is:

$$h_c = 0.19\, \Delta T^{1/3} \text{ BTU/hr-ft}^2\text{-°F, for } D^3 \Delta T > 100 \qquad [16, \text{Eq. } 4.4.12\text{d, Page } 4\text{-}88]$$

where:

ΔT = temperature difference between surface and air, °F
D = cylinder diameter, ft

For D = 7.667 ft and $\Delta T > 100°F$, the value of $D^3 \Delta T > 45{,}000$ is significantly larger than 100.

The expression can be converted into:

$$h_c = 0.00132\ \Delta T^{1/3}\ \text{Btu/hr-in}^2\text{-°F}.$$

Table 3.2-1 Thermal Properties of Solid Neutron Shield (NS-4-FR)

Property (units)	**Value**
Conductivity (Btu/hr-in-°F) [6]	0.0311
Density (Borated) (lbm/in^3) [6]	0.0589
Specific heat (Btu/lbm-°F) [6]	0.39

the cask (the sections of the cask body covered by the impact limiters are modeled as adiabatic). The three-dimensional finite element model for the cask loaded with PWR fuel is described in Section 3.4.1.1.1. The three-dimensional finite element model for the cask loaded with BWR fuel is described in Section 3.4.1.2.1.

The models of the cask/internal components (both PWR and BWR) are constructed of ANSYS three-dimensional, solid brick, thermal conduction elements (SOLID70) to model heat conduction/combined conduction and thermal radiation, as well as two-node thermal radiation link elements (LINK31) to model thermal radiation. The analyses of the cask models correspond to steady-state conditions.

In the three-dimensional cask models, the fuel assemblies are modeled as homogeneous regions with effective temperature-dependent thermal conductivity. The effective thermal conductivity of the fuel region in the plane perpendicular to the major axis of the cask is determined for each fuel (PWR and BWR) by using two-dimensional finite element models representing the cross-section of a single fuel assembly. The two-dimensional finite element models of the fuel assemblies consist of the UO_2 fuel pellets; Zircaloy cladding; and gas between the fuel pellets and cladding and between the fuel rods (fuel pellet/cladding). Heat generation rates (multiplied by the respective peaking factors for each fuel) are applied to the elements representing the UO_2 and an isothermal temperature condition is applied to the edges of the model representing the outer surfaces of the fuel assembly. The effective conductivity of the fuel assembly is then calculated by determining the maximum temperature in the fuel and using a closed form expression for a square with uniform heat generation. The two-dimensional finite element model of the PWR fuel is also described in Section 3.4.1.1.2. The two-dimensional finite element model of the BWR fuel is also described in Section 3.4.1.2.2.

The models of the fuel assemblies are constructed of ANSYS two-dimensional thermal elements (PLANE55) to model heat conduction and two-node thermal radiation link elements (LINK31) to model thermal radiation. The analyses of the fuel assemblies models are steady-state.

Additionally, the fuel tube walls and BORAL plate are modeled in the three-dimensional cask models as homogeneous regions by using effective thermal conductivity properties. The effective thermal conductivity of the fuel tube walls and BORAL plate is determined for each fuel tube (PWR and BWR) by using two-dimensional finite element models representing the cross-section of a typical fuel tube. The two dimensional models of the fuel tube walls and BORAL plate consist of the stainless steel tube wall; the BORAL sheet, which is composed of a sheet of boron sandwiched between aluminum sheets; the stainless steel sheet covering the BORAL plate; and the gaps separating these components. A heat flux is applied to the inner face of the composite tube wall while a temperature is applied to the outer face. The change in temperature is then used to calculate the effective thermal conductivity. This method treats the thermal resistance of the different layers as being in series. The effective thermal conductivity for heat condition parallel to the axis of the cask is computed as a weighted average based on the thickness of each layer. The two-dimensional finite element model of the PWR fuel tube is described in Section 3.4.1.1.3. The two-dimensional finite element model of the BWR fuel tube is described in Section 3.4.1.2.3.

The models of the tube wall and BORAL plate are constructed of ANSYS two-dimensional thermal elements (PLANE55) to model heat conduction and two-node thermal radiation link elements (LINK31) to model thermal radiation. The analyses of the fuel tube and BORAL plate models are steady-state.

A separate thermal analysis from the cask models is performed to determine the volumetric average temperature of the cask impact limiters. The impact limiters are not explicitly modeled in the cask thermal analyses previously discussed—the cask surfaces covered by the impact limiters are modeled as adiabatic. The impact limiter thermal model consists of an axis-symmetric finite element model of one impact limiter, the cask lid, the cask upper forging, the fire block inside the impact limiter shell, and the gap between the cask upper forging and the impact limiter.

3.4.1.1 Analytical Models: Cask with PWR Fuel Canister

The thermal analysis of the cask transporting PWR fuel uses three finite element ANSYS models as previously described. A three-dimensional model is employed to evaluate the cask in a horizontal position with the basket in contact with the canister, which, in turn, is in contact with the cask inner shell. The fuel regions and the fuel tubes with BORAL plates in this model are modeled by using effective conductivities. The effective conductivity of the fuel is determined by a second model, which is a detailed two-dimensional thermal model of the fuel assembly. The effective conductivities of the fuel tube wall and BORAL plate are calculated by using a third model, which is a two-dimensional thermal model of the fuel tube. The three ANSYS thermal models are described in the following paragraphs.

3.4.1.1.1 Three-Dimensional Cask Model: Cask with PWR Fuel Canister

The three dimensional Universal Transport Cask model is a half-symmetry finite element model constructed by using ANSYS Revision 5.5. The model considers the fuel assemblies, fuel tubes, stainless steel support disks, aluminum heat transfer disks, canister shell, lids and bottom plate, spacers at the bottom of the canister, cask inner shell, lead, outer shell, neutron shield, and neutron shield shell. The gaps between the individual components are also considered. The ANSYS model is shown in Figure 3.4-1. As shown in Figure 3.4-1, the internal cavity of the canister contains the active fuel region: the top and bottom end fittings of the fuel assemblies, fuel tubes enclosing the fuel assemblies and the top and bottom end fittings, and the bottom weldment.

The gas inside the canister is modeled as helium. The gas inside the cask cavity is modeled as helium, because the cavity will be backfilled with helium following fuel loading prior to transport. The finite element model is constructed of ANSYS three-dimensional, solid brick, thermal conduction elements (SOLID70) to model heat conduction/combined conduction and thermal radiation and two-node thermal radiation link elements (LINK31) to model thermal radiation. The principal gaps applied to the model are shown in Figure 3.1-1 and described in Section 3.2.2.3. In establishing these gaps, the differential thermal expansion between the components is considered. The gap values selected are conservative.

Because the canister is in the horizontal position during transport, the elements for the canister shell are shifted downwards to simulate contact with the inner shell of the cask. Similarly, the support disks and the heat transfer disks are shifted downward to simulate contact with the canister shell. As shown in Figure 3.1-1, a 2-degree contact is considered for the gaps between the canister shell and the cask inner shell and between the support disk and the canister shell. At the 2-degree contact region in the model, an element 0.005-inch thick (in the radial direction) is modeled between the elements of the canister shell and cask inner shell, and between the elements for the support disk and canister shell. To simulate the contact condition, a conductivity of 100 Btu/hr-in-°F is assumed for the element. The value of conductivity used has a negligible effect on the thermal analysis results, since the thermal resistance across the element is negligible compared to the thermal resistance of the canister shell or the cask inner shell because the thickness of the element is only 0.005 inch. The aluminum heat transfer disks are assumed to have only a line contact with the canister shell because the heat transfer disks are not subjected to any loads other than their own weight.

To account for differential thermal expansion, gaps within the model are adjusted on the basis of temperature and defined physical contact conditions. Solar insolance and ambient temperature conditions are applied to the neutron shield shell when appropriate. Insolance is used at the exterior surface of the cask and is based on the amount of insolation required by 10 CFR 71 to be applied over a 12-hr period evaluated in the steady state (applied over 24 hr simulating 12-hr period of solar exposure and 12-hr period of no solar exposure). The heat flux resulting from insolation on a curved surface is calculated as follows:

$$1475 \frac{\text{Btu}}{12\ \text{hr - ft}^2} \times \frac{12\ \text{hr}}{24\ \text{hr}} \times \frac{1\ \text{ft}^2}{144\ \text{in}^2} = 0.427\ \text{Btu/hr-in}^2.$$

Multiplying this value by the emissivity of the cask surface, $\varepsilon = 0.36$, gives a heat flux resulting from insolance on curved surfaces of 0.154 Btu/hr-in^2. Using the same method and a heat flux of 2,950 Btu/12 hr-ft^2 (0.853 Btu/hr-in^2) gives a heat flux resulting from insolance on flat surfaces of 0.307 Btu/hr-in^2. Applying one-half of the required 12-hr insolance over a 24-hr period to achieve a steady state solution, as has been done previously in transport cask licensing, is conservative.

The model is analyzed to determine the maximum temperatures for the basket, canister, cask shells, radial shielding, and surface conditions under normal conditions of transport. All material properties are shown in Tables 3.2-1 through 3.2-13.

The fuel regions (inside tubes) are modeled as homogeneous regions with effective conductivities, determined by the two-dimensional fuel model as described in Section 3.4.1.1.2. The fuel assembly tube and the BORAL plate, including gaps on both sides of the BORAL sheet and the gap between the stainless steel cladding for BORAL and disk, are modeled as one element thick with effective conductivities, as established by using the two-dimensional tube model discussed in Section 3.4.1.1.3. Only the spacer plate is modeled with the spacer concentric cylinders. Therefore, only conduction through the helium (modeled using SOLID70 elements) and radiation from the spacer plate to the cask bottom (modeled using LINK31 thermal radiation links) are conservatively modeled.

The neutron shield of the Universal Transport Cask, consisting of NS-4-FR, steel, and Cu/SS fins, is also modeled with effective conductivities. The radial neutron shield effective conductivity is calculated using an electrical resistance analogy. The equivalent circuit corresponding to Cu/SS, fin, NS-4-FR and silicon foam is shown below.

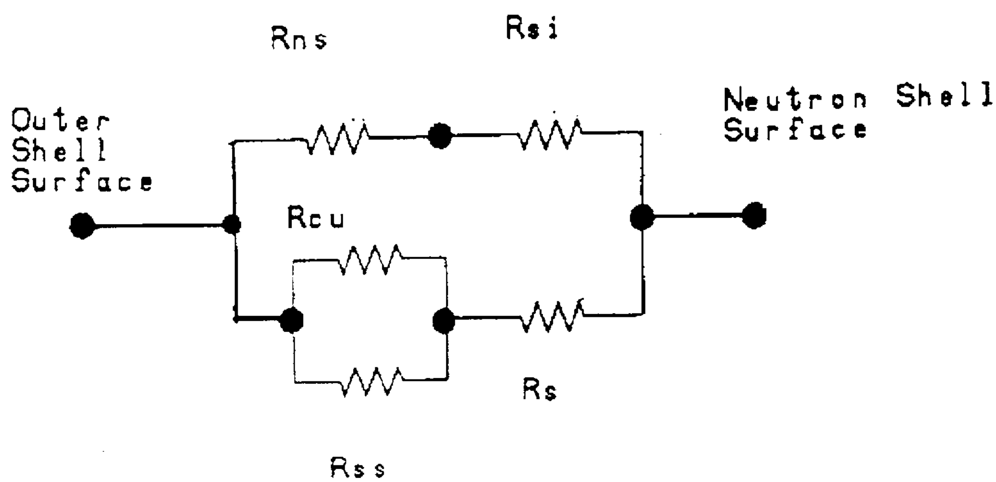

Rns = NS-4-FR material

Rsi = silicon foam between NS-4-FR and neutron shield shell

Rcu = 6 mm copper plate

Rss = 8 mm stainless steel

Rs = stainless steel connection to neutron shield shell

The axial conductivity, specific heat, and density are calculated on the basis of a weighted average of the axial cross sectional area and property. Conductivity of the neutron shield material NS-4-FR (0.031 Btu/hr-inch-°F) is used as the conductivity in the circumferential direction. The effective thermal conductivities for the neutron shield are :

Temperature	100°F	225°F	350°F
Radial Conductivity (Btu/hr in °F)	0.380	0.382	0.383
Axial Conductivity (Btu/hr in °F)	0.425	0.424	0.421
Specific heat (Btu/hr in °F)	0.39	0.39	0.39
Density (lbm/in^3)	0.0589	0.0589	0.0589

In the model, radiation heat transfer is considered from the top of the fuel region to the bottom surface of the canister shield lid, from the bottom of the fuel region to the top surface of the canister bottom plate, and from the exterior surfaces of the fuel tubes to the inner surface of the canister shell. This radiation is modeled by using LINK31 radiation elements. Radiation across gaps in the model is described in Section 3.2.2.3 and 3.2.2.4.

Radiation at the neutron shield shell surface to ambient is combined with the convection effect by using the method described in Section 3.2.2.2. The convection heat transfer coefficient is calculated on the basis of the formula shown in Section 3.2.3. Effective emissivities are used for all radiation calculations, with the form factor taken to be unity. Effective emissivity is computed by using the following formula [9] based on corresponding material emissivities:

$$\varepsilon_{eff} = 1/(1/\varepsilon_1 + 1/\varepsilon_2 - 1)$$

Solar insolance is applied to the neutron shield shell surface for the "Hot" condition (ambient temperature = 100°F). A cosine distribution is considered for the heat flux since the cask side surface is subjected to maximum insolation at the top and minimum (zero) insolation at the bottom while in the horizontal position. The heat flux is determined based on the average value of 0.154 Btu/hr-in^2 for the curved surface discussed previously.

Volumetric heat generation (Btu/hr-$inch^3$) is applied to the active fuel region on the basis of a total heat load of 20 kW, with an active fuel rod length of 144 inches, and an axial power the corresponding total heat is only 15.7 kW and the heat density is 88% of the 20 kW over 144 inches. The 20kW over 144 inches is considered to be controlling.

A sensitivity study was performed to assess the effect of variations in emissivity and convection heat transfer coefficient on temperature results. Two thermal analyses were performed using the thermal model described in this section with the following changes: The first analysis considered a 10% reduction of the emissivity of the transport cask inner and outer shells, the canister shell, and the basket (including support disks, heat transfer disks and fuel tubes); the second analysis considered a 10% reduction in the convection heat transfer coefficient at the transport cask outer surfaces. The analysis results indicate that the increase in the maximum fuel cladding and basket temperature is ≤ 6°F for both the reduced emissivity and reduced convection coefficient cases. Therefore, the effect of variation in emissivity and convection heat transfer coefficient on temperature results is not significant.

3.4.1.1.2 Two-Dimensional Fuel Assembly Model: PWR Fuel

The effective conductivity of the fuel is determined by a detailed two-dimensional finite element thermal model of the PWR 14x14 fuel assembly. Taking advantage of the symmetry of the cross-section of the fuel, the finite element model represents a one-quarter section of the fuel. The model includes the fuel pellets, cladding, gas between the fuel rods, and gas occupying the gap between the fuel pellets and cladding. Modes of heat transfer modeled include conduction and radiation between individual fuel rods for the steady-state condition. The model is shown in Figure 3.4-3. Thermal analyses of the other PWR fuel assemblies (i.e., 17x17, 16x16, and 15x15) are performed; however, because the PWR 14x14 fuel assembly results in the lowest effective thermal conductivities, only the analysis of that fuel assembly is presented in this section.

ANSYS PLANE 55 conduction elements and LINK31 radiation elements are used in the model, which includes a total of 49 fuel rods (representing a total of 196 fuel rods for the full cross-section). Each fuel rod consists of the pellet, Zircaloy cladding, and a gap between the pellet and clad. The gas in the gap between the pellet and clad, as well as the gas between the fuel rods, is modeled as helium. Radiation elements are defined between rods and from rods to the boundary of the model (inside surface of the fuel tube). Radiation across the gap between the boundary of the model (inside surface of the fuel tube). Radiation across the gap between the pellet and clad is conservatively ignored. Effective emissivities are determined by using the formula shown in Section 3.4.1.1.1.

The effective conductivity for the fuel is determined by using a two-step procedure. Using the fuel assembly model, a uniform temperature is applied to the exterior of the model (see Figure 3.4-3) in conjunction with the volumetric heat generation. From this analysis, the maximum temperature located at the center of the fuel assembly is determined. This maximum temperature occurs at the corner of the model, which represents the center of the entire fuel assembly.

A Sandia National Laboratory Report [10] defines an expression for use in determining the maximum temperature of a square cross section of an isotropic homogeneous fuel with uniform volumetric heat generation. At the boundary of this square cross section, the temperature is constrained to be uniform. The expression for the maximum temperature is given by:

$$T_c = T_e + 0.29468 \frac{Q a^2}{K_{eff}} \quad 1$$

where:

T_c = temperature at center of fuel (°F)
T_e = temperature applied at exterior of fuel (°F)
Q = volumetric heat generation rate (Btu/hr-in^3)
a = half-length of square cross section of fuel (inch)
K_{eff} = effective thermal conductivity for isotropic homogeneous fuel material (Btu/hr-in-°F).

Using the maximum temperature, located at the center of the fuel, from the detailed fuel assembly model, the preceding expression is used to determine the K_{eff} for an isotropic homogeneous representation of the fuel assembly.

Volumetric heat generation based on the design heat load of 20 kW with a peaking factor of 1.1 is applied to the fuel pellets. The temperature at the boundary of the model is constrained to be uniform. The effective conductivity is determined on the basis of the heat generated and the temperature difference from the center of the model to its edge. The temperature-dependent effective properties are established by using different boundary temperatures. The effective conductivity in the axial direction of the fuel assembly is calculated on the basis of a weighted average of the axial cross sectional area.

3.4.1.1.3 Two-Dimensional Fuel Tube Model: PWR Fuel

The effective conductivity of the fuel tube and BORAL plate, which is used in the three-dimensional canister model, is determined by the two-dimensional fuel tube model. As shown in Figure 3.4-4, this model includes the fuel tube, the BORAL plate (including the core matrix sandwiched by aluminum claddings), gaps on both sides of the BORAL plate, and a gap between the stainless steel cladding for the BORAL plate and the support disk or heat transfer disk. The BORAL plate in the PWR fuel tube is composed of 62.34% B_4C and 37.66% aluminum.

ANSYS PLANE55 conduction elements and LINK31 radiation elements are used to construct the model, which consists of eight layers of conduction elements and six radiation elements that are defined at the gaps (two per gap). The thickness of the model (x-direction) is the distance measured from the inside dimension of the fuel tube to the inside dimension of the slot in the support disk (assuming that the fuel tube is located at the center of the disk slot). The tolerance of the BORAL plate core thickness, 0.003 inch, is used as the gap size for both sides of the BORAL plate. The model height is defined to be the same dimension as the model thickness.

A heat flux is applied at the left side of the model and the temperature at the right boundary of the model is constrained. The heat flux is determined on the basis of design heat load of 20 kW with a peaking factor of 1.1. The maximum temperature of the model (at the left boundary where the heat flux is applied) is calculated by using ANSYS. The effective conductivity through the thickness of the tube is determined by using the following equation:

$$q = K_{eff}(A/L)\,\Delta T$$

or $K_{eff} = qL/(A\ \Delta T)$

where:

q = heat rate applied to inner surface of fuel tube (Btu/hr)
A = area (in^2)
L = thickness of composite tube model (in)
ΔT = temperature difference across the model (°F)
K_{eff} = effective conductivity (Btu/hr-in-°F).

The temperature-dependent conductivity for heat conduction through the wall (K_{eff}) is determined by varying the temperature constraint at the boundary of the model and then re-solving for the temperature difference. The effective conductivity for heat conduction parallel to the axis of the cask body or in the plane of the tube wall is calculated on the basis of the weighted average of the thickness and conductivity of the individual layers.

3.4.1.2 Analytical Models: Cask with BWR Fuel Canister

The finite element ANSYS models used in the thermal analysis of the cask transporting BWR fuel are similar to those used in the thermal analysis of the cask with PWR fuel canister discussed in previous sections. A three-dimensional model is employed to evaluate the cask in a horizontal position with the basket in contact with the canister, which, in turn, is in contact with the cask inner shell. The fuel regions and the fuel tubes with BORAL plates are modeled by using effective conductivities. A detailed two-dimensional thermal model of the fuel assembly is used to determine the effective conductivity of the fuel. A two-dimensional thermal model of the fuel tube is used to calculate the effective conductivities of the fuel tube wall and BORAL plate. Another two-dimensional thermal model for the fuel tube is used to calculate the effective conductivity of the fuel tube wall with no BORAL plate present. These four ANSYS thermal models are described in the following sections.

3.4.1.2.1 Three-Dimensional Cask Model: Cask with BWR Fuel Canister

The three dimensional Universal Transport Cask model is a half-symmetry finite element model constructed by using ANSYS Revision 5.5. The model considers the fuel assemblies, fuel tubes, stainless steel support disks, aluminum heat transfer disks, canister shell, lids and bottom plate, spacers at the bottom of the canister, cask inner shell, lead, outer shell, neutron shield, and neutron shield shell. The ANSYS model is shown in Figure 3.4-5. As shown in the figure, the internal cavity of the canister contains the active fuel region: the top and bottom fittings of the fuel assemblies, fuel tubes enclosing the top and bottom fittings, and the first stainless steel support.

For the BWR configuration, the gas inside the canister and the cask cavity is modeled as helium because the cavity will be backfilled with helium prior to transport. Conduction and radiation are modeled by using ANSYS "SOLID70" and "LINK31" elements, respectively. The principal gaps applied to the model are shown in Figure 3.1-2 and are described in Section 3.2.2.3. In establishing these gaps, the differential thermal expansion between the components is considered.

Because the canister is in horizontal position during transport, the elements for the canister shell are shifted downwards to simulate contact with the inner shell of the cask. Similarly, the support disks and the heat transfer disks are shifted downward to simulate contact with the canister shell. As shown in Figure 3.1-2, a 2-degree contact is considered for the gaps between the canister shell and the cask inner shell and between the support disk and the canister shell. This contact is simulated by using appropriate conductivity (100 Btu/hr-inch-°F) for elements at the contact locations. The aluminum heat transfer disks are assumed to have only a line contact with the canister shell because the heat transfer disks are not subjected to any loads other than their own weight.

To account for differential expansion, gaps within the model are adjusted on the basis of temperature and defined physical contact conditions. Solar insolance and ambient temperature conditions are applied to the neutron shield shell when appropriate. Insolance is used at the exterior surface of the cask and is based on the amount of insolation required by 10 CFR 71 to be applied over a 12-hr period evaluated in the steady state (applied over 24 hr simulating 12-hr period of solar exposure and 12-hr period of no solar exposure). The heat flux resulting from insolation on a curved surface is calculated as follows:

$$1475 \frac{\text{Btu}}{12\ \text{hr - ft}^2} \times \frac{12\ \text{hr}}{24\ \text{hr}} \times \frac{1\ \text{ft}^2}{144\ \text{in}^2} = 0.427\ \text{Btu/hr-in}^2$$

Multiplying this value by the emissivity of the cask surface, $\in = 0.36$, gives a heat flux resulting from insolance on curved surfaces of 0.154 Btu/hr-in^2. Using the same method and a heat flux of 2,950 Btu/12 hr-ft^2 (0.853 Btu/hr-in^2), gives a heat flux resulting from insolance on flat surfaces of 0.307 Btu/hr-in^2.

The model is analyzed to determine the maximum temperatures for the basket, canister, cask shells, radial shielding, and surface conditions under normal conditions of transport. All material properties are shown in Tables 3.2-1 through 3.2-13.

The fuel regions (inside tubes) are modeled as homogeneous regions with effective conductivities determined by the two dimensional fuel model as described in Section 3.4.1.2.2. All sides of the BWR fuel tubes do not contain the BORAL plate. Therefore, two different two-dimensional BWR fuel tube models are analyzed to establish the effective conductivities used in the three dimensional analysis of the cask with BWR fuel. The models consist of the BORAL plate (where applicable), including gas gaps on both sides of the BORAL sheet (where applicable), and the gap between the stainless steel cladding for the BORAL and the support disks and heat transfer disks. These models are discussed in Section 3.4.1.2.3.

The radial neutron shield of the transport cask for the BWR configuration is identical to PWR configuration. The modeling of the radial neutron shield is described in Section 3.4.1.1.

In the model, radiation heat transfer is considered from the top of the fuel region to the bottom surface of the canister shield lid, from the bottom of the fuel region to the top surface of the canister bottom plate, and from the exterior surfaces of the fuel tubes to the inner surface of the canister shell. This radiation is modeled by using LINK31 radiation elements. Radiation across gaps in the model is described in Sections 3.2.2.3 and 3.2.2.4.

Radiation at the neutron shield shell surface to ambient is combined with the convection effect by using the method described in Section 3.2.2.2. The convection heat transfer coefficient is calculated on the basis of the formula shown in Section 3.2.3. Effective emissivities are used for all radiation calculations, with the form factor taken to be unity. Effective emissivity is computed by using the following formula [9] based on corresponding material emissivities:

$$\varepsilon_{eff} = 1/\,(1/\varepsilon_1 + 1/\,\varepsilon_2 - 1)$$

Solar insolance is applied to the neutron shield shell surface for the "Hot" condition (ambient temperature = 100°F). A value of 0.154 Btu/hr-inch^2 is used as the heat flux at the neutron shield shell surface on the basis of the 1,475 Btu/hr-ft^2 heat flux for a curved surface. Calculation of the heat flux resulting from insolation on a curved surface is discussed earlier in this section.

Volumetric heat generation (Btu/hr-inch^3) is applied to the active fuel region on the basis of a total heat load of 16 kW, a shortest active fuel rod length of 144 inches, and an axial power with a peaking factor of 1.22 as shown in Figure 3.4-6.

3.4.1.2.2 Two-Dimensional Fuel Assembly Model: BWR Fuel

The effective conductivity of the fuel is determined by a detailed two-dimensional finite element thermal model of the BWR 9x9 fuel assembly. Taking advantage of the symmetry of the cross-section of the fuel, the finite element model represents a one-quarter section of the fuel. The model includes the fuel pellets, cladding, gas between the fuel rods, and gas occupying the gap between the fuel pellets and cladding. Modes of heat transfer modeled include conduction and radiation between individual fuel rods for the steady-state condition. The model is shown in

Figure 3.4-7. Thermal analyses of the other BWR fuel assemblies (i.e., 7x7 and 8x8) are performed; however, because the BWR 9x9 fuel assembly results in the lowest effective thermal conductivities, only the analysis of that fuel assembly is presented in this section.

ANSYS PLANE55 conduction elements and LINK31 radiation elements are used in the model, which includes a total of 20.25 fuel rods (representing a total of 81 fuel rods for the full cross-section). Each fuel rod consists of the pellet, Zircaloy cladding, and a gap between the pellet and clad. The gas in the gap between the pellet and clad, as well as the gas between the fuel rods, is modeled as helium. Radiation elements are defined between rods and from rods to the boundary of the model (inside surface of the fuel tube). Radiation effect at the gaps between the pellet and clad is conservatively ignored. Effective emissivities are determined by using the formula shown in Section 3.4.1.1.1.

The effective conductivity for the fuel is determined by using a two-step procedure. Using the fuel assembly model, a uniform temperature is applied to the exterior of the model (see Figure 3.4-7) in conjunction with the volumetric heat generation. From this analysis, the maximum temperature located at the center of the fuel assembly is determined. This maximum temperature occurs at the corner of the model, which represents the center of the entire fuel assembly.

A Sandia National Laboratory Report [10] defines an expression for use in determining the maximum temperature of a square cross section of an isotropic homogeneous fuel with uniform volumetric heat generation. At the boundary of this square cross section, the temperature is constrained to be uniform. The expression for the maximum temperature is given by:

$$T_c = T_e + 0.29468 \frac{Q a^2}{K_{eff}}$$

where:

T_c = temperature at center of fuel (°F)
T_e = temperature applied at exterior of fuel (°F)
Q = volumetric heat generation rate (Btu/hr-in^3)

portion of the model corresponding to the cask surface constrains both the horizontal and vertical components of the velocity to be zero.

The cask and personnel barrier are not explicitly modeled in this analysis—only the air surrounding the cask is modeled. It is conservative that the personnel barrier is not explicitly modeled because it will not have a temperature greater than the temperature of the air in contact with it. The temperatures of nodes in the model that correspond to the air adjacent to the cask surface are constrained as boundary conditions of the model. The temperature is considered to be linearly distributed, with the bottom and top temperatures equal to 267°F and 244°F, respectively.

Since the personnel barrier is not explicitly modeled, its temperature is considered to be the temperature of the air at coordinates that correspond the location of the personnel barrier surface. The maximum temperature of the personnel barrier occurs at the top most location at the centerline of the model. The temperatures at key points from the analysis using the model described above are shown in Figure 3.4-12.

3.4.1.5 Test Model

The methods previously described have been used in previous transport cask licensing and are sufficient to show that the Universal Transport Cask meets the criteria set forth in Section 3.4. Therefore, no thermal test model is created.

3.4.2 Maximum Temperatures

Using the thermal models described in Sections 3.4.1.1 and 3.4.1.2, temperatures for the PWR and BWR cask body, canister, basket, and fuel rod cladding are determined for three normal conditions of transport: (1) maximum decay heat, 100°F ambient temperature, and solar insolance; (2) maximum decay heat, -40°F ambient temperature, and no insolance; and (3) no decay heat, -40°F ambient temperature, and no insolance. The maximum temperatures of the principal PWR and BWR cask components, canister, basket components, and fuel rod cladding are shown in Tables 3.4-1 and 3.4-2 for the first two environmental conditions listed above. For the third environmental condition (i.e., no decay heat, -40°F ambient temperature, and no insolance), no analysis is necessary because all package temperatures will equilibrate to -40°F. The cask body maximum allowable component temperatures are shown in Section 3.3.2 and Table 3.4-3.

Using the thermal model described in Section 3.4.1.3, the volumetric average temperature of the redwood in the impact limiters is 135°F.

3.4.3 Minimum Temperatures

The minimum temperatures of the cask and components occur with no heat load and -40°F. These conditions yield a uniform -40°F temperature throughout the Universal Transport Cask package. All package components are capable.

3.4.4 Maximum Internal Pressures

In the following sections, the maximum internal operating pressures for normal conditions of transport are calculated for the PWR and BWR Transportable Storage Canisters and for the Universal Transport Cask cavity. The maximum operating pressure for the canister and cask cavity are summarized in Table 3.4-4.

3.4.4.1 Maximum Internal Pressure for PWR Fuel Canister and Transport Cask

The internal pressures within the PWR fuel canister and transport cask are a function of fuel type, fuel condition (failure fraction), burnup, canister type, and the backfill gases in the canister and cask cavity. Gases included in the pressure evaluation include rod-fill, rod fission and rod backfill gases, expected to be loaded into the UMS® system is separately evaluated to arrive at a bounding canister pressure.

Fission gases include all fuel material generated gases including long-term actinide decay generated helium. Based on detailed SAS2H calculations of the maximum fissile material mass assemblies in each canister class, the quantity of gas generated by the fuel rods rises as burnup and cool time is increased and enrichment is decreased. To assure the maximum gas is available for release, the PWR inventories are extracted from conservatively high 60,000 MWD/MTU burnup cases at an enrichment of 1.9 wt. % ^{235}U and a cool time of 40 years. Gases included are all krypton, iodine, and xenon isotopes in addition to helium and tritium (^{3}H). Molar quantities for each of the maximum fissile mass assemblies are summarized in Table 3.4-5. Fuel generated gases are scaled by fissile mass to arrive at molar contents of other UMS® fuel types.

Fuel rod backfill pressure varies significantly between the PWR fuel types. The maximum reported backfill pressure is listed for the Westinghouse 17x17 fuel assembly at 500 psig. With the exception of the B&W fuel assemblies, which are limited to 435 psig, all fuel assemblies evaluated are set to the maximum 500 psig backfill reported for the Westinghouse assembly. Backfill quantities are based on the free volume between the pellet and the clad and the plenum volume. The fuel rod backfill gas temperature is conservatively assumed to have an initial temperature of 68°F.

Burnable poison rod assemblies (BPRAs) placed within the UMS® canister may contribute additional molar gas quantities due to (n, alpha) reactions of fission generated neutrons with ^{10}B. during in-core operation. ^{10}B forms the basis of a portion of the neutron poison population. Other neutron poisons, such as gadolinium and erbium, do not produce a significant amount of helium nuclides (alpha particles) as part of their activation chain. Primary BPRAs in existence include Westinghouse Pyrex (borosilicate glass) and WABA (wet annular burnable absorber) configurations, as well as B&W BPRAs and shim rods employed in CE cores. The CE shim rods replace standard fuel rods to form a complete assembly array. The quantity of helium available for release from the BPRAs is directly related to the initial boron content of the rods and the release fraction of gas from the matrix material in question. Release from either of the low temperature, solid matrix materials is likely to be limited, but no release fractions were available in open literature. Therefore, a 100% release fraction is assumed based on a boron content of 0.0063 g/cm ^{10}B per rod, with the maximum number of rods per assembly. The maximum number of rods is 16 for Westinghouse core 14 x 14 assemblies, 20 rods for Westinghouse and B&W 15 x 15 assemblies, and 24 rods for Westinghouse and B&W 17 x 17 assemblies. The length of the absorber is conservatively taken as the active fuel length. CE core shim rods are modeled at 0.0126 g/cm ^{10}B for 16, 12, and 12 rods applied to CE manufactured 14 x 14, 15 x 15 and 16 x 16 cores, respectively.

The canister backfill gases are conservatively assumed to be at 250°F. The initial pressure of the canister backfill gas is 1 atm (0.0 psig). The cask backfill temperature and pressure are assumed to be 68°F and 1 atm. Free volume inside each PWR canister class is listed in Table 3.4-6. Also included are the total canister and cask free volumes. The listed free volumes do not include fuel assembly components since these components vary for each assembly type and fuel insert. By subtracting the rod and guide tube volumes and all hardware component volumes from the listed free volume, the free volume of the canisters including fuel assemblies and a load of 24 BPRAs can be determined. For the Westinghouse BPRAs, the Pyrex volume is employed since it displaces more volume than the WABA rods.

The total pressure for each of the UMS® payloads is found by calculating the releasable molar quantity of each gas (30% of the fission gas, 100% of the rod backfill, BPRA and shim rod gasses adjusted for the 3% fuel failure fraction and the canister and cask backfill gases), and summing the quantities directly. The quantity of gas is then employed in the ideal gas equation in conjunction with the average gas temperature at normal operating conditions to arrive at system pressures. The normal condition average temperature of the gas within the PWR canister and cask is considered to be 453°F. Each of the UMS® PWR fuel types is individually evaluated for normal condition pressure, and the maximum normal condition canister and cask pressures are determined to be 6.15 psig and 6.91 psig, respectively. A summary of the maximum pressure in the canister and in the cask for each PWR canister class is shown in Table 3.4-7. The table also includes the fuel type producing the listed maximum pressures.

3.4.4.2 Maximum Internal Pressure for BWR Fuel Canister and Transport Cask

BWR canister and cask maximum pressures are determined in the same manner as those documented for the PWR cases. Primary differences between PWR and BWR analysis include a maximum normal condition average gas temperature of 366°F, rod backfill gas pressures of 132 psig, and pressurizing gases are limited to fission gases (including helium actinide decay gas), rod backfill gases, and canister and cask backfill gas. The 132 psig employed in this analysis is significantly higher than the 6 atmosphere maximum pressure reported in open literature. BWR assemblies do not contain an equivalent to the PWR BPRAs and, therefore, do not require ^{10}B helium generated gases to be added. Fissile gas inventories for the maximum fissile material assemblies in each of the three BWR lattice configurations (7 x 7, 8 x 8, and 9 x 9) are shown in Table 3.4-8. Free volumes, without fuel components, in UMS® canister classes 4 and 5 are shown in Table 3.4-9. Cask and canister maximum pressures for each canister class are listed in Table 3.4-10. The maximum normal condition pressure of 3.47 psig is based on a GE 7 x 7 assembly designed for a BWR/2-3 reactor and burned to 60,000 MWD/MTU. Cask maximum pressure for the GE 7 x 7 fuel is 3.65 psig. High burnups, greater than 45,000 MWD/MTU, are typically obtained from updated assembly designs such as the GE 9 x 9 assembly. The normal condition pressure for a UMS® canister containing the GE 9 x 9 fuel assembly with 79 fuel rods is 3.33 psig. Similar fuel masses and displaced volume account for similar system pressures.

3.4.5 Maximum Thermal Stresses

The ANSYS computer code is used to obtain temperatures for use in the structural analyses of Chapter 2.0. These temperatures are presented in Tables 3.4-1 and 3.4-2. The thermal stress calculations for normal conditions of transport are performed in Sections 2.6.1 and 2.6.2.

3.4.6 Maximum Allowable Cladding Temperature and Canister Heat Load

The maximum allowable cladding temperatures are calculated for PWR and BWR systems based on fuel assembly type, maximum burnup, and minimum initial cool time. Allowable heat loads are determined by relating cladding temperature to canister heat load.

Cladding stresses are calculated for a set of representative PWR and BWR assemblies at 40,000 MWD/MTU and 380°C. The limiting, highest stress assemblies, the Westinghouse 14x14 and GE 9x9 (150-inch fuel region), are then evaluated at various burnups to determine the maximum allowable fuel cladding temperature based on PNL-6364 criteria [28]. Maximum allowable cladding temperatures are generically calculated for PWR and BWR burnups ranging from 35,000 MWD/MTU to 45,000 MWD/MTU. PWR burnups are extended to 50,000 MWD/MTU to envelop the Maine Yankee specific inventory. After applying a bias to the maximum allowable cladding temperatures, the maximum allowable heat load is calculated as a function of burnup and minimum initial cool time.

3.4.6.1 Maximum Allowable Cladding Temperature

Based on PNL-6364, the cladding temperature limit is expressed as a function of initial dry storage temperature, initial cladding stress at the dry storage temperature, and initial storage time. For this evaluation, the transport temperatures and transport times are applied.

The initial cladding stress is a function of the rod internal pressure, temperature, diameter of the fuel rod, and fuel cladding thickness. The initial cladding stress (σ_{mhoop}) for a particular assembly is calculated as [28]:

$$\sigma_{mhoop} = \frac{(P)(D_{mid})}{2t} \times \alpha \times \frac{T_2}{T_1} \times \frac{69.684}{10{,}000}$$

where:

σ_{mhoop} = dry storage cladding hoop stress, MPa
P = internal gas pressure of the rod, psi
T_1 = temperature at which P was determined, K
t = cladding wall thickness, in.
D_{mid} =cladding midwall diameter, in.
α = a factor, 0.95 for PWR rods or 0.90 for BWR rods
T_2 = allowable storage temperature for σ_{mhoop}, K

To account for cladding oxidation during in-core fuel assembly operation and storage of the fuel in the spent fuel pool, the nominal cladding thickness is reduced by 0.06 mm and 0.125 mm for

PWR and BWR fuel rods, respectively [3]. For higher burnup PWR fuels (i.e., rod peak burnup up to 50,000 MWD/MTU), Maine Yankee experience is that the maximum oxide layer thickness on the fuel cladding is 120 microns [30]. The allowable cladding temperature calculations at 50,000 MWD/MTU therefore employ an oxide layer thickness of 0.012 cm.

The pressure in the fuel assembly rods is produced by the combination of fill gas and fission gas.

For a given fuel assembly design, the fill gas quantity is fixed and does not vary with discharge burnup. Based on the initial pressure and temperature of the fill gas, the number of moles of gas are calculated using the ideal gas law:

$$PV = NRT$$

where:

P = Pressure
V = Volume (free volume inside fuel rod)
N = Number of moles of gas
R = Universal gas constant
T = Temperature of the gas

The number of moles of fill gas are added to the fission gas quantity and converted to a cladding internal pressure at storage conditions.

The fission gas quantity pressurizing the fuel cladding is calculated on the basis of the burnup and a fission gas release fraction. While the amount of fission gas produced is a predictable quantity (directly correlated to the number of fissions required to produce the desired burnup), the release fraction of the gas from the pellet into the pellet-cladding void depends on fill gas pressure and reactor operating conditions.

The number of fissions (Z) is related to the burnup by:

$$Z = X \text{ Burnup } \frac{\text{MWd}}{\text{MTU}} \times 1.0 \times 10^{6} \frac{\text{W}}{\text{MW}} \times 86{,}400 \frac{\text{sec}}{\text{d}} \times \frac{1 \text{ MeV}}{1.602 \times 10^{-13} \text{ J}} \times \frac{1 \text{ Fission}}{200 \text{ MeV}}$$

$$\times \frac{1 \text{ Mole}}{6.02 \times 10^{23} \text{ Atoms}} \times \text{Mass} \frac{\text{MTU}}{\text{Assembly}} \times \frac{\text{Assembly}}{\#\text{ Rods}}$$

Multiplying the number of fissions by 0.3125 (0.25 x 1.25) atoms/fission then derives the quantity of fission gas produced. Olander's "Fundamental Aspects of Nuclear Reactor Fuel Elements" [11] lists the number of gas atoms from a single fission as 0.25. Based on a detailed SAS2H isotope generated fission gas inventory, this fraction is increased by 25% to account for decay chains not included in Olander (particularly those leading to ^{136}Xe). By employing a conservative fission gas fraction rather than the SAS2H output itself, the allowable cladding temperature calculation is decoupled from source term calculations.

Based on Sandia Report 90-2406, "A Method for Determining the Spent-Fuel Contribution to Transport Cask Containment Requirements" [10], gas release fractions from the fuel pellets are assumed to be 12% for PWR fuel rods and 25% for BWR fuel rods. Relying on a gas diffusion model (as applied to pre-pressurized light water reactor fuel rods), the Sandia report indicates a release fraction of approximately 1% for PWR rods and approximately 2% for BWR rods [10]. Experimental release fractions reach as high as 16% for PWR rods and 25 % for BWR rods [10]. The higher release fractions are associated with unpressurized fuel rods or those rods run at uncharacteristically high temperatures and linear heat generation rates. While these rods show higher release rates, they are not expected to produce higher "burned fuel" pressures, since the partial pressure of the fill gas is not present, thereby allowing a larger number of fission gas molecules to accumulate before reaching limiting cladding pressure. The 12% PWR fission gas release fraction excludes the unpressurized Maine Yankee rod data while including the 43,000 MWD/MTU Calvert Cliff data to approximate the upper bound 45,000 MWD/MTU burnup. An additional analysis is performed comparing the 12% PWR and 25% BWR release fractions to the element specific release fractions in Reg. Guide 1.25 [29]. The 12% PWR release fraction results in gas releases similar to those indicated by the Regulatory Guide, while the BWR 25% release fraction is twice the Regulatory Guide indicated gas release. Note that both the Sandia report and the Regulatory Guide release fractions are for punctured fuel rods where the release of the pressurizing gas allows additional gaseous isotopes to migrate from the fuel matrix. Using the 12% PWR and 25% BWR fuel rod release fractions, therefore, results in a conservative cladding pressurization assumption for the intact rod analysis. For higher burnup PWR fuels (i.e., rod peak burnup up to 50,000 MWD/MTU), Maine Yankee experience is that the maximum gas release rate (fuel pellet to rod plenum in intact fuel rods) is less than 3% [30]. Therefore, the 12% release fraction established for standard PWR fuel burned up to 45,000 MWD/MTU is conservatively applied to the higher burnup PWR fuel.

Fuel rod free volume is calculated based on the fuel characteristics in Tables 3.4-11 and 3.4-12 for PWR and BWR fuel, respectively. Not all assemblies requested for loading are included in the tables, since assemblies with significantly higher free volume or lower fuel mass are bounded by the cladding stress evaluations presented.

Substituting the internal gas pressure resulting from the releasable gas inventories produced by 40,000 MWD/MTU burned fuel into the initial cladding stress (σ_{mhoop}) equation at a temperature of 380°C results in the assembly-specific maximum cladding stresses shown in Table 3.4-11 and Table 3.4-12. The Westinghouse 14 x 14 and GE 9 x 9 (150-inch fuel region) are the limiting PWR and BWR assembly types at 113.9 and 70.5 MPa stress levels, respectively.

The stress levels in the limiting assemblies are then evaluated at burnups ranging from 35,000 MWD/MTU to 50,000 MWD/MTU for PWR fuel and 35,000 MWD/MTU to 45,000 MWD/MTU for BWR fuel at temperatures of 300°C and 400°C for PWR fuels and 300°C and 450°C for BWR fuel. The evaluation results are presented in Table 3.4-13. This data is overlaid on generic stress versus limiting temperature curves to arrive at cool time and burnup-specific maximum cladding allowable temperatures. The data, shown in Table 3.4-14, from which the generic curves are constructed, is taken from Table 3.1 of PNL-6189 [27].

The cladding temperature limit curves for the limiting PWR and BWR fuel assemblies are provided in Figures 3.4-13 and Figure 3.4-14. The intercept of each of the curves represents the maximum allowable cladding temperature at a given cool time and maximum assembly burnup. Fuel rod peak cladding stress level and the allowable cladding temperature are calculated using the assembly average burnup, even though some rods experience a higher burnup than the average. The average burnup is used, since the quantity of fission gas formation and the fuel rod gas temperature are conservatively determined. As shown in Table 3.4-15, allowable cladding temperature varies only slightly over a wide range of burnup for a given required cooling time. Consequently, the variation in cladding stress with burnup is also small.

3.4.6.2 Maximum Allowable Canister Heat Load

Thermal analysis was performed at three heat loads for PWR fuel and one heat load for BWR fuel to determine the corresponding maximum fuel cladding temperature. Only one heat load is analyzed for BWR fuel because the maximum computed clad temperature is 548°F (286.7°C) at the maximum heat load of 16 kW, which is already lower than the minimum allowable temperature limit for any BWR fuel (Table 3.4-15). Therefore, BWR fuel was not further analyzed and a fixed maximum decay heat of 16 kW is allowable for transport of BWR fuel.

The thermal models and methods, described in Section 3.4.1, used to determine the temperature of fuel cladding and system components for the design basis heat load are applied to determine the cladding temperature at reduced heat loads. The ANSYS calculated temperatures that provide input for correlating allowable cladding temperature to allowable heat load are:

	Fuel Clad Temperature		Heat Load
Fuel Type	(°F)	(°C)	(kW)
PWR	537	280.6	14
PWR	610	321.1	17
PWR	677	358.3	20
BWR	548	286.7	16

The PWR temperature versus heat load curve is plotted in Figure 3.4-15. To provide adequate design margin, the maximum allowable cladding temperatures are reduced by a temperature bias, shown in Table 3.4-17, prior to their use in the calculation of maximum allowable canister heat load. Maximum allowable canister heat loads are calculated for initial cool times ranging from 5 to 15 years and burnups ranging from 35,000 MWD/MTU to 50,000 MWD/MTU for PWR fuel and 35,000 MWD/MTU to 45,000 MWD/MTU for BWR fuel. The results of the PWR and BWR analysis are presented in Table 3.4-16. Since these temperatures are based on the PWR and BWR assemblies having the highest cladding stress levels, the maximum heat loads can be applied to all UMS® design basis contents.

3.4.7 Evaluation of Package Performance for Normal Conditions of Transport

Results of thermal analysis of the Universal Transport Cask containing PWR and BWR fuel under normal conditions of transport are summarized in Tables 3.4-1 through 3.4-3. The maximum fuel rod cladding temperature is maintained below 810°F (432°C); temperatures of safety-related cask components are maintained within their safe operating ranges; and thermally induced stresses in combination with pressure and mechanical load stresses are shown in the structural analysis of Chapter 2.0 to be less than the allowable stresses. As shown in Section 3.4.2, the personnel barrier temperature of 153°F is below the allowable temperature of 185°F for exclusive use shipment. Therefore, the Universal Transport Cask can safely transport the design basis fuel under the normal conditions of transport specified in 10 CFR 71.71.

Figure 3.4-1 Three-Dimensional PWR Cask Finite Element Model

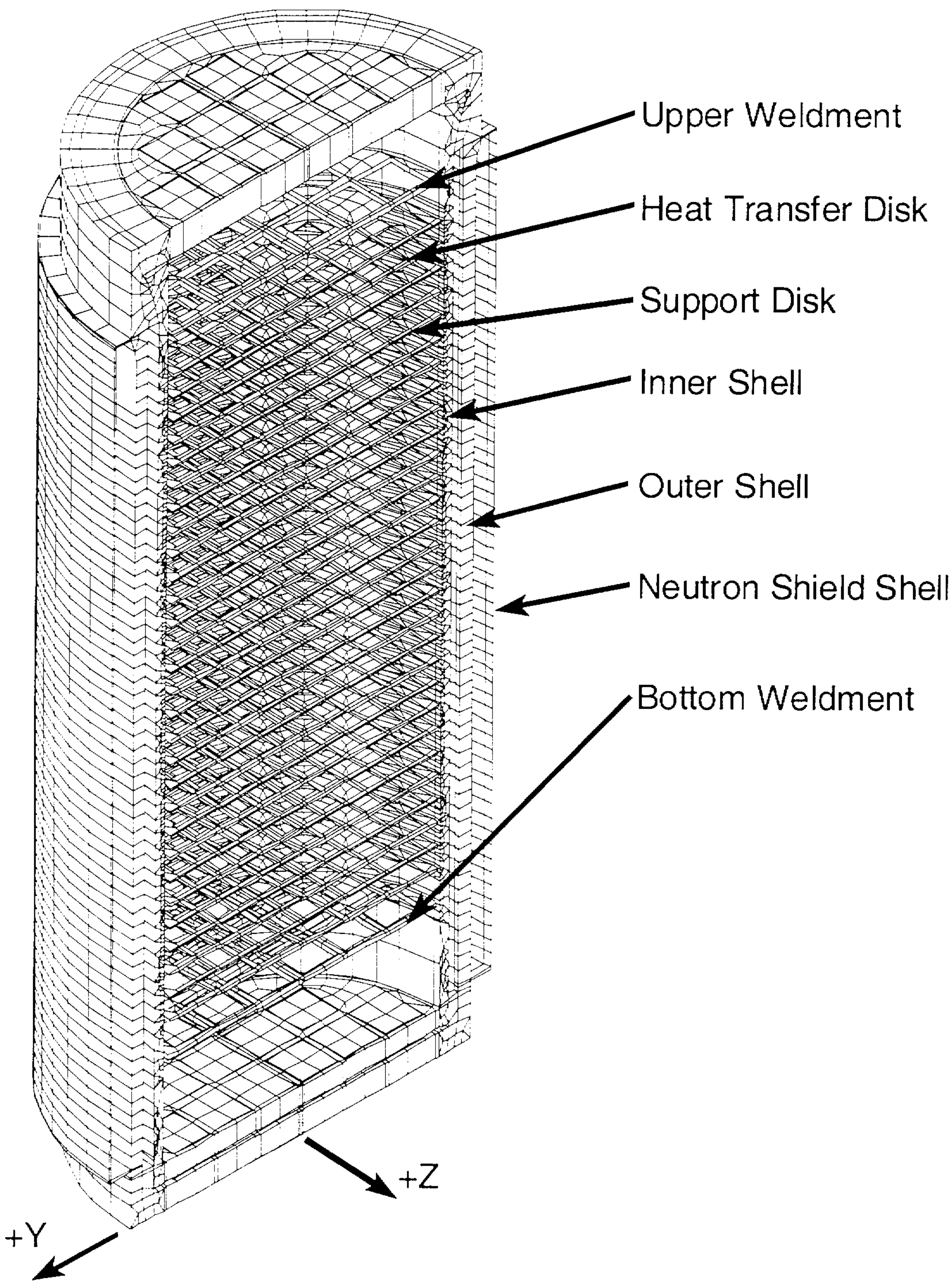

Figure 3.4-2 Design Basis PWR Fuel Assembly Axial Power Distribution

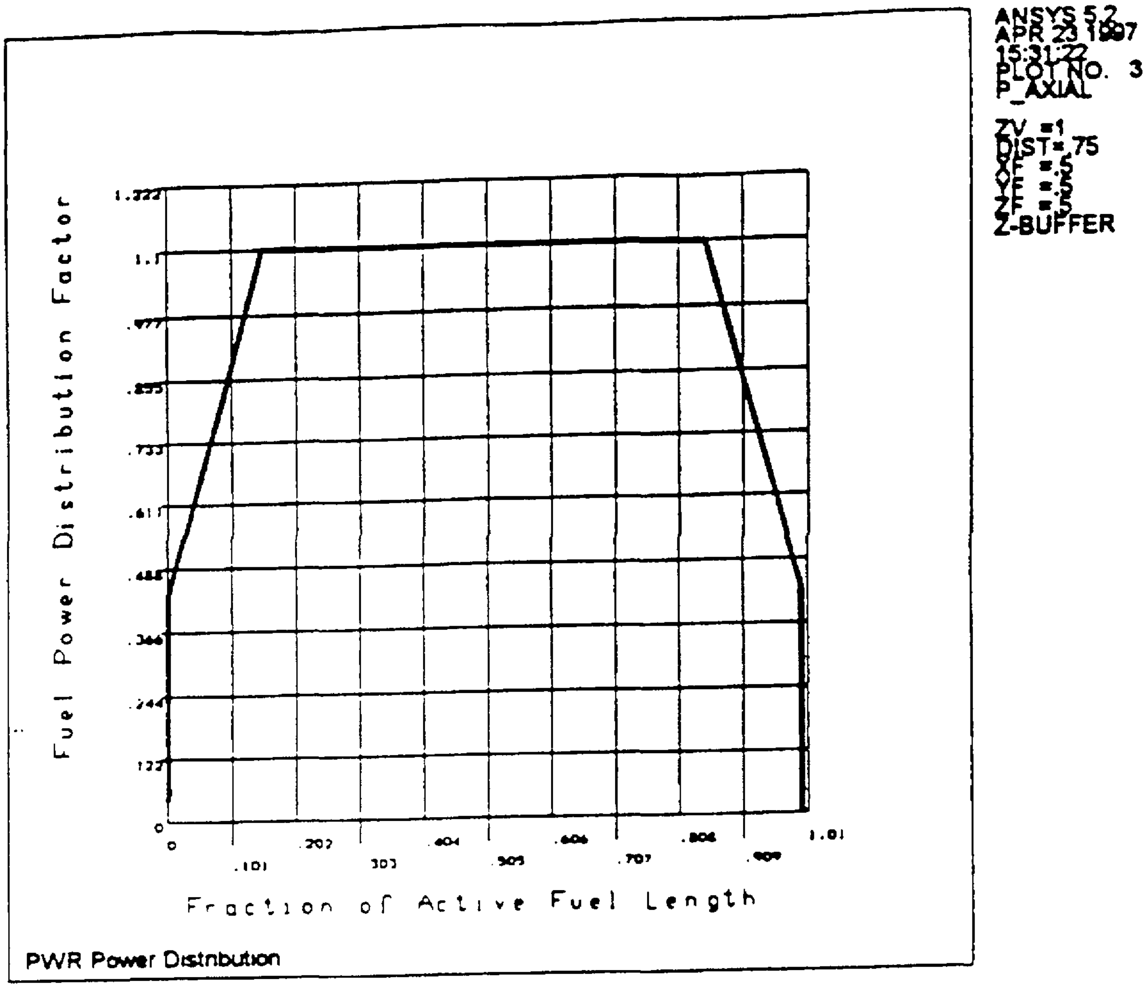

Figure 3.4-3 PWR 14x14 Fuel Assembly Two-Dimensional Finite Element Model

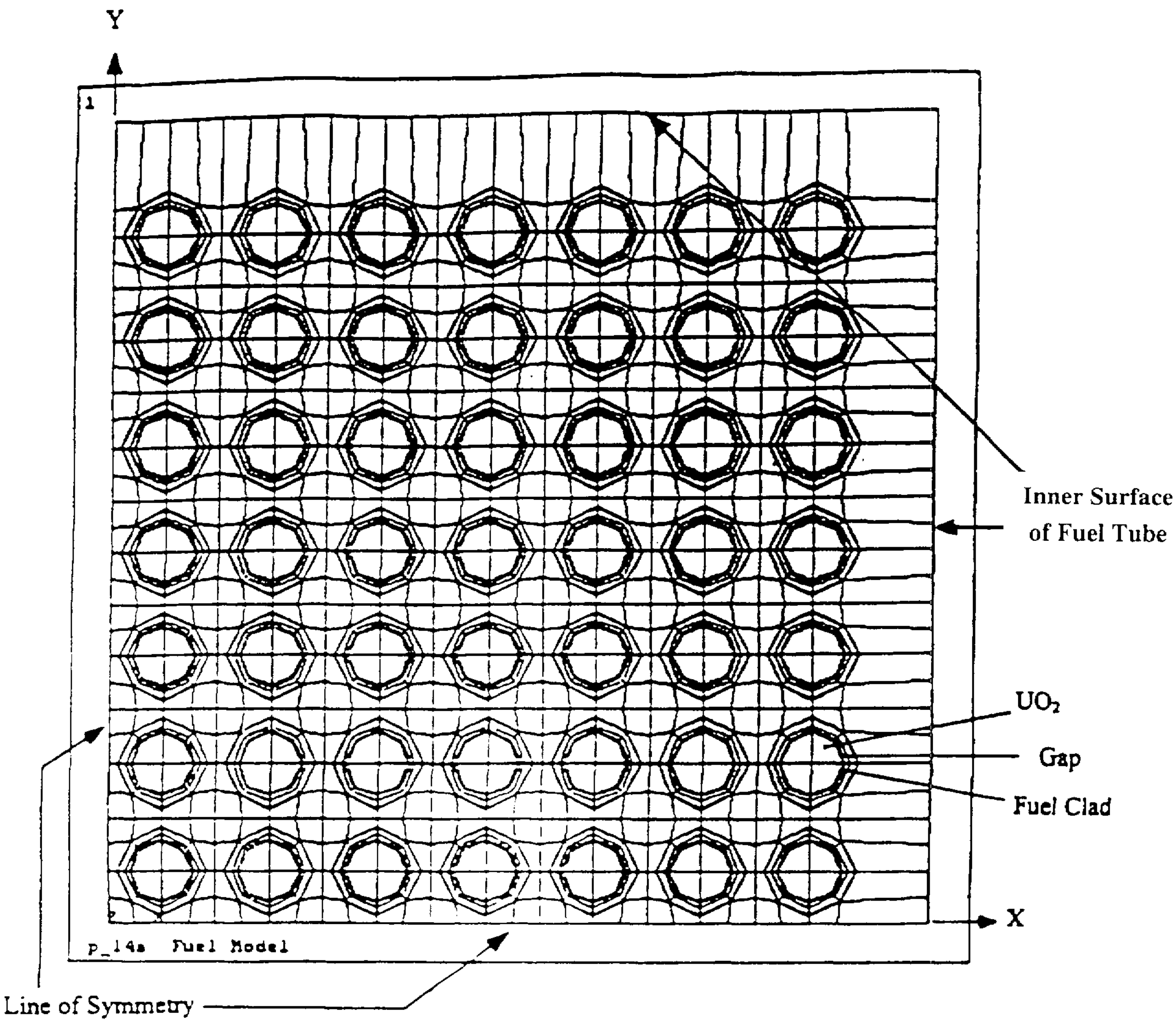

Figure 3.4-4 Two-Dimensional PWR Fuel Tube Model

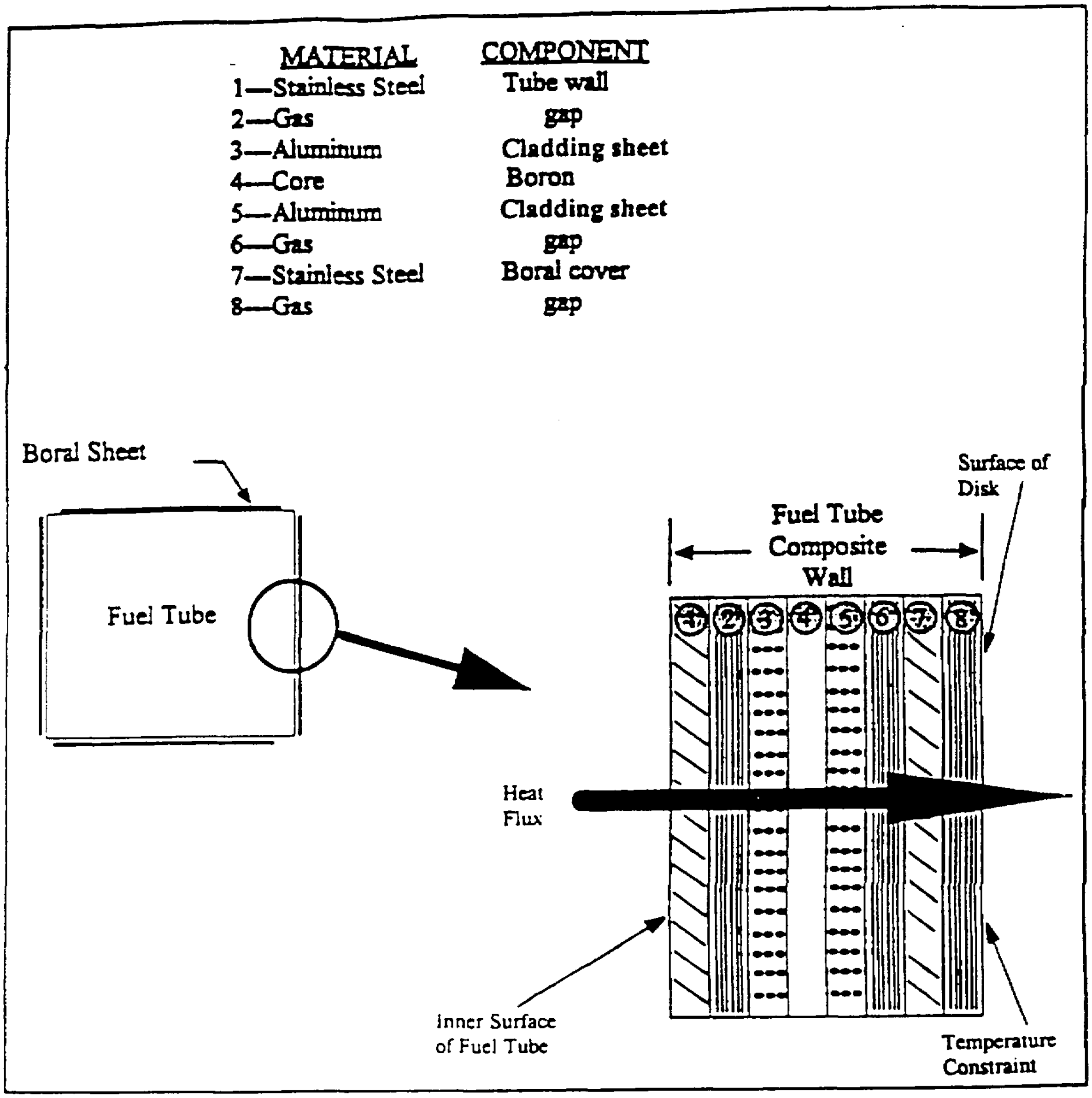

Figure 3.4-5 Three-Dimensional BWR Cask Finite Element Model

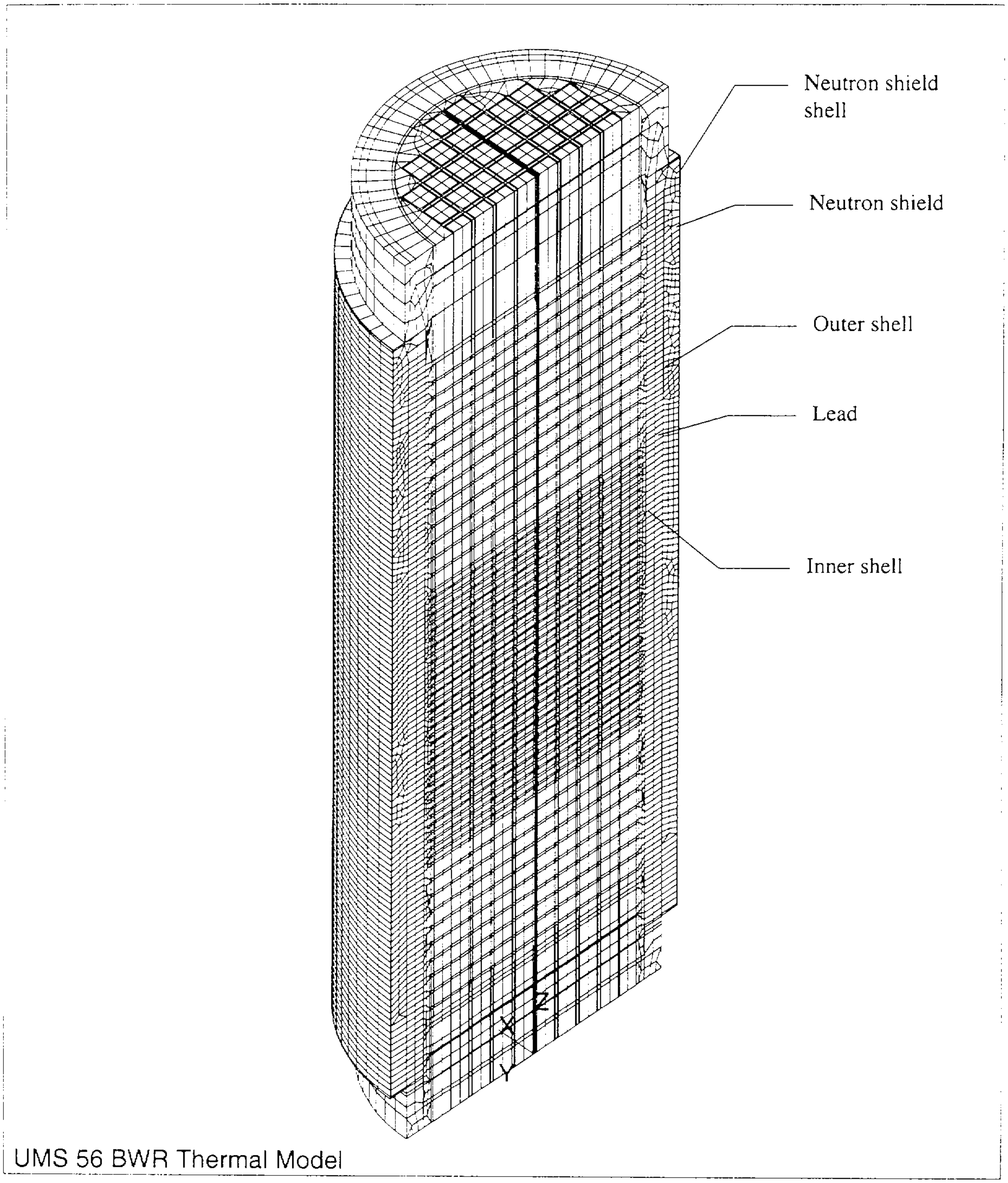

Figure 3.4-6 Design Basis BWR Fuel Assembly Axial Power Distribution

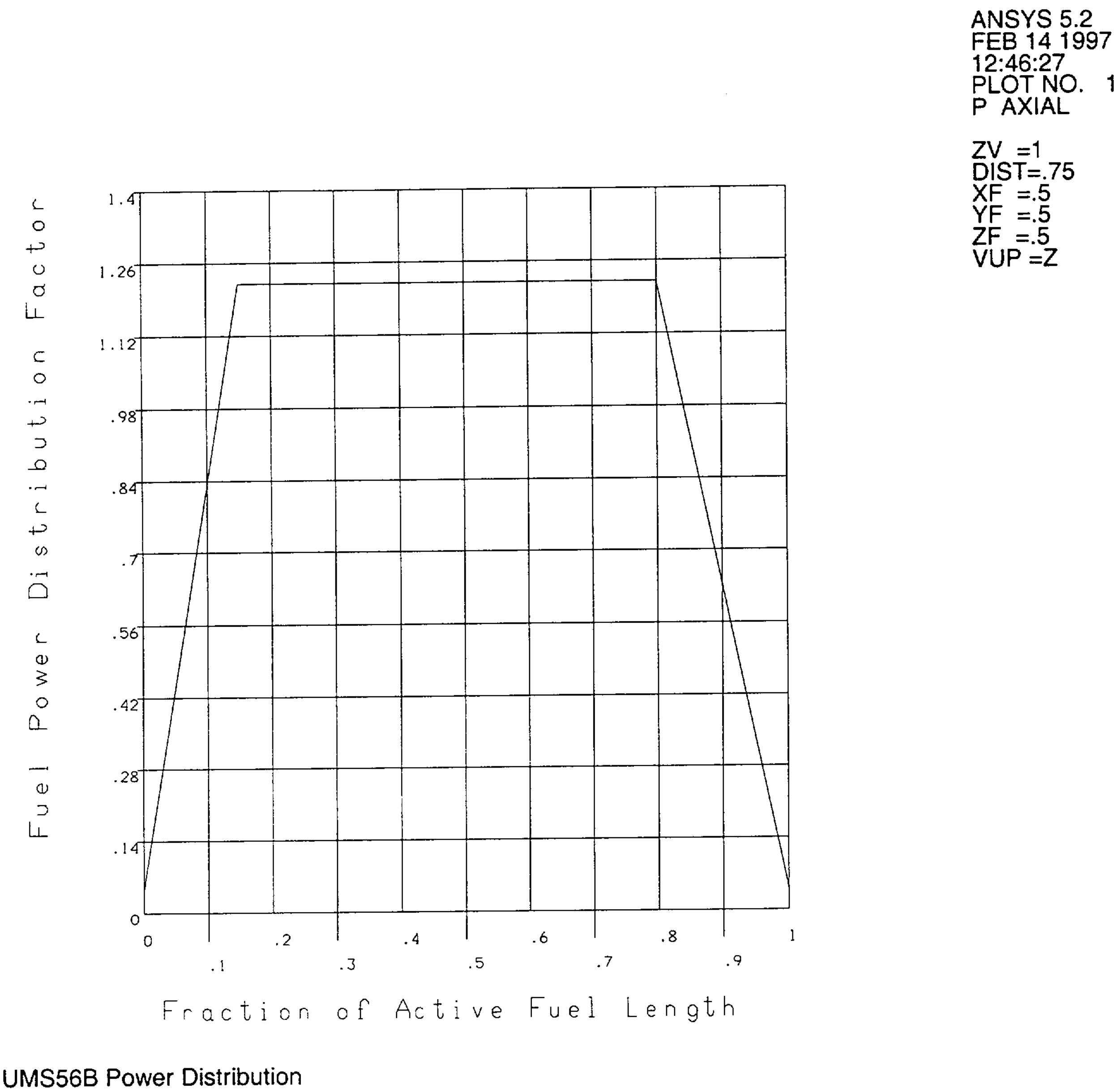

Figure 3.4-7 BWR 9x9 Fuel Assembly Two-Dimensional Finite Element Model

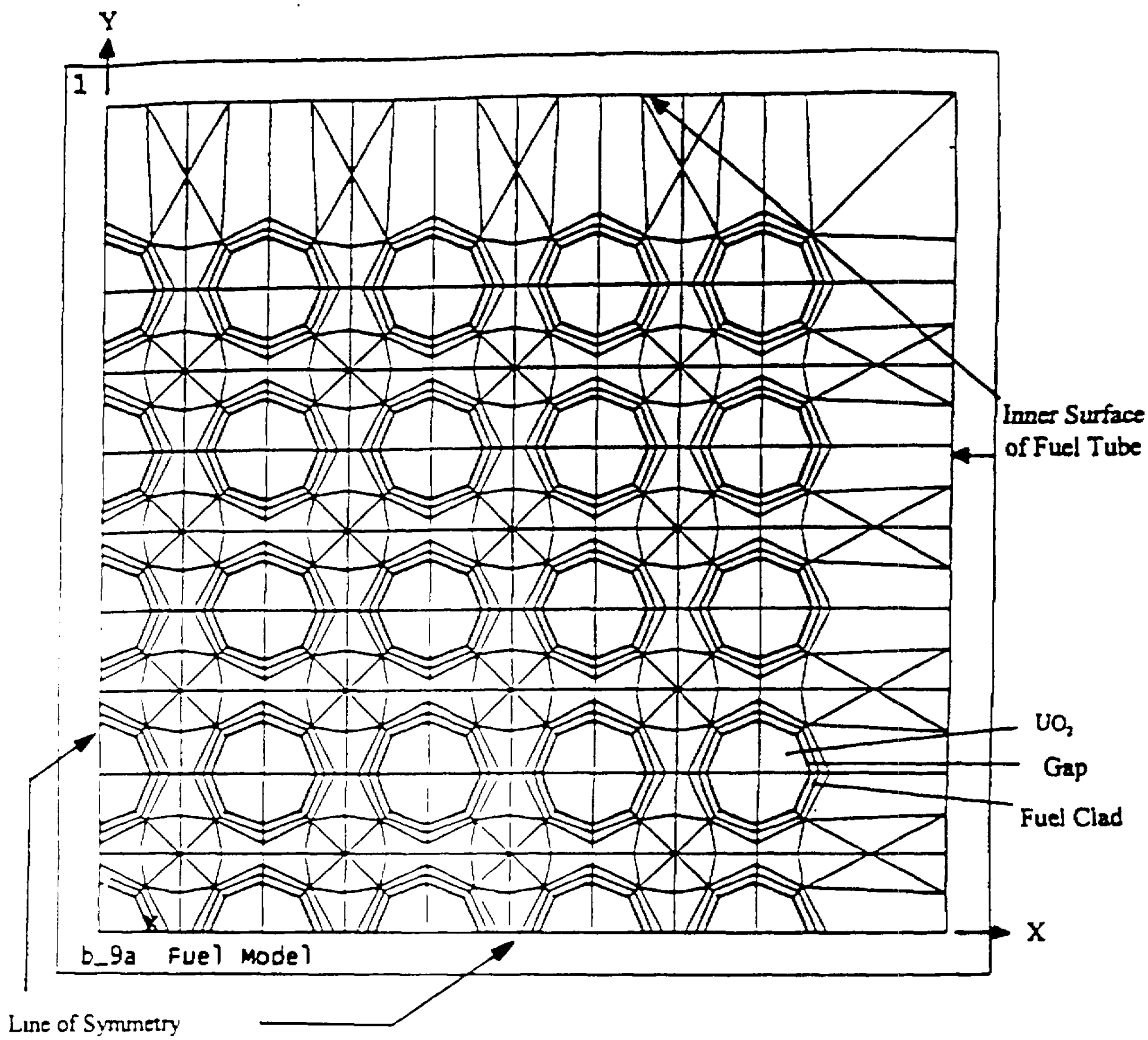

Figure 3.4-8 Two-Dimensional BWR Fuel Tube (with BORAL) Model

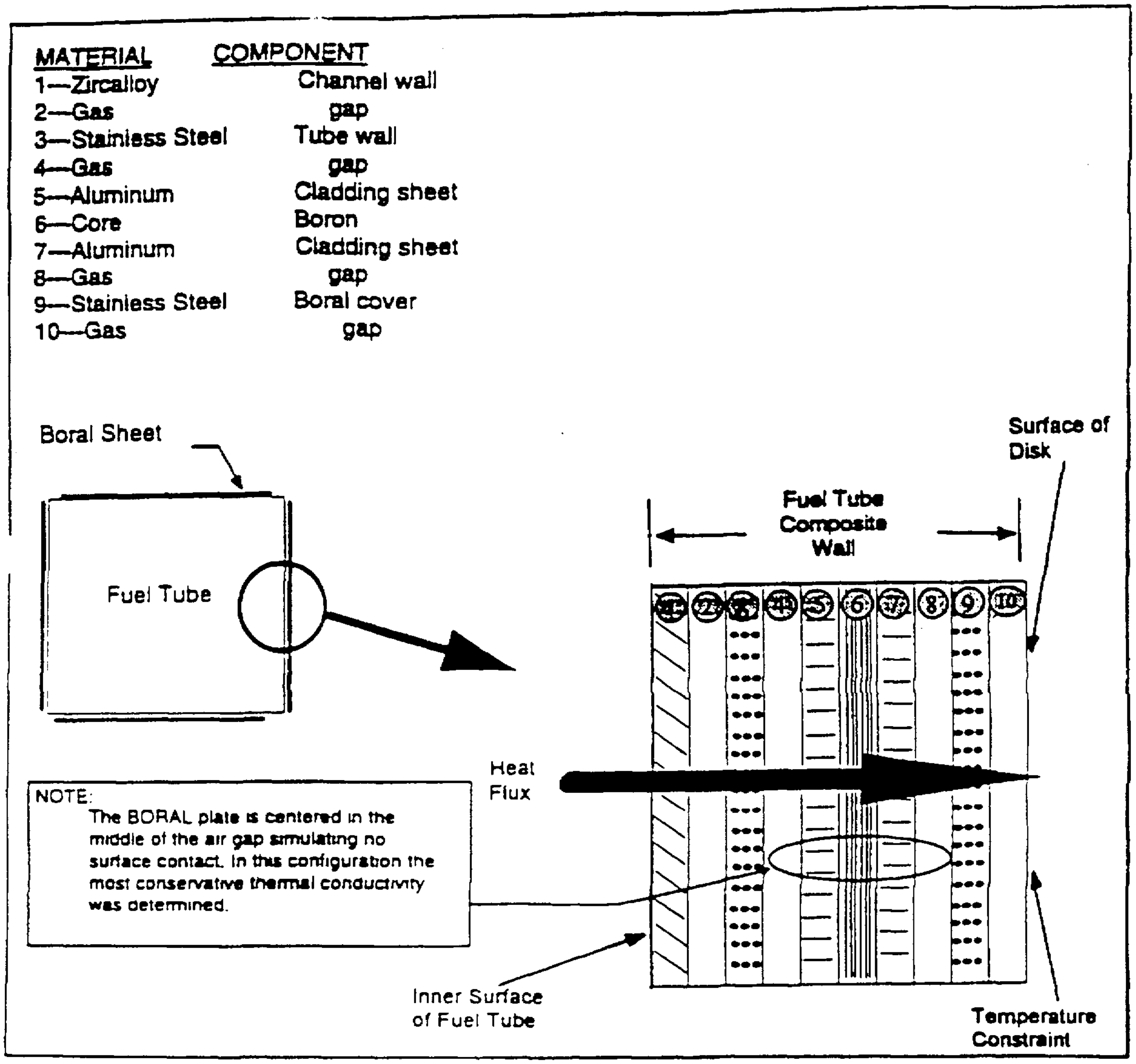

Figure 3.4-9 Two-Dimensional BWR Fuel Tube (without BORAL) Model

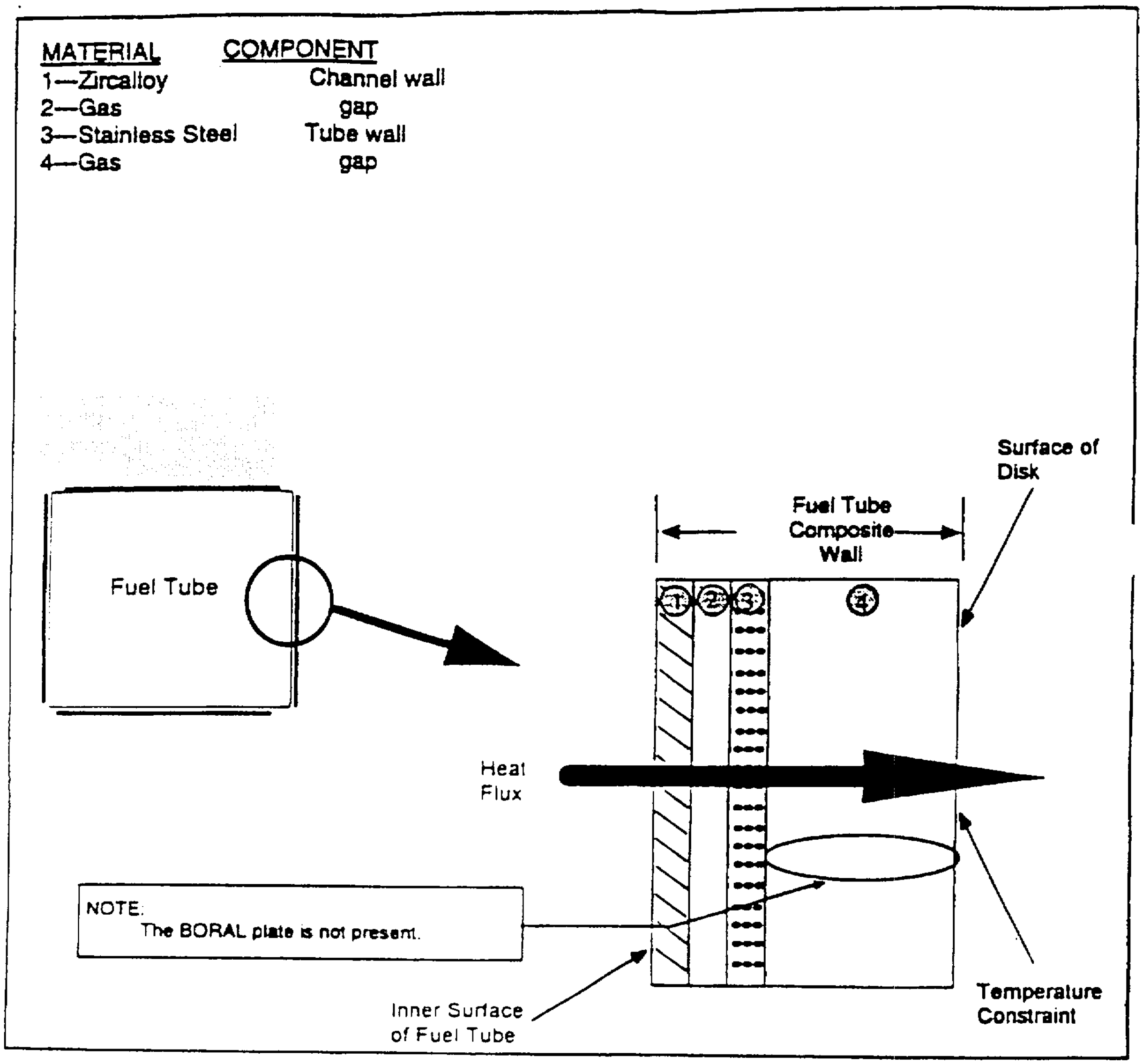

Figure 3.4-10 Cask Impact Limiter Thermal Model

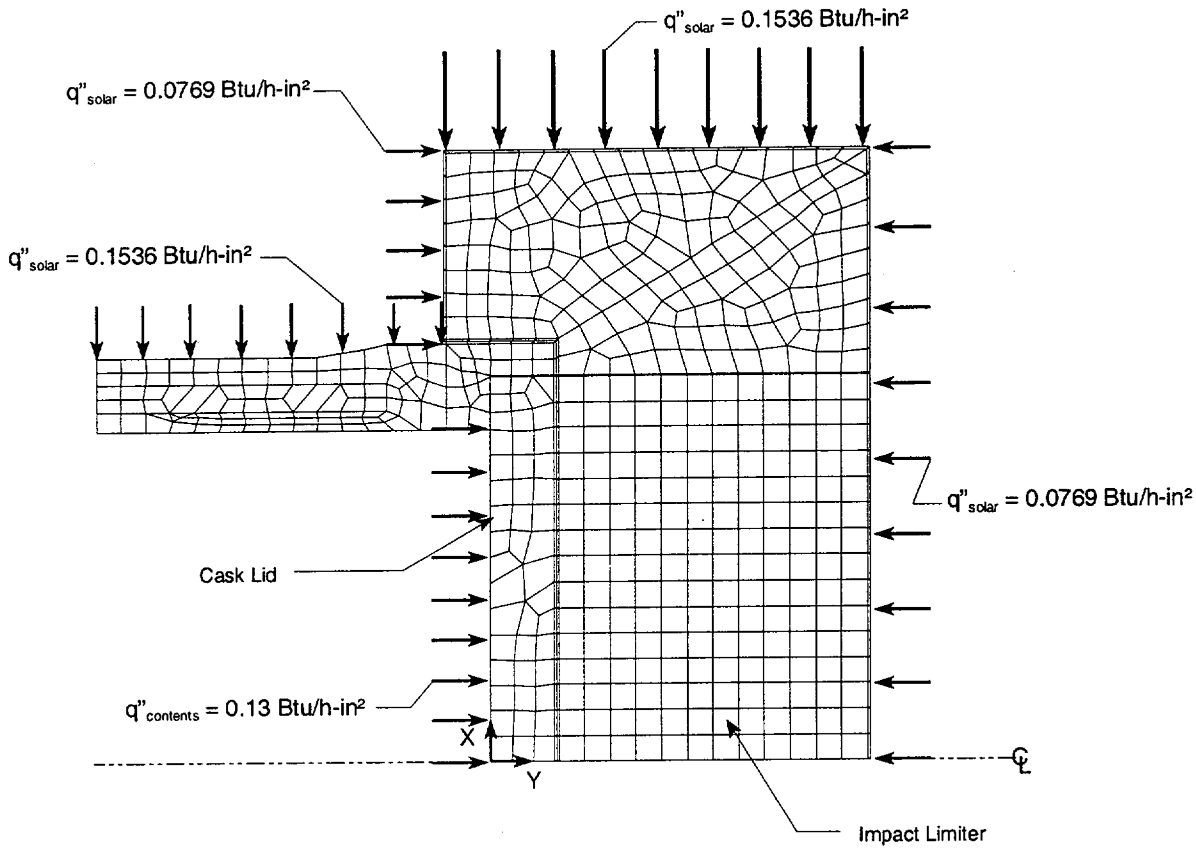

Figure 3.4-11 Personnel Barrier Thermal Model

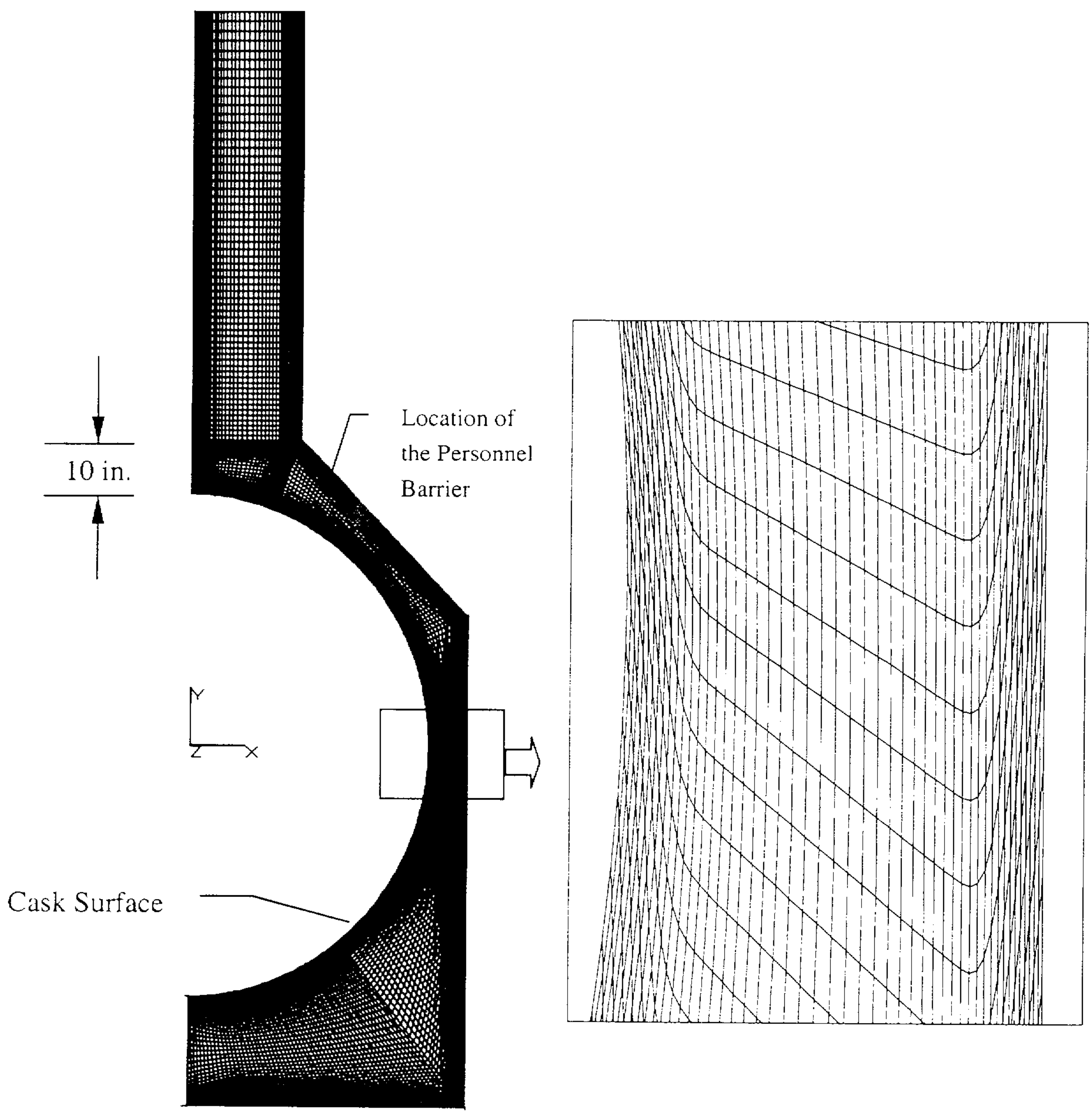

Figure 3.4-12 Temperature Results at Key Points of the Personnel Barrier

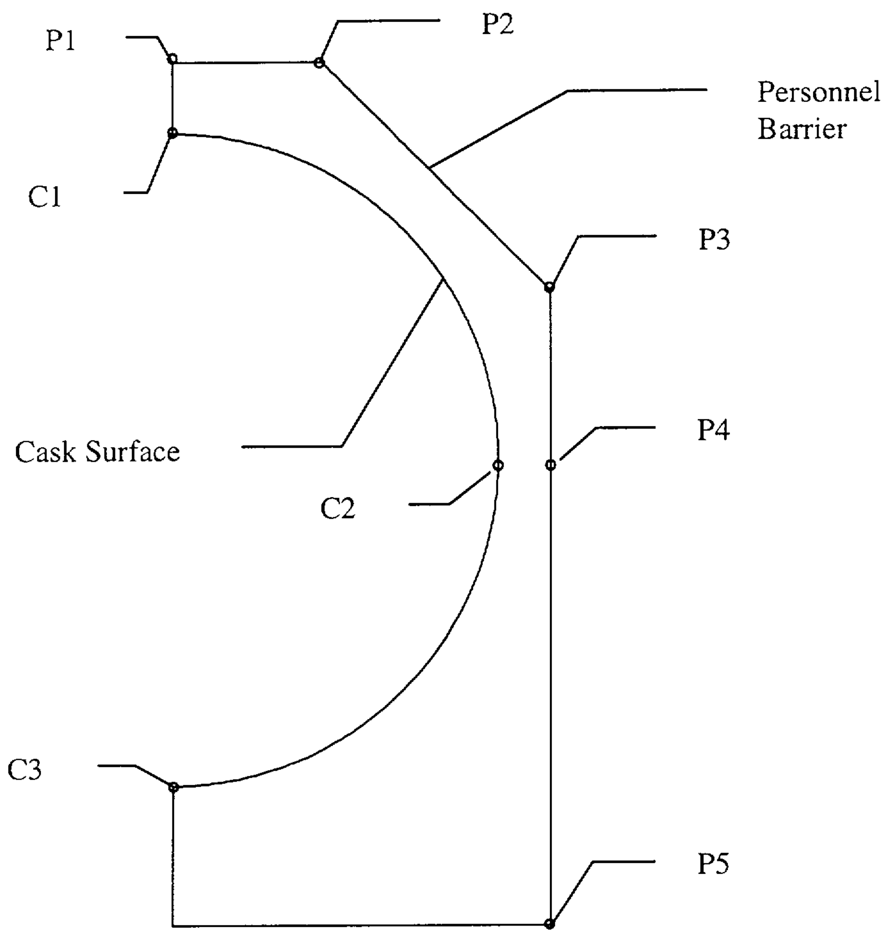

	Boundary Conditions			Calculated Temperature (°F)				
Location	C1	C2	C3	P1	P2	P3	P4	P5
Temperature	244	256	267	153	108	133	131	100

Figure 3.4-13 PWR Fuel Dry Storage Temperature versus Cladding Stress

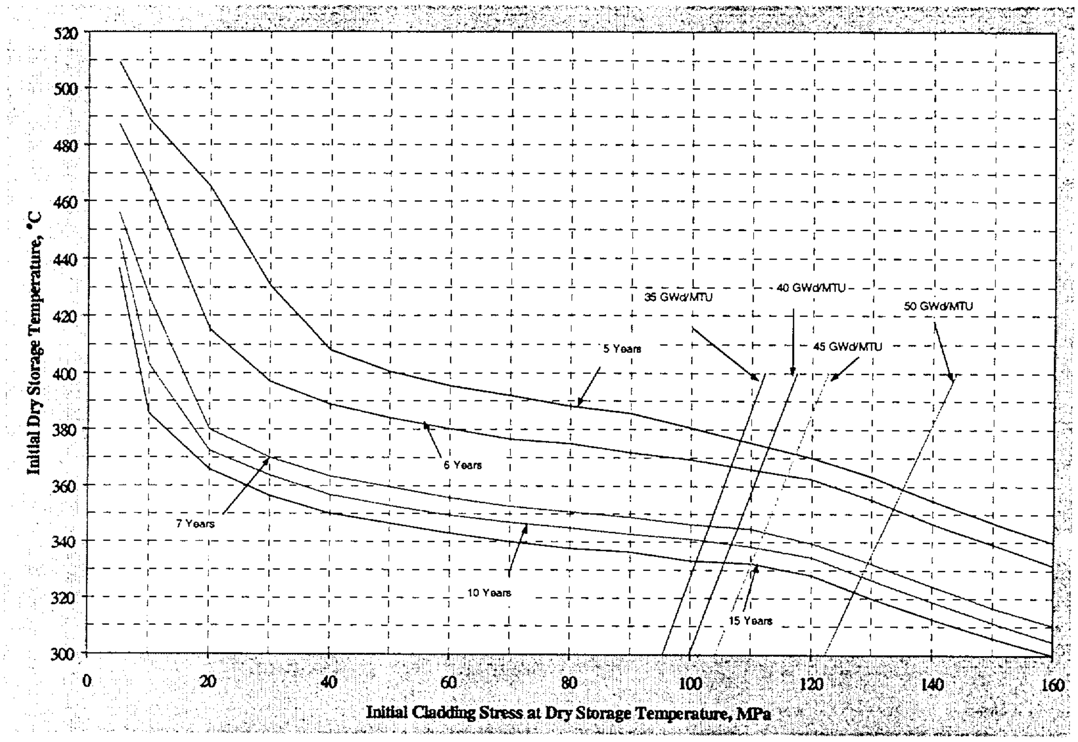

Figure 3.4-14 BWR Fuel Dry Storage Temperature versus Cladding Stress

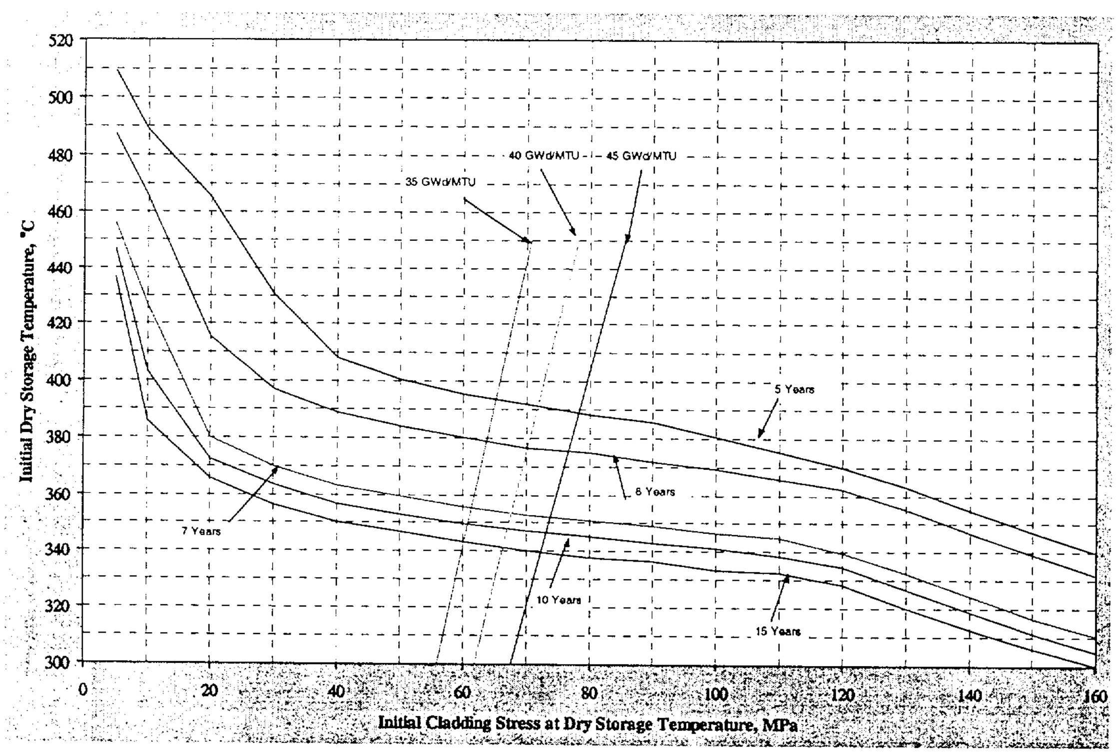

Figure 3.4-15 PWR Fuel Cladding Dry Storage Temperature versus Basket Heat Load

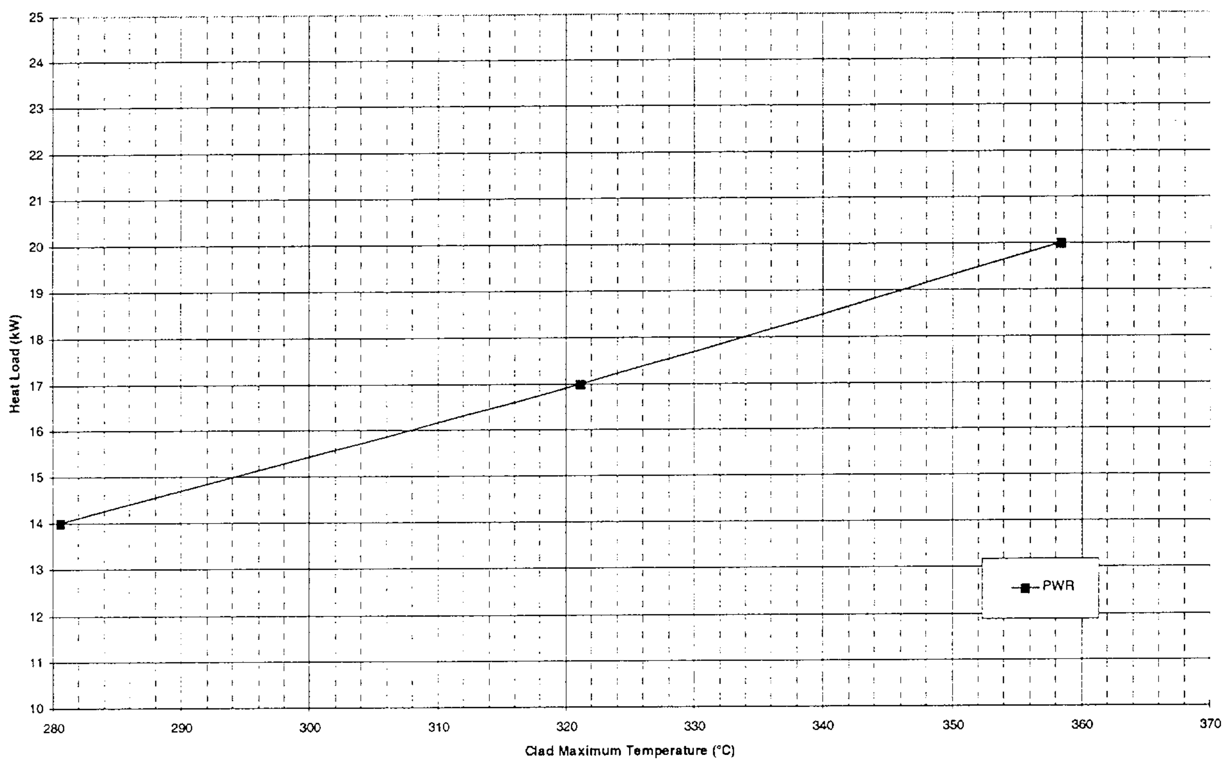

Table 3.4-1 Maximum Component Temperatures - Normal Conditions of Transport, Maximum Decay Heat, Maximum Ambient Temperature

Component	Temperature (°F) Cask with PWR Fuel Canister		Temperature (°F) Cask with BWR Fuel Canister	
		Canister Gas: Helium		Canister Gas: Helium
Cask Lid O-Rings/Vent Port O-ring[1]		266		204
Lower Drain Port O-ring[4]		224		230
Cask Radial Outer Surface		266		256
Radial Neutron Shield		293		286
Lead Gamma Shield		306		298
Aluminum Disk Exterior		268		298
Aluminum Disk Interior		605		515
Support Disk Exterior		255		208
Support Disk Interior		608		512
Canister Shell		408		363
Canister Shield Lid		270		208
Canister Bottom Plate		324		262
Maximum Fuel Rod Cladding		673		548
Cask Bottom		217		228
Bottom Forging		224		230
Inner Shell		344		312
Outer Shell		301		293
Top Forging[2]		250		194
Cask Lid		266		204
Cask Lid Bolt[3]		266		204
Average Gas Temperature in the Canisters[5]		453		366

Conditions:
100°F ambient temperature
20 kW decay heat load, 1.1 peaking factor - PWR
16 kW decay heat load, 1.22 peaking factor - BWR
Solar insolation
Cask cavity gas: helium
Canister cavity gas: helium

1. Cask lid O-rings and vent port O-rings not explicitly modeled—taken to be the maximum cask lid temperature.
2. Average temperature.
3. Cask lid bolts not explicitly modeled—taken to be the maximum temperature of the cask lid.
4. Lower drain port O-ring not explicitly modeled - taken to be the maximum temperature of the bottom forging.
5. Calculated as a volumetric average.

Table 3.4-2 Maximum Component Temperatures - Normal Conditions of Transport, Maximum Decay Heat, Minimum Ambient Temperature

Component	Temperature (°F) Cask with PWR Fuel Canister		Temperature (°F) Cask with BWR Fuel Canister	
		Canister Gas: Helium		Canister Gas: Helium
Cask Lid O-Rings/Vent Port O-ring[1]		140		62
Cask Radial Outer Surface		151		132
Radial Neutron Shield		178		162
Lead Gamma Shield		191		174
Maximum Basket[2]		505		404
Canister Shell		289		238
Canister Shield Lid		145		66
Canister Bottom Plate		205		127
Maximum Fuel Rod Cladding		578		440

Conditions:
-40°F ambient temperature
20 kW decay heat load, 1.1 peaking factor - PWR
16 kW decay heat load, 1.22 peaking factor - BWR
No insolation
Cask cavity gas: helium
Canister cavity gas: helium

1. Cask lid O-ring and vent port O-rings not explicitly modeled—taken to be the maximum cask lid temperature.
2. Taken to be the greater of the maximum support disk and the maximum aluminum heat transfer disk temperatures.

Table 3.4-3 Universal Transport Cask Thermal Performance Summary for Component Operating Temperature

Temperature	Cask with PWR Fuel Canister (helium in cask cavity/helium in canister)	Cask with BWR Fuel Canister (helium in cask cavity/helium in canister)	Allowable Temperature Range
Maximum cladding temperature(°F)	673	548	< 716[1]
Component safe operating temperature ranges			
Cask lid O-rings	-40 to 266°F	-40 to 208°F	-40 to 300°F
Vent port coverplate O-ring	-40 to 266°F	-40 to 208°F	-40 to 300°F
Drain port coverplate-O-rings	-40 to 224°F	-40 to 230°F	-40 to 300°F
Radial NS-4-FR neutron shield	-40 to 293°F	-40 to 286°F	-40 to 300°F
Lead gamma shield	-40 to 306°F	-40 to 298°F	-40 to 600°F
Aluminum heat transfer disk	-40 to 605°F	-40 to 515°F	-40 to 700°F
PWR support disk	-40 to 608°F		-40 to 650°F
BWR support disk		-40 to 517°F	-40 to 700°F

1. In accordance with PNL-6189, the temperature limit of 380°C (716°F) is used for the evaluation of fuel considered in the design basis heat load (20 kW). For temperature limits corresponding to different burnup and cooling times, refer to Table 3.4-8.

Table 3.4-4 Maximum Internal Pressures for Transport

Fuel	Cavity	Condition	Pressure (psig)
PWR	Canister	3% fuel rod failure	6.15
		100% fuel rod failure	74.3
	Cask	3% fuel rod failure	6.91
		100% fuel rod failure	69.3
BWR	Canister	3% fuel rod failure	3.47
		100% fuel rod failure	43.8
	Cask	3% fuel rod failure	3.65
		100% fuel rod failure	42.8

Table 3.4-5 PWR Per Assembly Fuel Generated Gas Inventory

Array	Assy Type	MTU	Moles
14x14	WE Standard	0.4144	35.52
15x15	B&W	0.4807	41.32
16x16	CE	0.4417	38.10
17x17	WE Standard	0.4671	40.18

Table 3.4-6 PWR Canister Free Volume (No Fuel or Inserts)

Canister Class	1	2	3
Basket Volume (in^3)	69800	74490	77460
Canister Height (inch)	175.05	184.15	191.75
Canister Free Volume w/o Fuel (liter)	7970	8400	8770
Canister and Cask Free Volume w/o Fuel (liter)	9030	8980	8970

Table 3.4-7 PWR Maximum Normal Condition Pressure Summary

Canister Class	Fuel Type	Canister Pressure (psig)	Cask Pressure (psig)
Class 1	West. 17x17 Standard	6.13	6.91
Class 2	B&W 17x17 Mark C	6.15	6.62
Class 3	CE 16x16	5.81	6.02

Table 3.4-8 BWR Per Assembly Fuel Generated Gas Inventory

Array	Assy Type	MTU	Moles
7x7	GE 7x7 (49 Rods)	0.1985	16.78
8x8	GE 8x8 (63 Rods)	0.1880	16.07
9x9	GE 9x9 (79 Rods)	0.1979	16.86

Table 3.4-9 BWR Canister Free Volume (No Fuel or Inserts)

Canister Class	4	5
Basket Volume (in^3)	73110	74680
Canister Height (inch)	185.55	190.35
Canister Free Volume w/o Fuel (liter)	8500	8740
Canister and Cask Free Volume w/o Fuel (liter)	8710	8930

Table 3.4-10 BWR Maximum Normal Condition Pressure Summary

Canister Class	Fuel Type	Canister Pressure (psig)	Cask Pressure (psig)
Class 4	GE 7 x 7	3.47	3.65
Class 5	GE 7 x 7	3.41	3.55
Class 5	GE 9 x 9	3.33	3.48

Table 3.4-11 PWR Cladding Stress Level Comparison Chart

Fuel Type	B&W 15x15	B&W 17x17	CE 14x14	CE 16x16	WE 14x14	WE 15x15	WE 17x17
Rod OD (inch)	0.43	0.379	0.44	0.382	0.422	0.422	0.374
Cladding Thickness (inch)	0.0265	0.024	0.028	0.025	0.0225	0.0242	0.0225
Pellet OD (inch)	0.3686	0.3232	0.3765	0.325	0.3674	0.3659	0.3225
Active Fuel Length (inch)	144	143	137	150	145.2	144	144
Plenum Length (inch)	7.755	8.318	8.528	9.927	5.790	7.386	6.260
Spring Weight (lb)	0.042	0.026	0.1	0.1	0.07	0.044	0.037
Backfill Pressure (psig)	435	435	500	500	500	500	500
Fuel Mass (MTU)	0.4807	0.4658	0.4037	0.4417	0.4144	0.4646	0.4671
# of Fuel Rods	208	264	176	236	179	204	264
Free Volume (inch^3)	1.427	1.198	1.252	1.052	1.217	1.300	0.882
Pressure (psia) (380°C)	1525	1478	1739	1722	1762	1713	1795
Stress Level (Mpa)	83.1	78.9	91.2	88.5	113.9	101.7	102.1

Table 3.4-12 BWR Cladding Stress Level Comparison Chart

Fuel Type	EX 7x7	EX 8x8	EX 9x9	GE 7x7	GE 8x8a	GE 8x8b	GE 9x9
Rod OD (inch)	0.57	0.484	0.424	0.563	0.493	0.483	0.441
Cladding Thickness (inch)	0.036	0.036	0.03	0.032	0.034	0.032	0.028
Pellet OD (inch)	0.49	0.4045	0.3565	0.487	0.416	0.41	0.376
Active Fuel Length (inch)	144	150	150	144	144	150	150
Plenum Length (inch)	10.200	10.024	9.578	11.190	10.960	9.580	9.580
Spring Weight (lb)	0.13	0.1	0.047	0.083	0.066	0.066	0.047
Backfill Pressure (psig)	44.1	132.0	132.0	44.1	132.0	132.0	132.0
Fuel Mass (MTU)	0.196	0.1793	0.1666	0.1977	0.1855	0.1847	0.1979
# of Fuel Rods	48	62	74	49	63	62	79
Free Volume (inch^3)	2.426	1.708	1.469	3.236	2.181	1.970	1.758
Pressure (psia) (380°C)	1264	1469	1359	971	1236	1345	1286
Stress Level (MPa)	66.7	65.1	65.4	58.2	59.8	68.7	70.5

Table 3.4-13 Cladding Stress as a Function of Fuel Assembly Average Burnup and Temperature

Burnup	PWR		BWR	
	300°C	400°C	300°C	450°C
35,000 MWD/MTU	95.4 Mpa	112.3 Mpa	55.9 Mpa	70.8 Mpa
40,000 MWD/MTU	99.9 Mpa	117.4 Mpa	61.8 Mpa	78.2 Mpa
45,000 MWD/MTU	104.2 Mpa	122.6 Mpa	67.6 Mpa	85.5 Mpa
50,000 MWD/MTU	122.3 Mpa	143.9 Mpa	--	--

Table 3.4-14 Maximum Allowable Initial Storage Temperature (°C) as a Function of Initial Cladding Stress and Initial Cool Time

MPa	5 years	6 years	7 years	10 years	15 years
5	509.2	487.3	455.9	447	436.5
10	488.8	465.5	426.4	403	385.6
20	465.2	415.5	380.1	372.4	366
30	430.4	397	370.1	363.8	356.5
40	408.1	389	363.2	356.6	350
50	400.6	384	359.7	353.1	346.5
60	395.6	380.4	355.9	349.6	343.1
70	391.9	376.5	352.5	347	340
80	388.2	375	350.8	345.2	337.6
90	385.7	372	348.8	342.8	336.1
100	380.7	369.3	346.2	341	333.2
110	375.2	365.9	344.6	338	332.1
120	370	362.4	339.5	334.3	328.2
130	363.5	355.2	332.2	326.6	320
140	355	346.6	324.2	318.6	312.6
150	346.9	339.1	316.5	311.2	306
160	339.6	331.4	310.3	304.7	299.9

Table 3.4-15 Maximum Allowable Cladding Temperature for PWR and BWR Fuel

Cool Time [years]	PWR Clad Temperature Limit [°C] Burnup (MWD/MTU)				BWR Clad Temperature Limit [°C] Burnup (MWD/MTU)			
	35,000	40,000	45,000	50,000	35,000	40,000	45,000	50,000
5	376	374	371	359	394	391	389	--
6	367	365	364	352	379	376	376	--
7	346	345	343	333	355	353	352	--
10	340	339	338	328	349	348	346	--
15	333	333	332	322	343	341	339	--

Table 3.4-16 Maximum Allowable Decay Heat for PWR and BWR Systems

Cool Time [years]	PWR Decay Heat Limit[1] [kW] Burnup (MWD/MTU)				BWR Decay Heat Limit[1] [kW] Burnup (MWD/MTU)			
	35,000	40,000	45,000	50,000	35,000	40,000	45,000	50,000
5	20.00	20.00	19.90	19.30	16.00	16.00	16.00	--
6	19.50	19.30	19.20	18.70	16.00	16.00	16.00	--
7	17.80	17.80	17.70	17.20	16.00	16.00	16.00	--
10	17.40	17.30	17.20	16.80	16.00	16.00	16.00	--
15	16.80	16.80	16.70	16.50	16.00	16.00	16.00	--

1 Based on maximum clad temperature and biases shown in Table 3.4-17.

Table 3.4-17 Temperature Bias Applied to Maximum Allowable Decay Heats

Cool Time [years]	PWR Clad Temperature Bias [°C] Burnup (MWD/MTU)				BWR Clad Temperature Bias [°C] Burnup (MWD/MTU)			
	35,000	40,000	45,000	50,000	35,000	40,000	45,000	50,000
5	-15	-15	-14	-9	-18	-17	-18	--
6	-15	-15	-16	-10	-18	-17	-19	--
7	-15	-15	-14	-10	-16	-16	-17	--
10	-15	-15	-15	-10	-16	-16	-15	--
15	-15	-16	-16	-9	-15	-16	-16	--

3.5 Thermal Evaluation for Hypothetical Accident Conditions

This section provides thermal evaluation of the Universal Transport Cask containing PWR or BWR fuel under hypothetical accident conditions. The objective of the thermal analysis of the cask under hypothetical accident conditions is to demonstrate that the cask containment boundary structural components are maintained within their safe operating temperature ranges.

Because the fire accident is considered to be of short duration, the limit for maximum cladding temperature may be higher than that for normal conditions of transport. A cladding temperature limit of 1,058°F, however, is conservatively applied [3]. To determine their cumulative effect on the package, the tests specified in 10 CFR 71.73 are to be performed or analyzed in sequence. Thus, the Universal Transport Cask is analyzed for the fire transient, specified in 10 CFR 71.73(c)(4), assuming that the package is in a form consistent with the damage sustained in the free-drop and puncture tests of 10 CFR 71.73.

3.5.1 Thermal Models

Finite element models are used in the thermal evaluation of the Universal Transport Cask under hypothetical accident conditions. The same model is used to evaluate the cask transporting the PWR and the BWR fuel. Heat flux is applied to the inner shell surface of the cask model to simulate the decay heat generation. The distribution of the heat flux corresponds to the power distribution shown in Figures 3.4-2 and 3.4-6 for PWR and BWR fuel, respectively.

The environmental conditions and decay heat loads for the analysis are provided as discussed in Section 3.5. Convection during the fire accident has been considered. Results are given in the form of maximum component temperatures in Tables 3.5-1 (PWR) and 3.5-2 (BWR).

3.5.1.1 Analytical Models

Taking advantage of the symmetry of geometry and thermal loads of the cask about its major axis, the two finite element models of the cask (with PWR and with BWR fuel) are two-dimensional axis-symmetric representations of the cask. The finite element models are constructed by using ANSYS two-dimensional thermal elements (PLANE55) with the axis-symmetric option activated. The spent fuel and basket are not explicitly modeled. The maximum temperatures of the basket components and fuel cladding are calculated by adding the maximum temperature difference between the cask inner shell and the component of interest from the normal condition results (Table 3.4-1) to the peak temperature of the inner shell. The inner shell peak temperatures for the hypothetical accident case are provided in Tables 3.5-1 and 3.5-2 for the PWR and BWR fuel, respectively. The cask model for PWR and BWR used in the accident condition evaluation are shown in Figures 3.5-1 through 3.5-3.

In each model, the cask body is modeled as three concentric shells: the inner stainless steel shell, the lead shielding, and the outer stainless steel shell. The portions of the lead region which extend above and below the neutron shield are protected by a layer of low conductivity material that effectively insulates the lead from the heat of the fire. Because the canister, fuel basket, and fuel assemblies are not explicitly modeled, no gas gaps occur in the models—all heat transfer through the models is by means of conduction only. The gap between the cask and lead is conservatively ignored, resulting in a greater heat input to the cask.

The analyses of the finite element models are composed of three distinct phases:

1. Initial conditions (steady-state): Maximum decay heat of the fuel; ambient temperature = 100°F; solar insolance.

2. 30-min fire (transient): Maximum decay heat of the fuel; fire temperature = 1,475°F (including convection and radiation); no solar insolance.

3. Postfire cool-down (transient): Maximum decay heat of the fuel; ambient temperature = 100°F; solar insolance.

For the first two phases of the analyses, the effective conductivity of the radial neutron shield is calculated in the same manner presented in Section 3.4.1.1.1. At the end of the 30-min fire transient, the neutron shield is considered to be voided of NS-4-FR, so that only the Cu/SS fins and stainless steel shell remain. The effective conductivity for this arrangement is then recalculated as discussed in Section 3.4.1.1.1. Air is substituted for the NS-4-FR material. The thickness of the fireblock material in an uncompressed state is .12 inches, but in the model .03 in. is used.

The effect of impact limiters is included in the model for the fire analysis. Previous scale model tests of the NAC-STC cask have demonstrated that the impact limiters remain on the cask after the 30-ft drop imposed by the hypothetical accident condition. The UMS® impact limiters are nearly identical to those of the NAC-STC. The fire transient models include natural convection and thermal radiation boundary conditions during all phases of the analyses and account for solar insolation effects in the pre- and postfire transient phase. The natural convection during the fire is modeled with a convection coefficient of 0.01222 $\Delta T^{(1/3)}$ Btu/hr in^2°F [12]. After the fire, the convection coefficient as described in Section 3.2.3 is used. The natural convection and thermal radiation boundary conditions are applied to all external cask surfaces not covered by the impact limiters. The solar insolance boundary condition is applied to the external surface of the neutron shield shell. During all phases of the analyses, the areas of the cask covered by the impact limiters are modeled as adiabatic surfaces.

3.5.1.2 Test Model

The thermal analyses presented in Section 3.5.3 demonstrate that the Universal Transport Cask is capable of meeting the design basis temperature requirements under hypothetical accident conditions. The methodology used in this analysis is conservative, consistent with those used in prior transport cask licensing, and sufficient to show that the cask meets the criteria set forth in Section 3.5. Therefore, no thermal test model is created.

3.5.2 Package Conditions and Environment

As demonstrated in Chapter 2.0, the Universal Transport Cask body sustains no major damage as a result of the free-drop and puncture events as demonstrated in Chapter 2.0. Therefore, the cask body is modeled in an undamaged configuration.

The emissivity of stainless steel is 0.36. However, during the 30-min fire portion of the transient analysis, the emissivity is assumed to be 0.9. Also, the emissivity of the fire is assumed to be 1.0.

At the end of the fire, the NS-4-FR in the neutron shield is assumed to be destroyed. The result is a lower conductivity and thus a greater resistance to heat leaving the cask. The emissivity of stainless steel is again assumed to be 0.36, also providing a greater resistance to heat leaving the cask. The cooldown is analyzed for a period of 18 hr after the end of the fire. At the end of the cooldown period, all cask components have already reached their maximum temperatures and have begun to cool down to their postfire, steady state temperatures.

3.5.3 Package Temperatures

The ANSYS computer code is used to evaluate the Universal Transport Cask for the hypothetical accident fire. A steady-state initial temperature profile is calculated on the basis of a 100°F ambient temperature and solar insolance and used as input for the 30-min fire transient, which considers exposure of the cask to a 1,475°F radiant environment. This exposure is followed by an 18-hr cooldown period, which considers exposure of the cask to a 100°F ambient temperature and solar insolance.

The safe operating temperature ranges of the components specified in Section 3.3.2 are also evaluated for the fire accident. These components include the seals and lead gamma shielding. The radial neutron shield temperature is not considered to be significant; therefore its loss is assumed in this accident. The shielding consequences of loss of the radial neutron shield are provided in Section 5.4.2.3.

The maximum component temperatures during the hypothetical fire accident and cooldown period are provided in Tables 3.5-1 (PWR) and 3.5-2 (BWR). The tables also show the maximum component temperatures for the fuel cladding, and the lead in the cask body. None of the safety-related components, with the exception of the radial neutron shield as noted previously, exceeds its safe operating temperature as a result of the fire accident. The temperature histories of the major cask components are shown in Figures 3.5-4 through 3.5-11 for PWR and Figures 3.5-12 through 3.5-19 for BWR.

3.5.4 Maximum Internal Pressures

The analysis requires the calculation of the free volume of the canister, calculation of the releasable quantity of fill and fission gas in the fuel assemblies, BPRA gases, and the subsequent calculation of the pressure in the canister and cask if these gases are added to the backfill helium pressure (initially at 1 atm) already present in the canister and cask (Sections 3.4.1.1 and 3.4.1.2). Canister and cask pressures are determined for a combined accident scenario of 100% fuel failure and the accident temperature maximum. The method employed in both of the accident analyses is identical to that employed in the normal condition evaluation of Section 3.4.1.

For the maximum temperature accident condition, the gas quantities are combined with the accident average gas temperatures of 588°F (PWR) and 515°F (BWR) to produce the desired system pressures. Maximum canister pressures under the 100% fuel rod failure and fire accident conditions are 74.3 psig (PWR) and 43.8 psig (BWR). The maximum transport cask pressures are 69.3 psig and 42.8 psig for PWR and BWR fuel, respectively, where the cask pressure assumes the loss of canister containment.

The maximum internal pressures for the hypothetical accident condition are summarized in Table 3.5-3.

3.5.5 Maximum Thermal Stresses

The maximum thermal stresses in the cask and the cask contents resulting from the hypothetical accident fire are not calculated. Thermal stresses are secondary stresses. Evaluation of secondary stresses is not required by the ASME code for accident conditions.

3.5.6 Evaluation of Package Performance for Hypothetical Accident Conditions

The Universal Transport Cask thermal performance has been assessed for the hypothetical accident fire transient, as specified in 10 CFR 71. Except for the radial neutron shield, which is assumed to be lost, all cask components important to safety remain within their safe operating ranges. The ability of the cask to safely contain its radioactive contents is not compromised.

Figure 3.5-1 Two-Dimensional Axis-Symmetric Finite Element Cask Model (PWR and BWR)

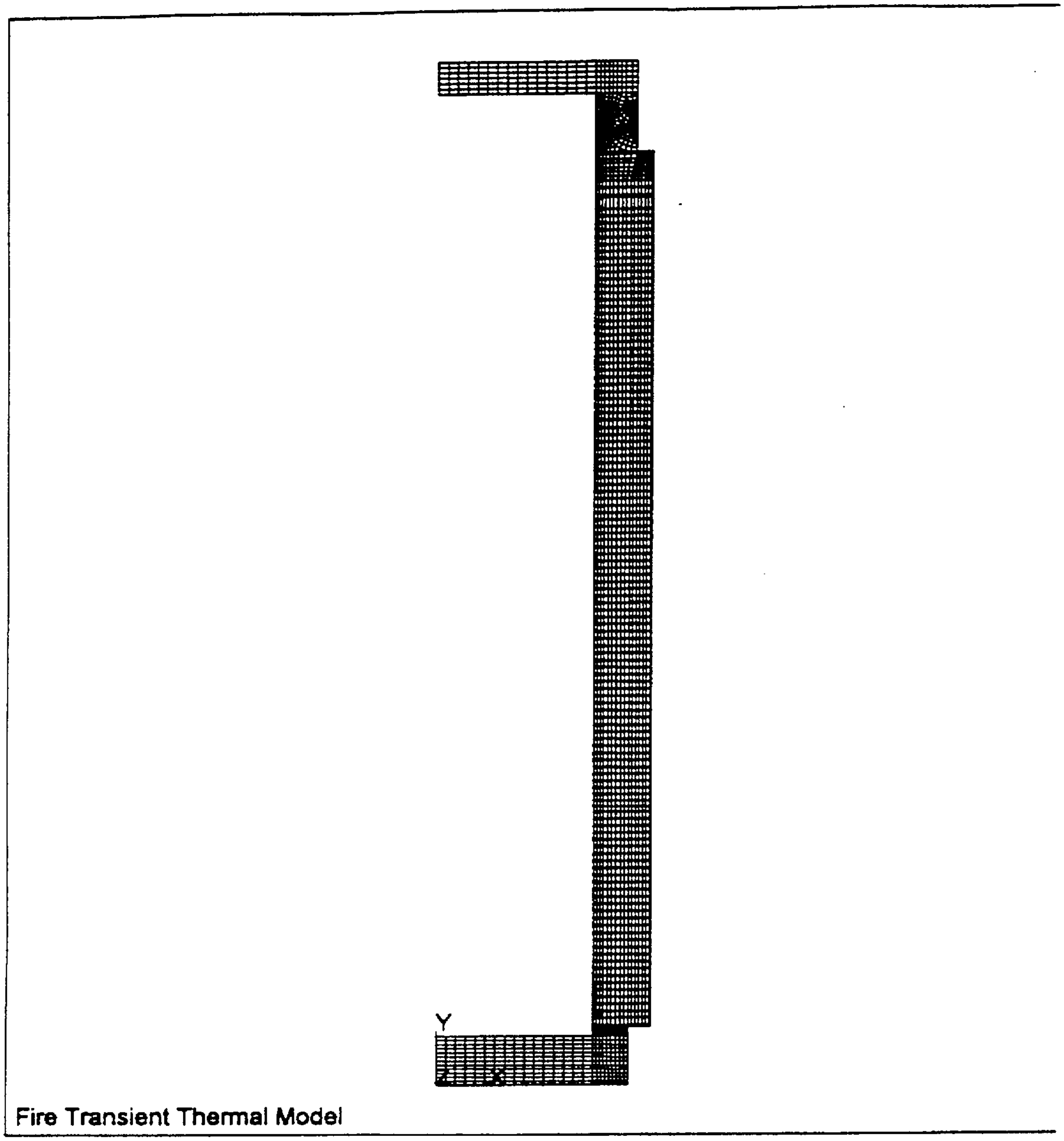

Figure 3.5-2 Upper Region of Two-Dimensional Axis-Symmetric Cask Finite Element Model (PWR and BWR)

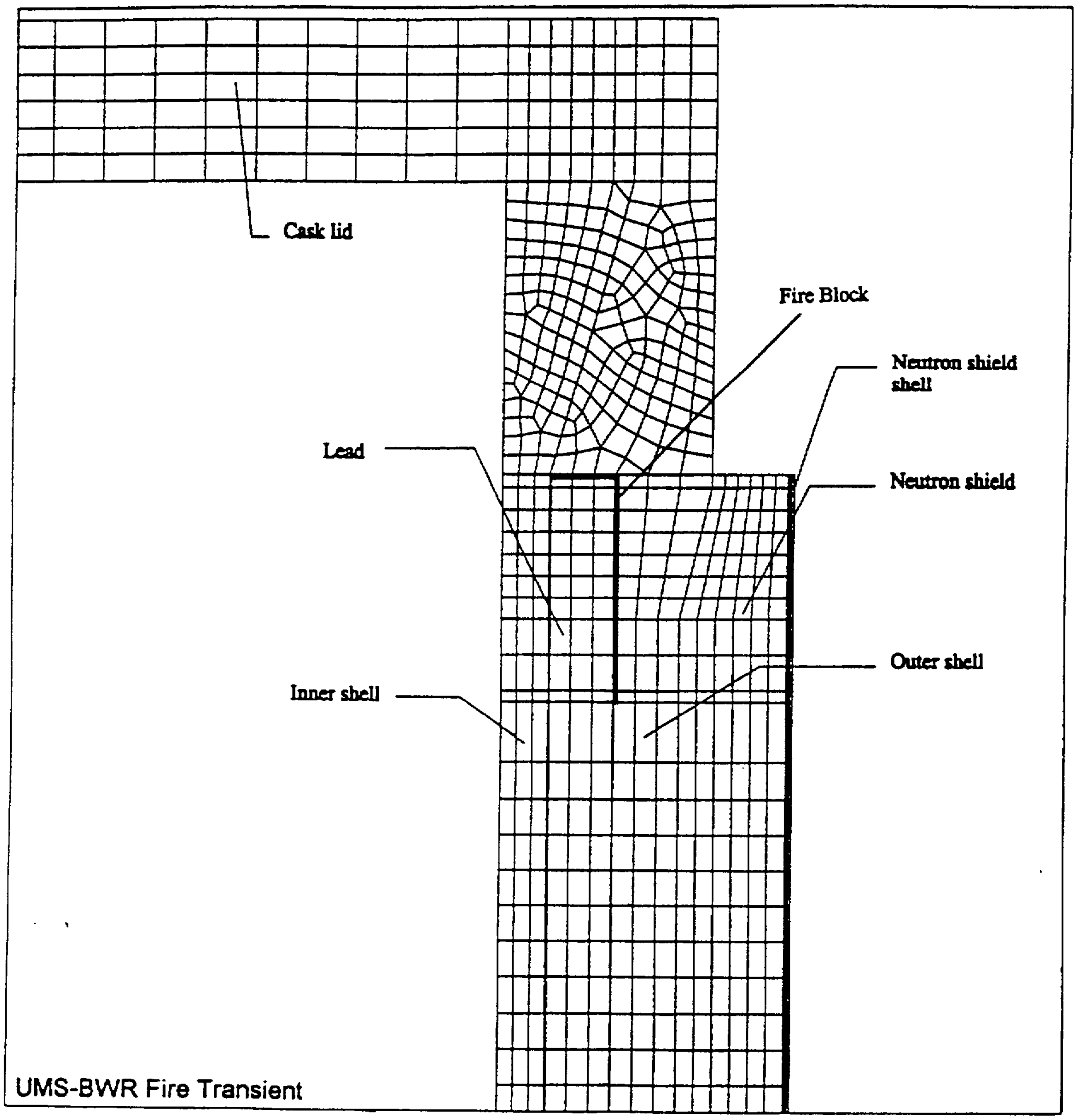

Figure 3.5-3 Lower Region of Two-Dimensional Axis-Symmetric Cask Finite Element Model (PWR and BWR)

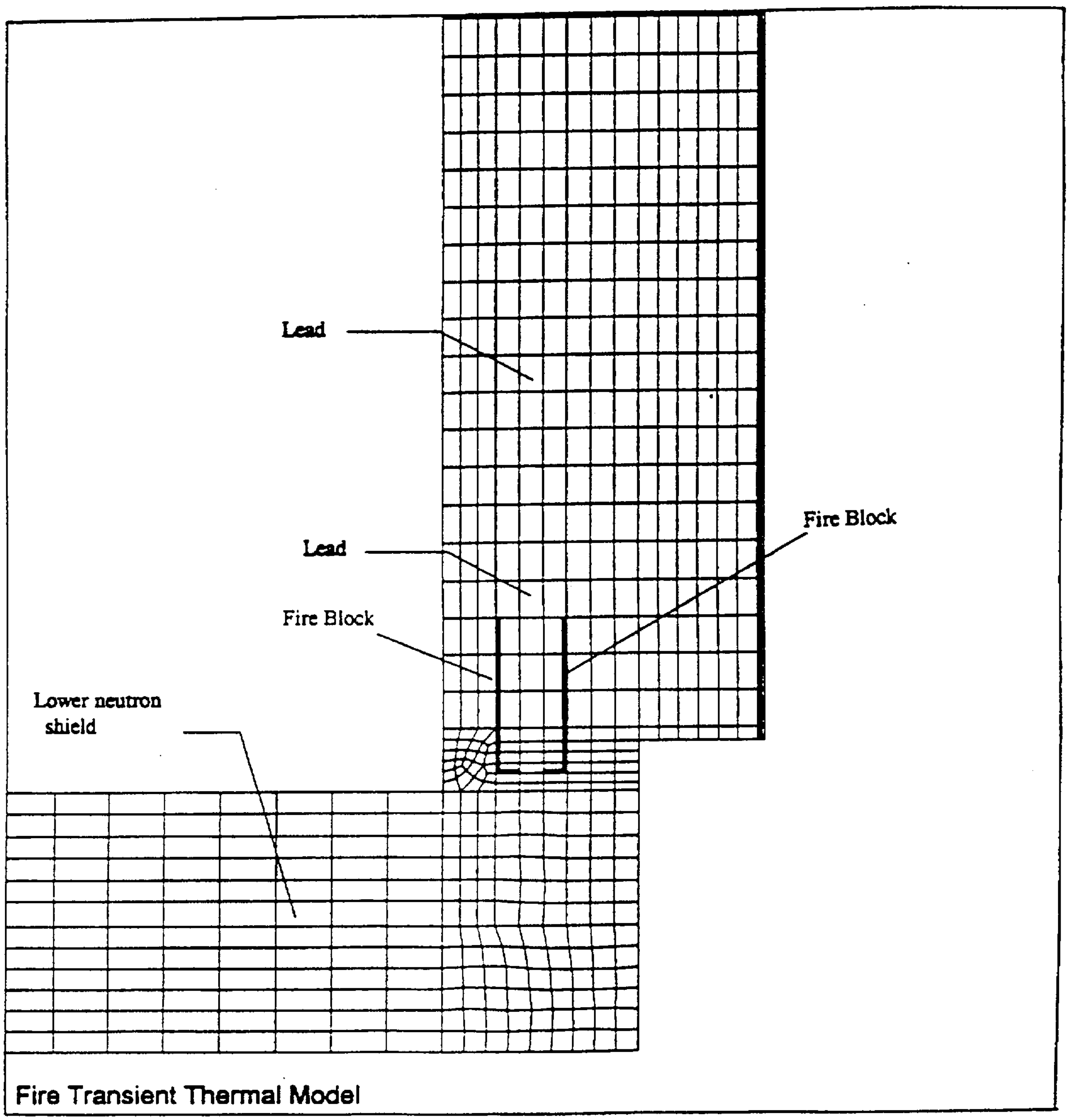

Figure 3.5-4 Hypothetical Accident Conditions Maximum Lead Temperature History (PWR)

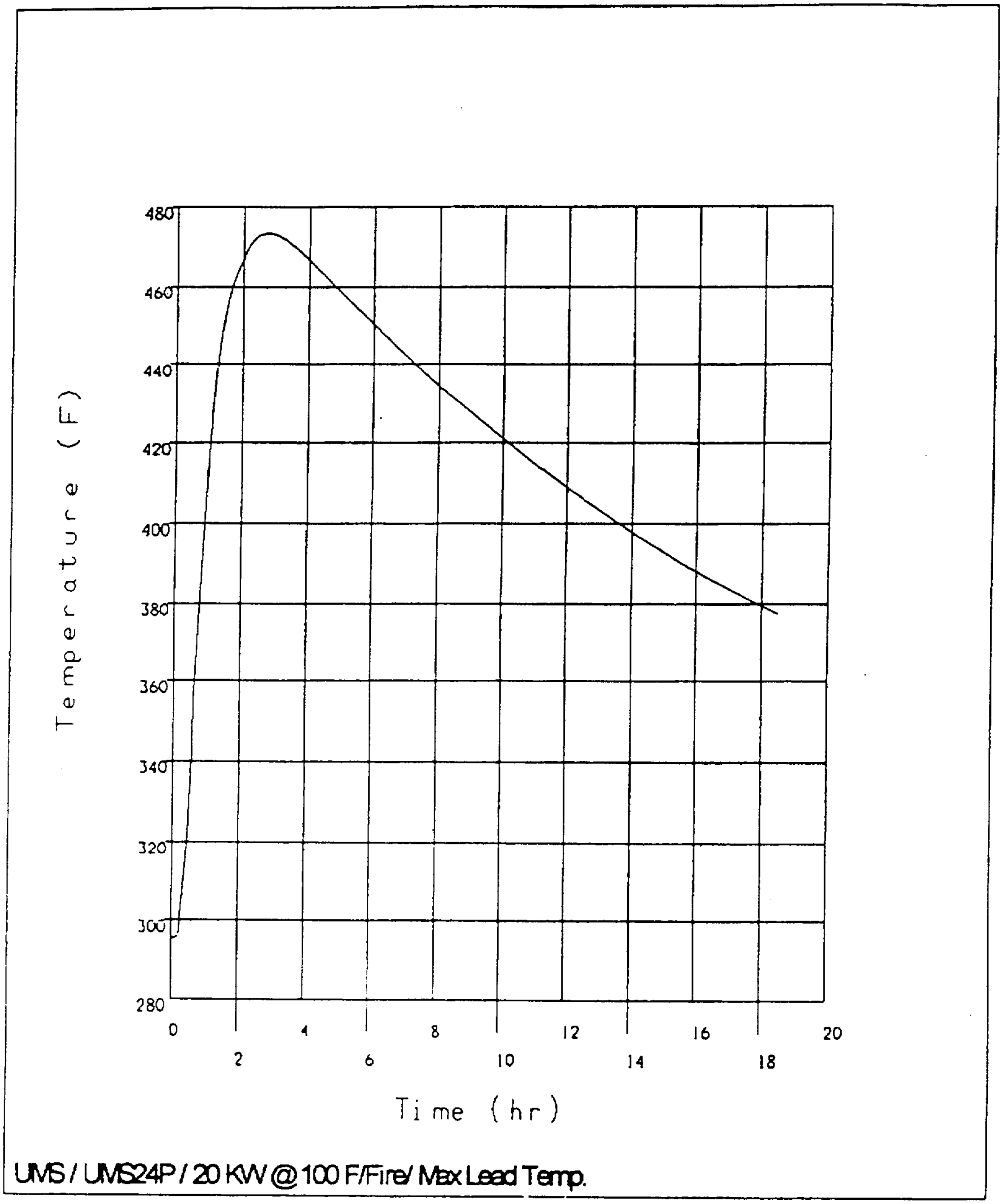

Figure 3.5-5 Hypothetical Accident Conditions Maximum Neutron Shield Exterior Temperature History (PWR)

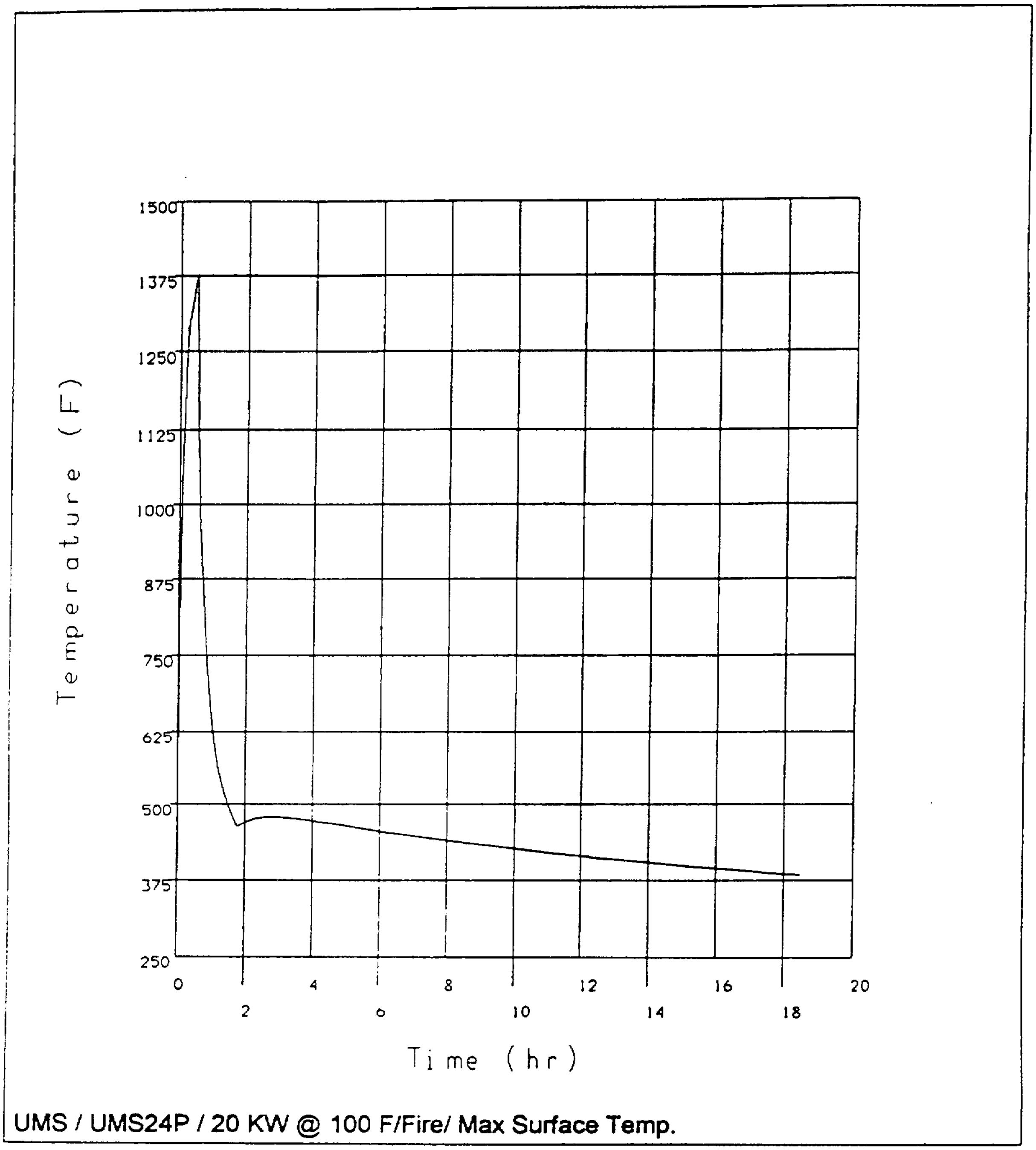

Figure 3.5-6 Hypothetical Accident Conditions Maximum Cask Inner Shell Temperature History (PWR)

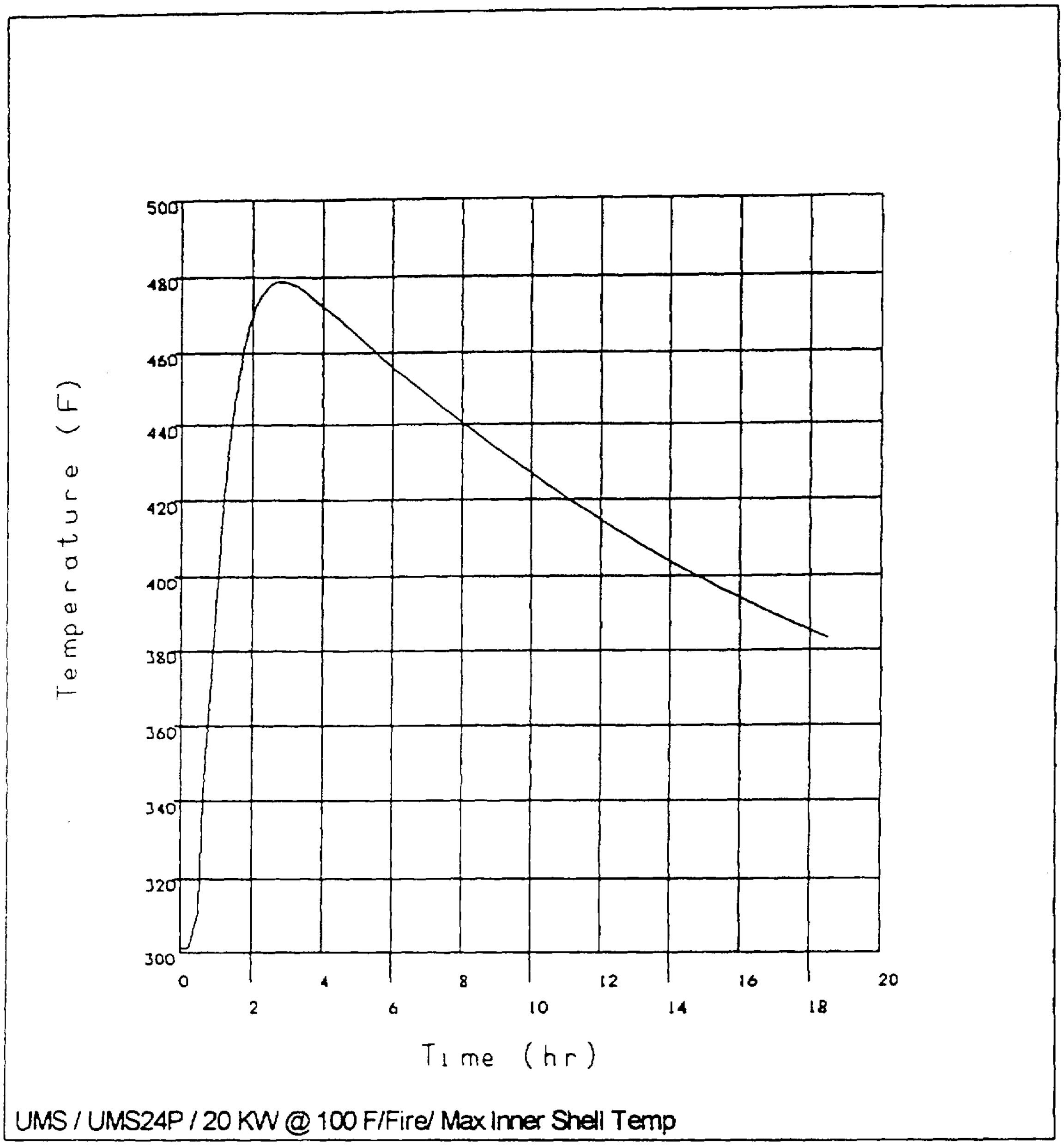

Figure 3.5-7 Hypothetical Accident Conditions Maximum Cask Outer Shell Temperature History (PWR)

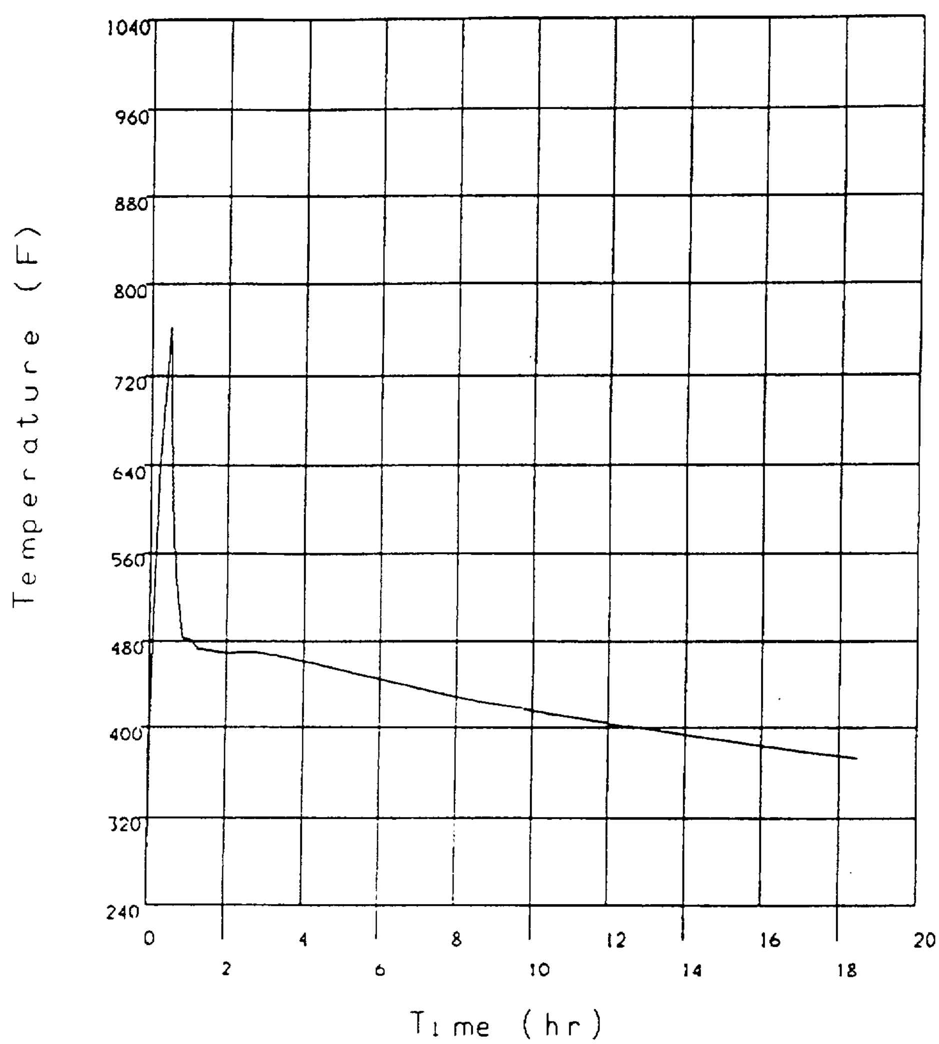

UMS / UMS24P / 20 KW @ 100 F/Fire/ Max Outer Shell Temp

Figure 3.5-8 Hypothetical Accident Conditions Maximum Lower Neutron Shield Temperature History (PWR)

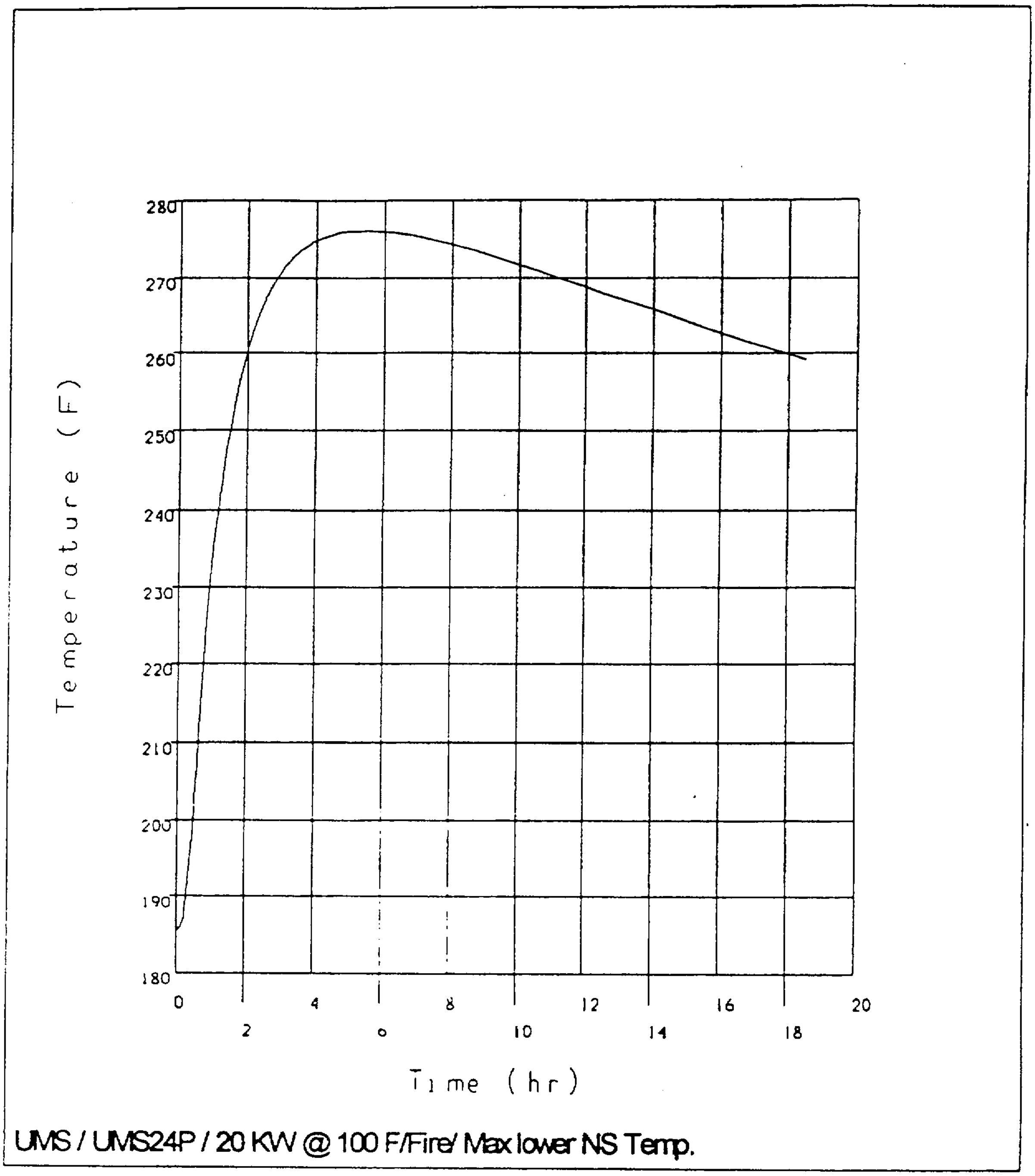

Figure 3.5-9 Hypothetical Accident Conditions Maximum Lower Drain Port O-Ring Temperature History (PWR)

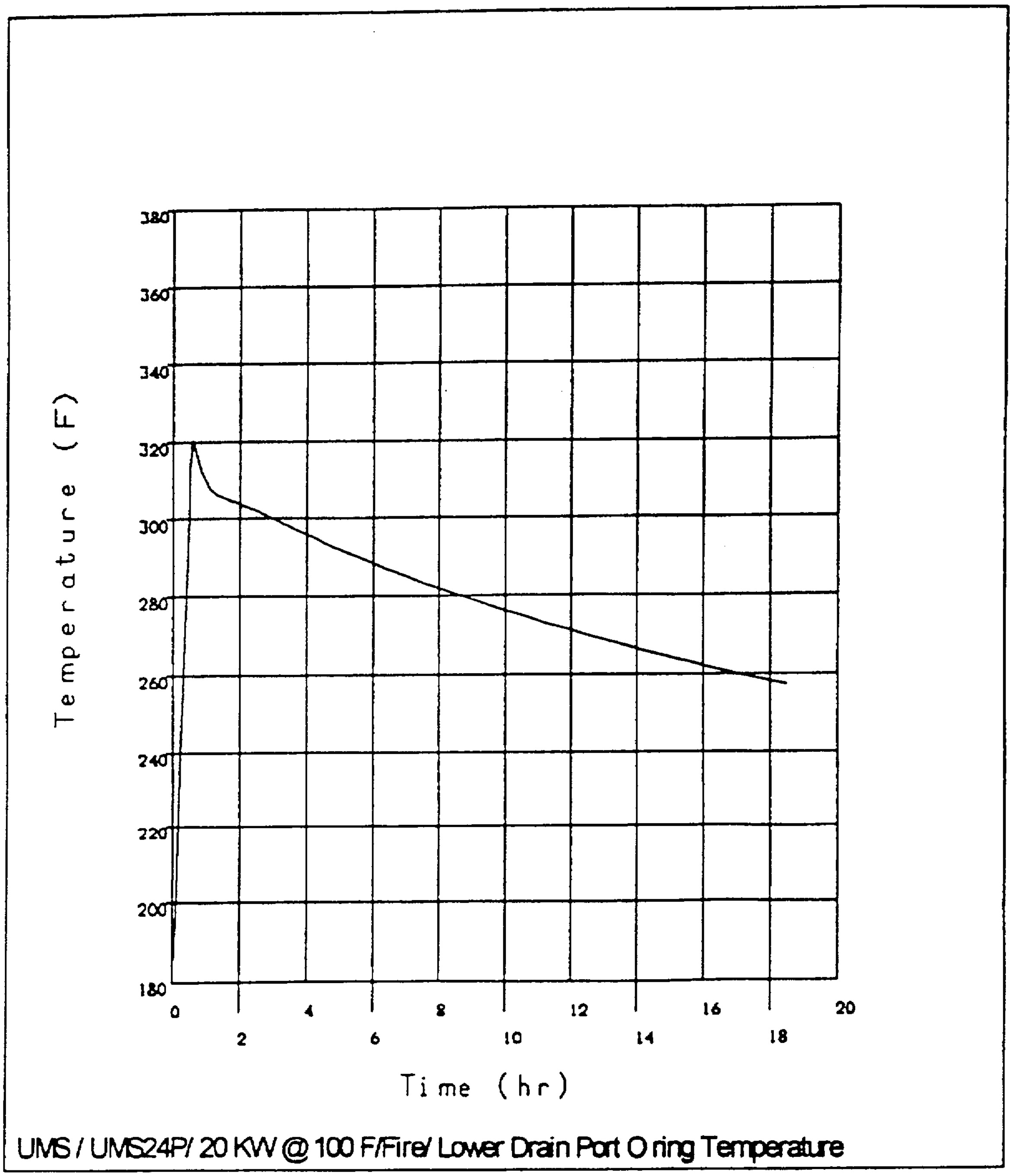

Figure 3.5-10 Hypothetical Accident Conditions Maximum Cask Lid Vent Port O-Ring Temperature History (PWR)

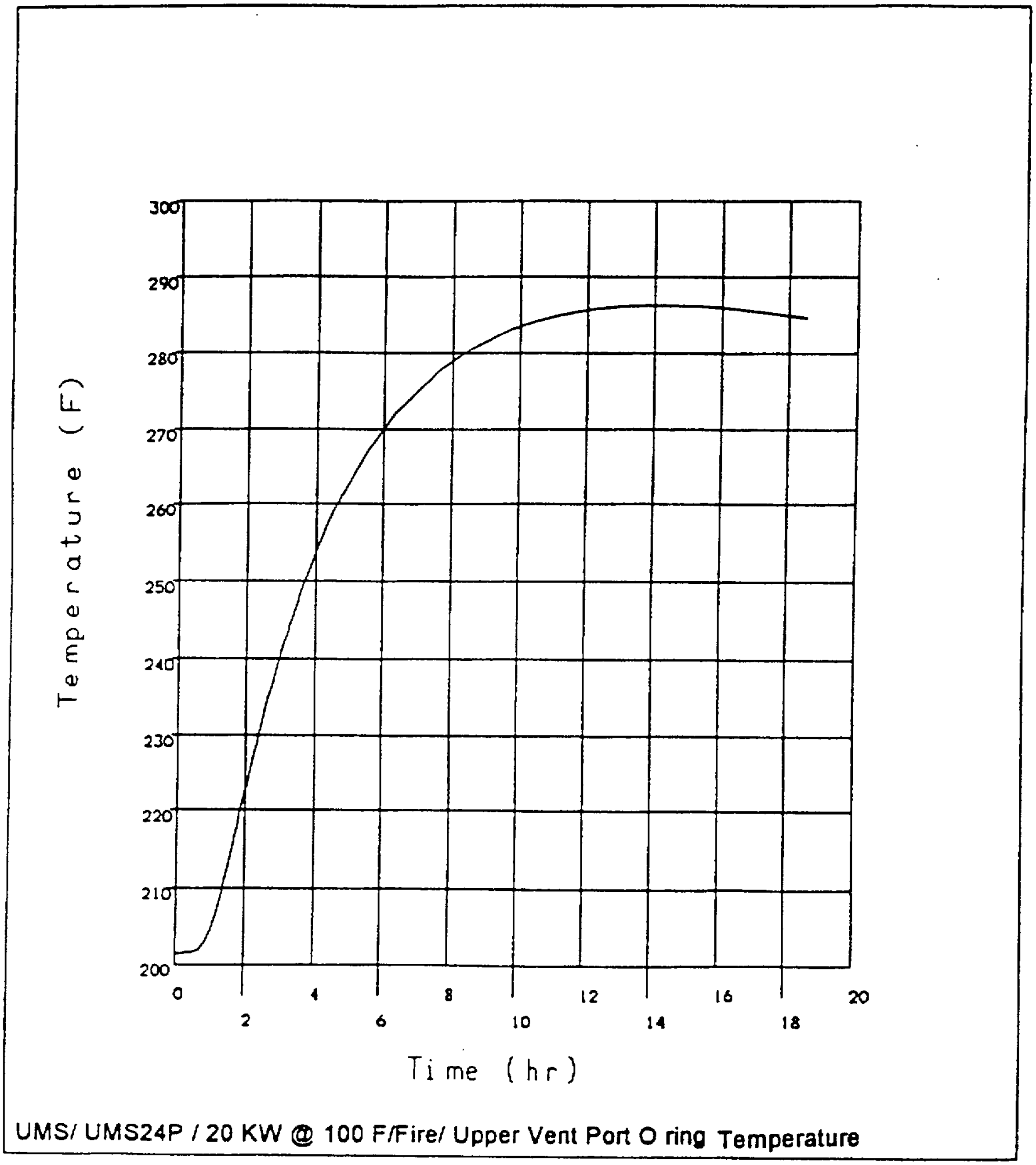

Figure 3.5-11 Hypothetical Accident Conditions Maximum Cask Lid O-Rings Temperature History (PWR)

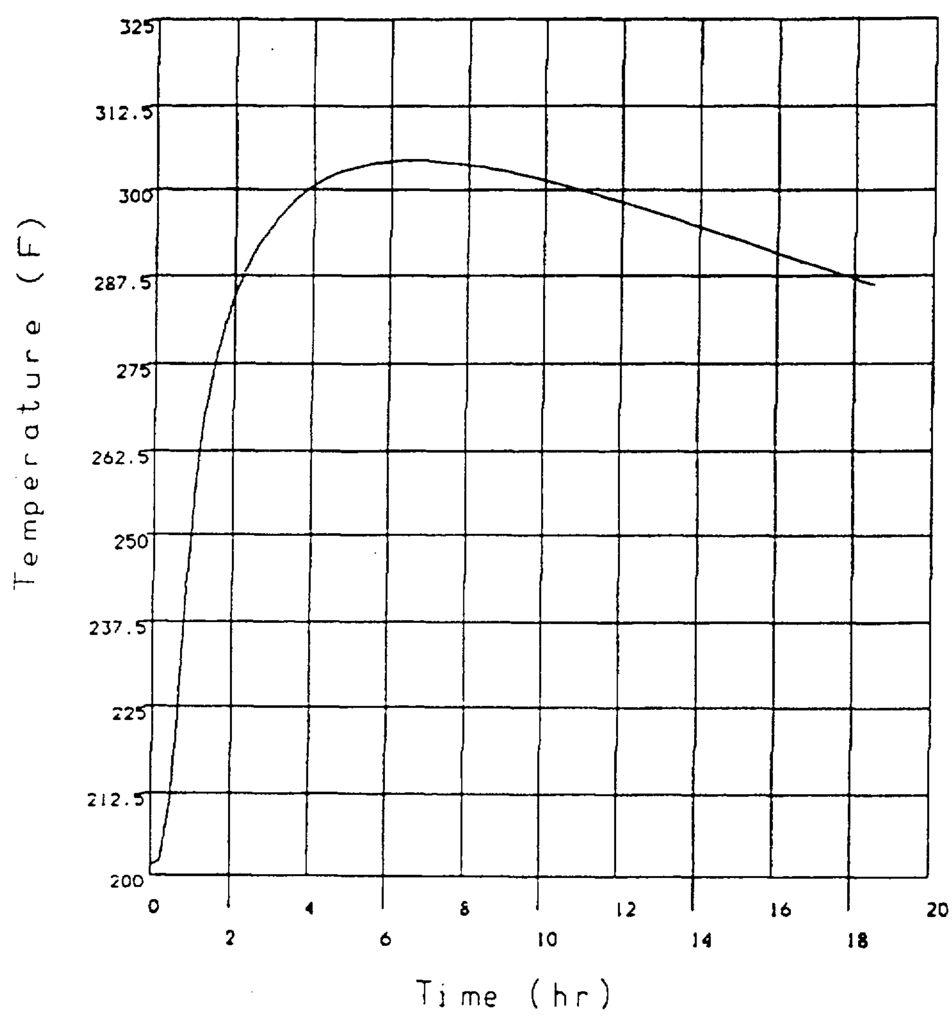

UMS / UMS24P / 20 KW @ 100 F/Fire/ Cask Lid O ring Temp

Figure 3.5-12 Hypothetical Accident Conditions Maximum Lead Temperature History (BWR)

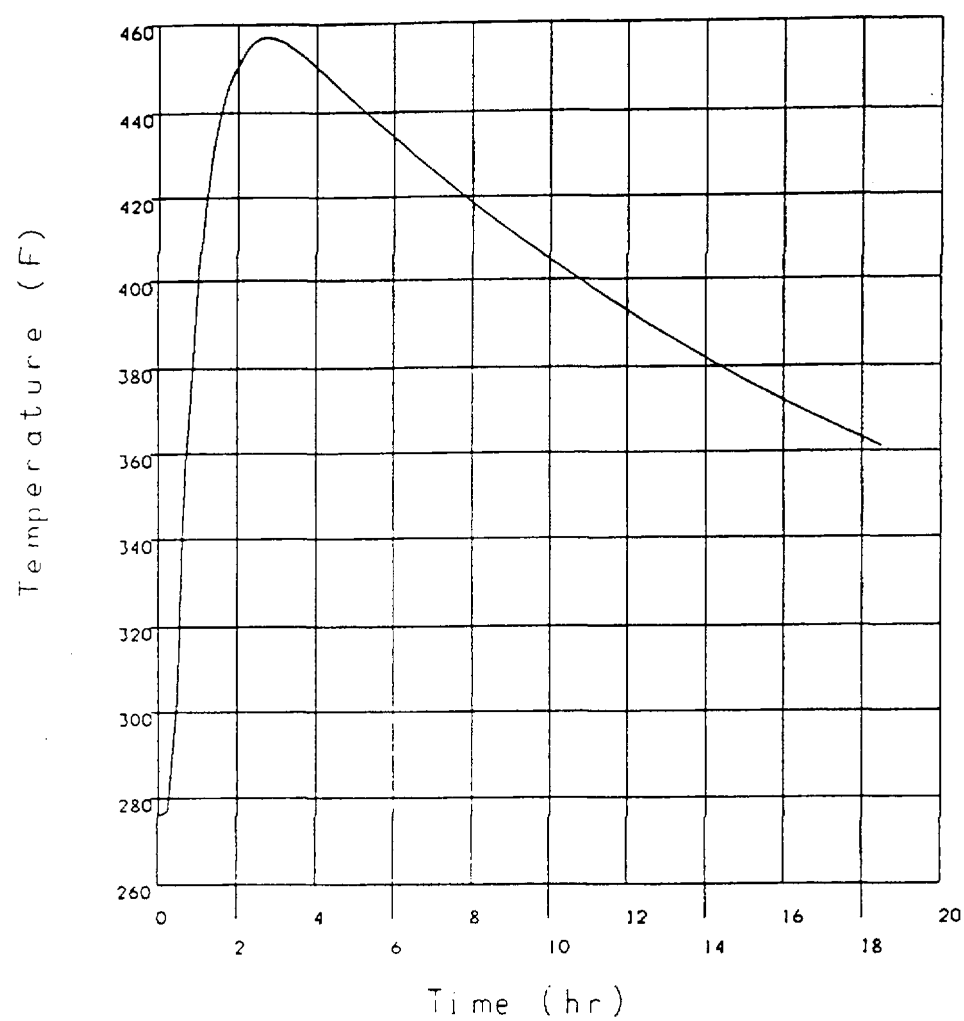

UMS / BWR / 16 KW @ 100 F/Fire/ Max Lead Temp.

Figure 3.5-13 Hypothetical Accident Conditions Maximum Neutron Shield Exterior Temperature History (BWR)

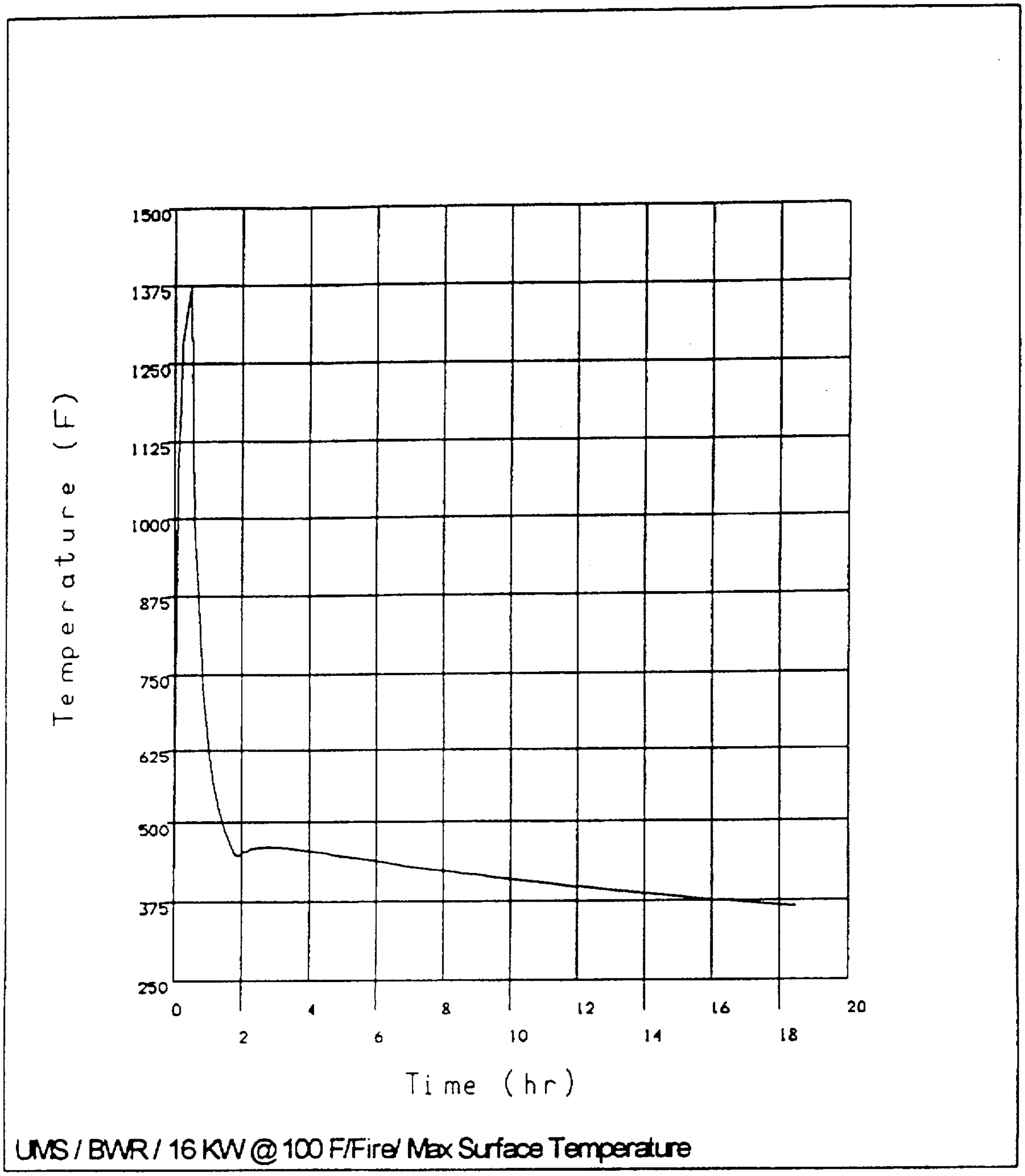

Figure 3.5-14 Hypothetical Accident Conditions Maximum Cask Inner Shell Temperature History (BWR)

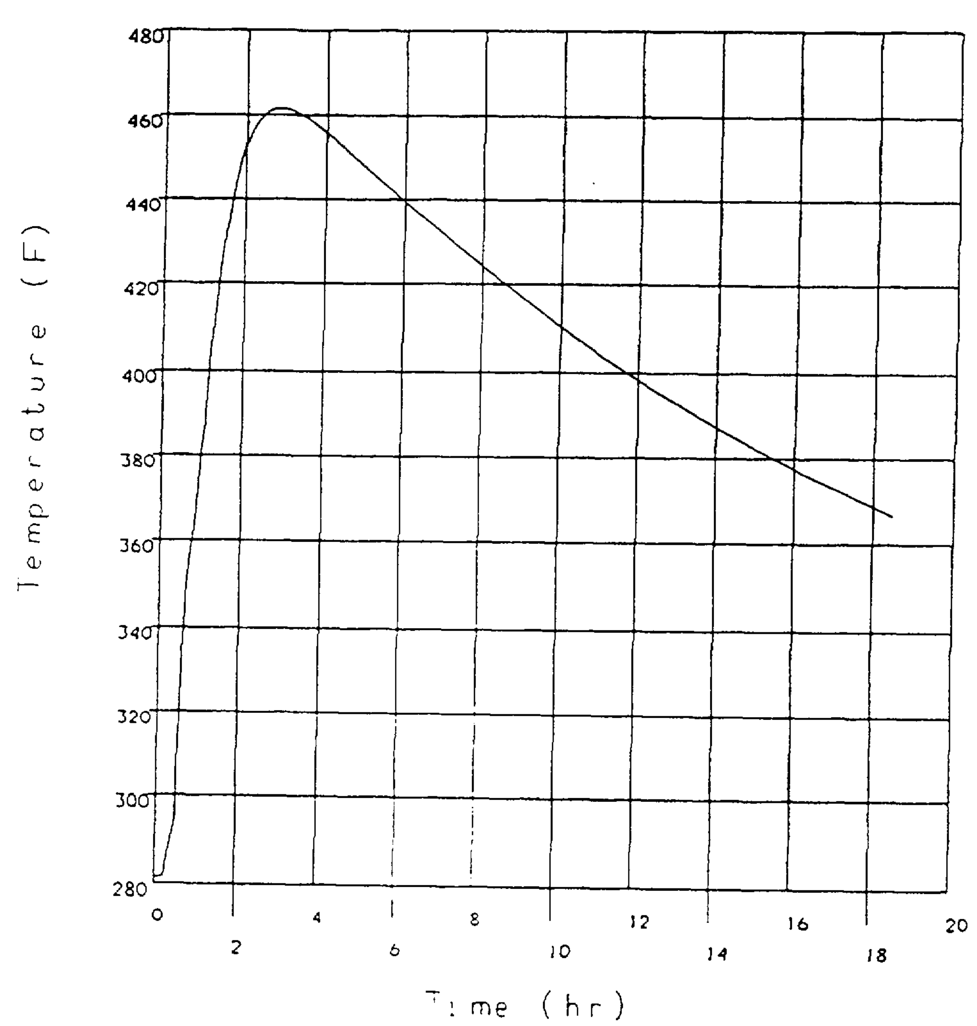

UMS / BWR/ 16 KW @ 100 F/Fire/ Max Inner Shell Temperature

Figure 3.5-15 Hypothetical Accident Conditions Maximum Cask Outer Shell Temperature History (BWR)

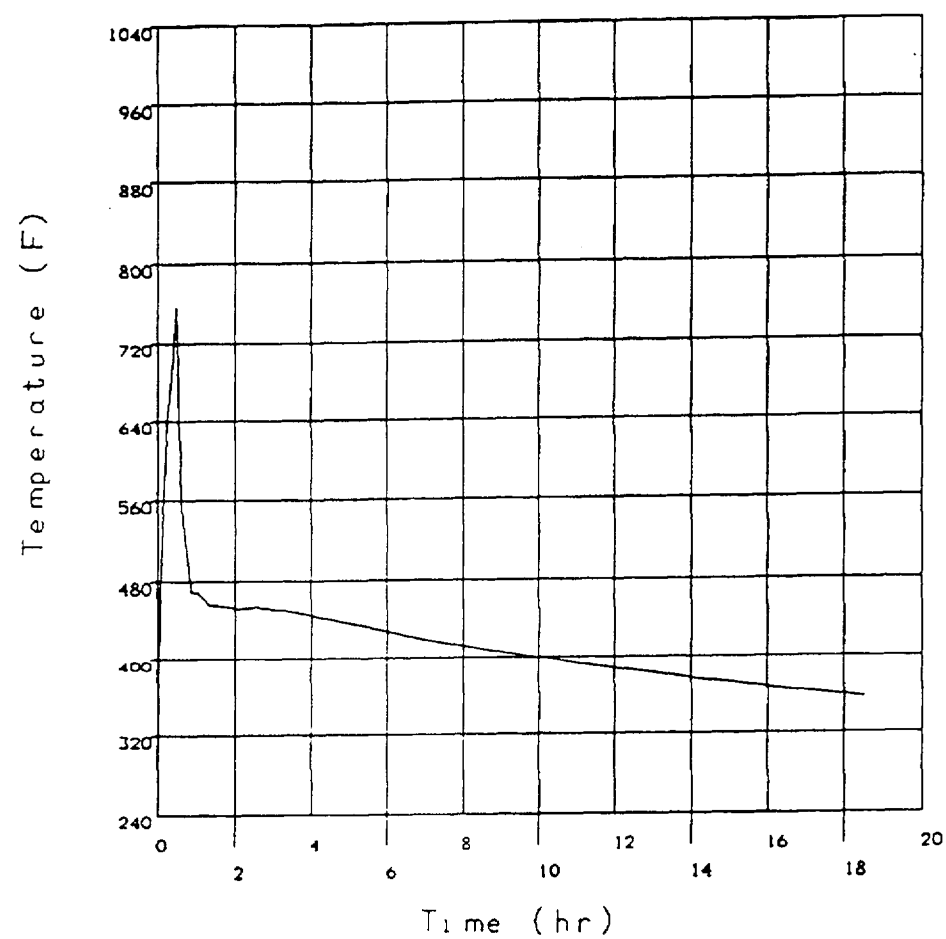

UMS / BWR/ 16 KW @ 100 F/Fire/ Max Outer Shell Temperature

Figure 3.5-16 Hypothetical Accident Conditions Maximum Lower Neutron Shield Temperature History (BWR)

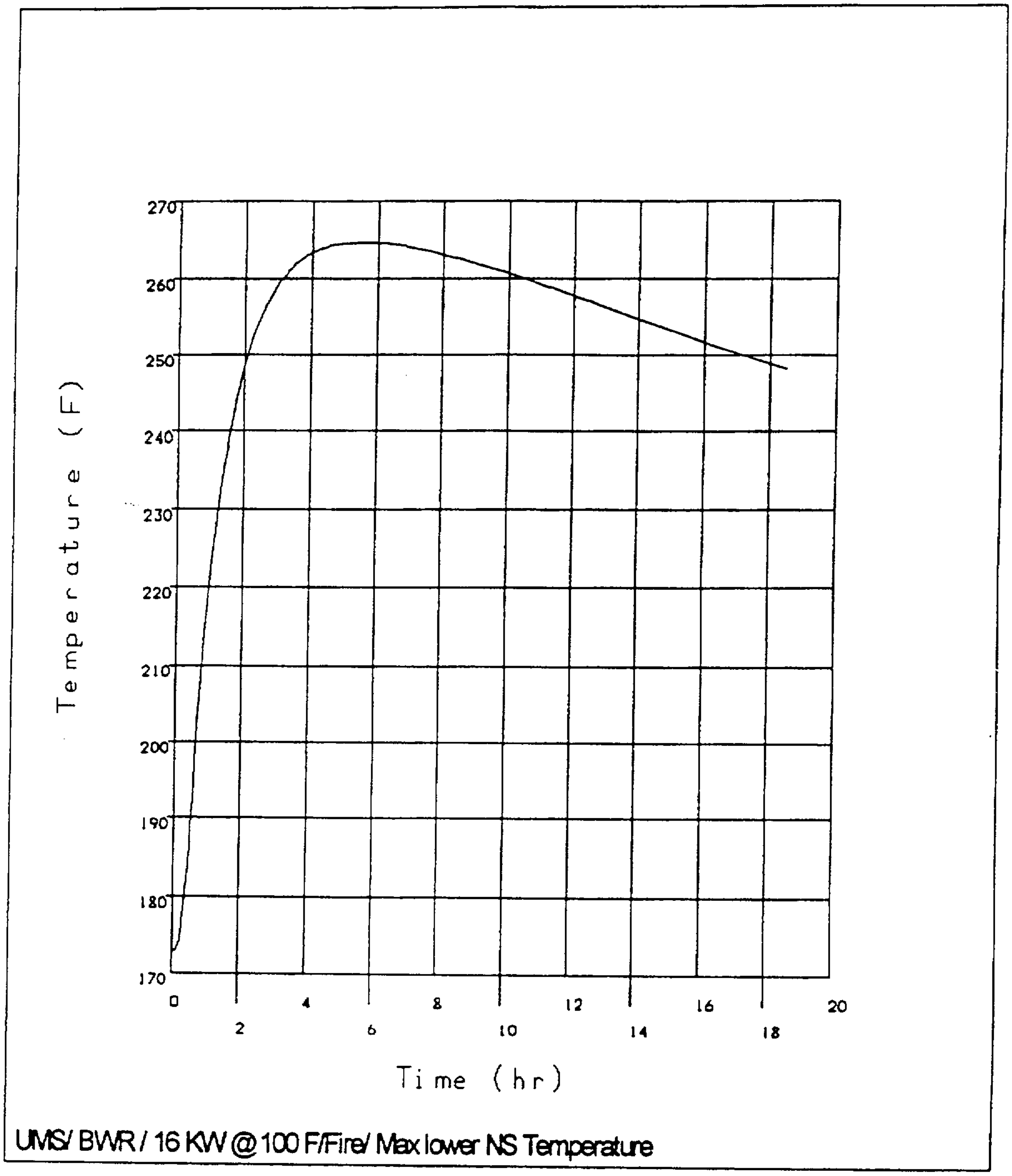

Figure 3.5-17 Hypothetical Accident Conditions Maximum Lower Drain Port O-Ring Temperature History (BWR)

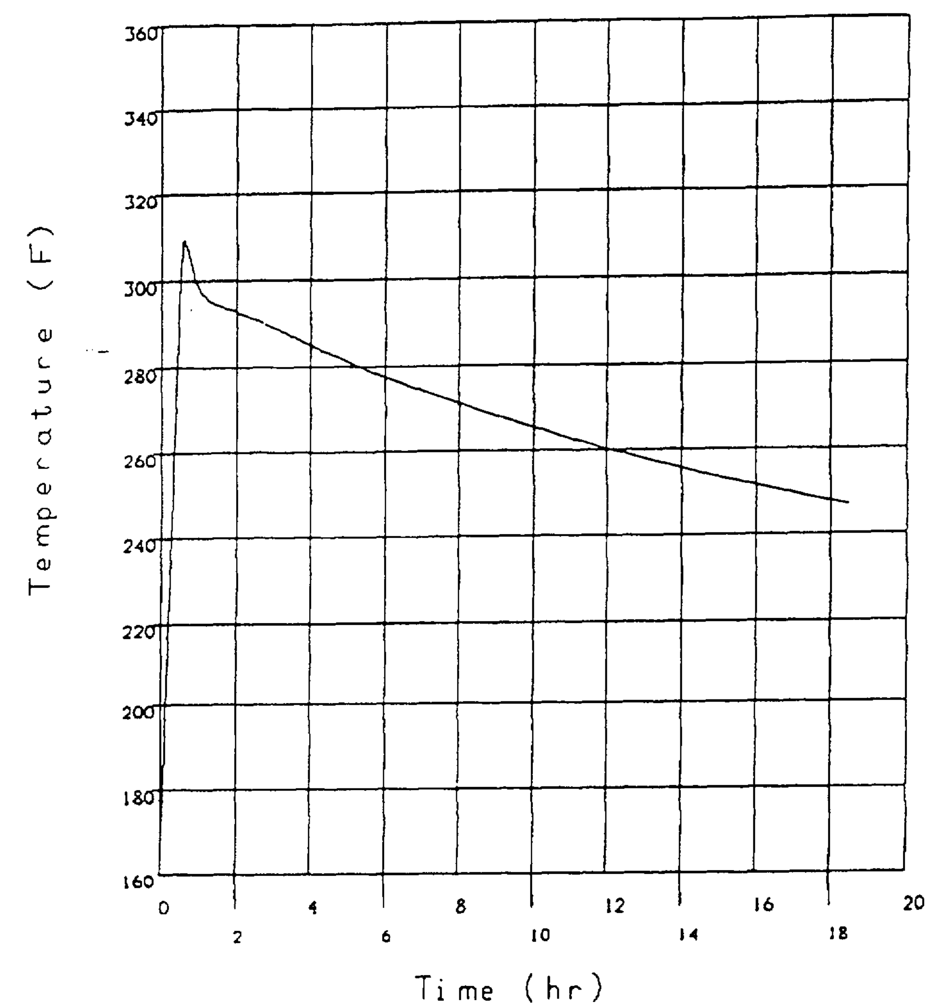

UMS / BWR / 16 KW @ 100 F/Fire/ Lower Drain Port O ring Temperature

Figure 3.5-18 Hypothetical Accident Conditions Maximum Cask Lid Vent Port O-Ring Temperature History (BWR)

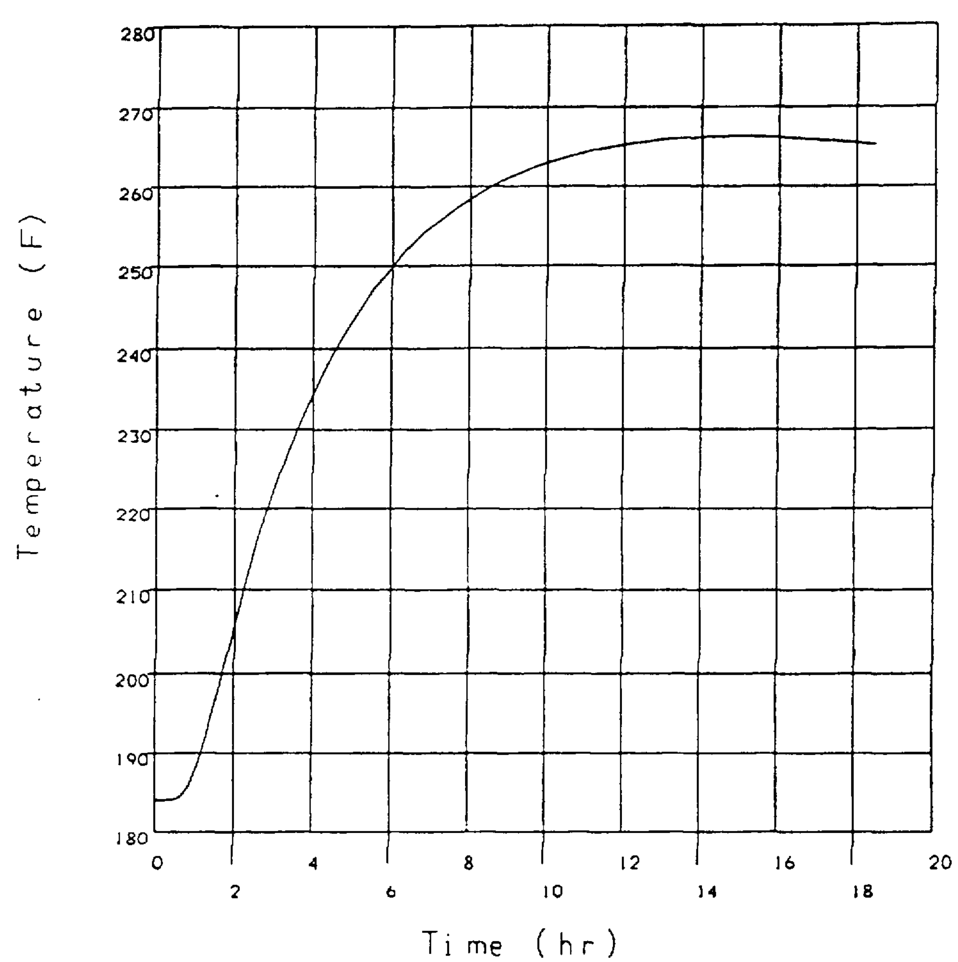

UMS/ BWR / 16 KW @ 100 F/Fire/ Upper Vent Port O ring Temperature

Figure 3.5-19 Hypothetical Accident Conditions Maximum Cask Lid O-Rings Temperature History (BWR)

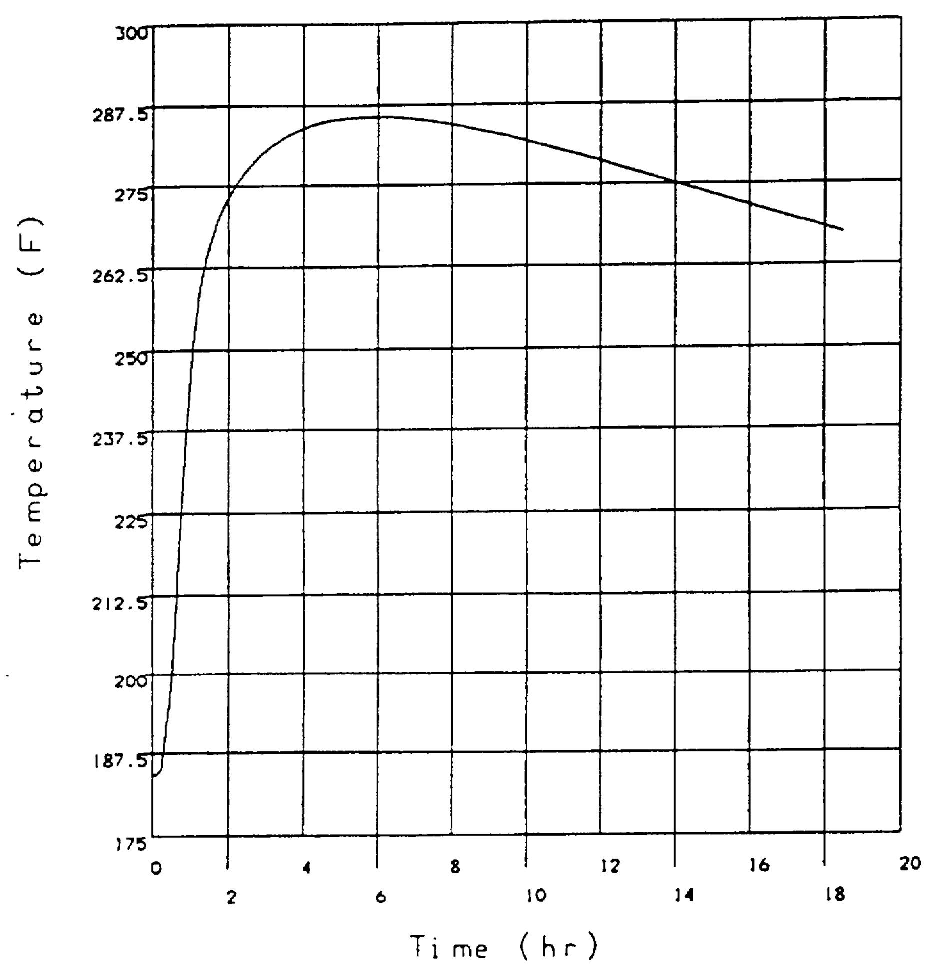

UMS/ BWR / 16 KW @ 100 F/Fire/ Cask Lid O ring Temperature

Table 3.5-1 Maximum Component Temperatures - Hypothetical Accident Condition Fire Transient (PWR Cask)

Component	Temperature (°F)	Time (Hours)	Temperature Limit (°F)
Cask Lid Bolt[1]	306	5.8	650
Cask Lid O-rings[2]	304	5.5	375[4]
Lower Drain Port O-ring[2]	320	0.8	375[4]
Cask Lid Vent Port O-ring[2]	286	13.0	375[4]
Cask Radial Outer Surface	1,376	0.5	—[5]
Lead Gamma Shield	473	2.9	600
Canister Gas[3]	588	—	—
Maximum Fuel Rod Cladding[3]	808	—	1,058
Cask Inner Shell	479	3.0	—[5]
Aluminum Heat Transfer Disks[3]	739	—	—[5]
Support Disks[3]	743	—	—[5]

Conditions: 30-min, 1475°F Fire
20 kW decay heat

1 Cask lid bolt not explicitly modeled—maximum temperature taken to be the maximum temperature of the cask lid.

2 O-rings not explicitly modeled - maximum temperature taken at the O-ring region in the component of interest.

3 Estimated by adding the maximum temperature gradient between the cask inner shell and component of interest from normal conditions results to the peak temperature of the cask inner shell during the hypothetical accident analysis.

4 Accident temperature limit is 375°F for 10-hr or less durations.

5 These components remain well below their respective material melting temperatures during the hypothetical accident condition fire; therefore, the intended performance of these components is not adversely affected by the hypothetical accident condition fire.

Table 3.5-2 Maximum Component Temperatures - Hypothetical Accident Condition Fire Transient (BWR Cask)

Component	Temperature (°F)	Time (Hours)	Temperature Limit (°F)
Cask Lid Bolt[1]	287	5.8	—
Cask Lid O-rings[4]	286	5.0	375[3]
Lower Drain Port O-ring[4]	309	0.8	375[3]
Cask Lid Vent Port O-ring[4]	266	13.0	375[3]
Cask Radial Outer Surface	1,376	0.5	—[5]
Lead Gamma Shield	457	2.9	600
Canister Gas[2]	515	—	—
Maximum Fuel Rod Cladding[2]	697	—	1,058
Cask Inner Shell	462	3.0	—[5]
Aluminum Heat Transfer Disks[2]	665	—	—[5]
Support Disks[2]	666	—	—[5]

Conditions: 30-min, 1475°F Fire
16 kW decay heat

1 Cask lid bolt not explicitly modeled—maximum temperature taken to be the maximum temperature of the cask lid.

2 Estimated by adding the maximum temperature gradient between the cask inner shell and component of interest from normal conditions results to the peak temperature of the cask inner shell during the hypothetical accident analysis.

3 Accident temperature limit is 375°F for 10-hr or less durations.

4 O-rings are not explicitly modeled - maximum temperature taken at the O-ring region in the component of interest.

5 These components remain well below their respective material melting temperatures during the hypothetical accident condition fire; therefore, the intended performance of these components is not adversely affected by the hypothetical accident condition fire.

Table 3.5-3 Maximum Internal Pressures for Hypothetical Accident Conditions

Fuel	Cavity	Condition	Pressure[1] (psig)
PWR	Canister	100% fuel rod failure	74.3
	Cask[2]	100% fuel rod failure	69.3
BWR	Canister	100% fuel rod failure	43.8
	Cask[2]	100% fuel rod failure	42.8

1. The pressure calculation considers the fire accident condition maximum cavity temperature.
2. The cask cavity pressure assumes failure of the canister confinement boundary.

8. Damaged Fuel Assemblies

Damaged fuel assemblies are standard fuel assemblies with fuel rods that have known or suspected cladding defects greater than hairline cracks or pinhole leaks. Each damaged fuel assembly will be placed in a Maine Yankee fuel can. The primary function of the fuel can is to confine fuel material within the can and to facilitate handling and retrievability. The Maine Yankee fuel can is shown in Drawings 412-501 and 412-502. The placement of the loaded fuel cans is restricted by operating procedures and/or Technical Specifications to loading into the four fuel tube positions at the periphery of the fuel basket as shown in Figure 3.6.1.1-4. The heat load for each damaged fuel assembly is limited to the design basis heat load of 0.833 kW (20 kW/24).

A steady-state thermal analysis is performed using the three-dimensional cask model described in Section 3.4.1.1.1 simulating 100% failure of the damaged fuel rods held in the Maine Yankee fuel can. The canister is assumed to contain twenty (20) design basis PWR fuel assemblies and damaged fuel assemblies in fuel cans in each of the four corner positions.

A debris compaction length of 104 inches is considered in the analysis based on the volume of fuel rods and a 50% compaction of the debris. Additionally, this 104-inch debris region is assumed to be located at the center of the active fuel region of the design basis PWR fuel assemblies, as shown in Figure 3.6.1.1-4. The entire heat load for a single fuel assembly (i.e., 0.833 kW) is considered to be concentrated in the debris region. The effective thermal conductivities for the design basis PWR fuel assembly (Section 3.4.1.1.2) are used for the debris region. This is conservative, since the debris (100% failed rods) is expected to have a higher density (better conduction) and more surface area (better radiation) than an intact fuel assembly. In addition, the thermal conductivity of helium is used for the remainder of the active fuel length. Boundary conditions corresponding to normal transport are used at the outer surface of the cask (see Section 3.4.1.1.1). The results of the steady-state thermal analysis for 100% fuel rod, fuel cladding and guide tube failure are:

Description	Maximum Temperature (°F)			
	Fuel Cladding	Damaged Fuel	Support Disk	Heat Transfer Disk
Configuration with damaged fuel loaded in four basket corner locations	682	633	618	614
Design basis PWR fuel	673	N/A	608	605
Allowable	716	N/A	650	700

As shown in the previous table, the maximum temperatures for the fuel cladding, damaged fuel assembly, support disks, and heat transfer disks for the configuration with damaged fuel loaded in four (4) basket corner locations are within the allowable temperature range. Additionally, the maximum temperature of the support disk remains bounded by that used in the structural analyses of the fuel basket (Table 3.4-1, Canister Gas: Air).

Damaged high burnup fuel must be loaded into damaged fuel cans. These fuel assemblies have more than 1% of rods with oxide layers greater than 80 microns or more than 3% of rods with oxide layers greater than 70 microns and burnup greater than 45,000 MWD/MTU. The cask pressure for this condition is used as input to the containment analysis. Consistent with the containment analysis, a basket release fraction of 20% is applied. This release fraction accounts for up to 12 high burnup assemblies, including up to four classified as damaged. Applying this release fraction to the pressure evaluation in Section 3.4.4.1 yields a normal conditions cask pressure of 15.61 psig, calculated using B&W 17x17 Mark C fuel assembly parameters.

3.7 References

1. Title 10 of the Code of Federal Regulations, Part 71 (10 CFR 71), "Packaging and Transportation of Radioactive Materials," April 1996.

2. IAEA Safety Series No. 6, "Regulations for the Safe Transport of Radioactive Materials," 1985 Edition, as amended 1990.

3. Johnson, A.B., and Gilbert, E.R., "Technical Basis for Storage of Zircaloy-Clad Fuel in Inert Gases," PNL-4835, 1985.

4. ARMCO Product Data Bulletin No. S-22, "17-4PH, Precipitation Hardening Stainless Steel," ARMCO, Inc., 1988

5. ANSYS Revision 5.5, Computer Program, ANSYS, Inc., Houston, PA.

6. NS-4-FR Fire Resistant Neutron and/or Gamma Shielding Material - Product Technical Data, Genden Engineering Services & Construction Company, Tokyo, Japan.

7. MIL-HDBK-5F, "Metallic Materials and Elements for Aerospace Vehicle Structures," U.S. Department of Defense, November 1990.

8.

9. Kreith, F., and Bohn, M.S., Principles of Heat Transfer, 5th Edition, West Publishing Company, 1993.

10. SAND90-2406, Sanders, T.L., et al., "A Method for Determining the Spent-Fuel Contribution to Transport Cask Containment Requirements," TTC-1019, UC-820, November 1992.

11. Olander, D.R., "Fundamental Aspects of Nuclear Reactors Fuel Elements," Technical Information Center (U.S. Department of Energy), 1985.

12. Proceedings of the 11th International Conference on the Packaging and Transportation of Radioactive Materials (PATRAM '95), Las Vegas, Nevada, December 3-8, 1995.

13. Kreith, F., Principles of Heat Transfer, 3rd Edition, New York, Intext Educational Publishers.

14. American Society of Mechanical Engineers, ASME Boiler and Pressure Vessel Code, SECTION II, PART D - PROPERTIES, 1995 Edition, New York, American Society of Mechanical Engineers, 1995.

15. Bucholz, J.A., Scoping Design Analyses for Optimized Shipping Casks Containing 1-, 2-, 3-, 5-, 7-, or 10-Year-Old Spent Fuel, Oak Ridge National Library, ORNL/CSD/TM - 149, 1983.

16. Baumeister T. and Mark, L.S., Standard Handbook for Mechanical Engineers, 9th Edition, New York, McGraw-Hill Book Co., 1987.

17. Chapman, A.J. Heat Transfer, 4th Edition, New York, MacMillan Publishing Company, 1987.

18. Edwards, TRUMP, A Computer Program for Transient and Steady State Temperature Distributions in Multimensional Systems, Lawrence Radiation Laboratory, Livermore, Rept, UCLR-14754, Rev. 1 (May 1, 1968).

19. AAR BORAL Sheet Manufacturers Data, Sheet Product Performance Report 624, Brooks & Perkins Advanced Structures Company©, 1983.

20. AAR Standard Specification Sheet for BORAL™ Composite Sheet, Brooks & Perkins Advances Structures Company, BRJREVO-940107.

21. UNIFRAX Product Specifications, Fiberfrax® Ceramic Fiber Paper, C-1423, Unifrax Corporation, Niagara Falls, NY, June 1996.

List of Figures

List of Tables

4.0 CONTAINMENT

This chapter presents the Universal Transport Cask containment evaluation. PWR and BWR fuel are evaluated separately.

The B&W 15 x 15 fuel assembly is the bounding PWR assembly because of its high fuel mass (maximum for PWR assemblies) and fission product inventory. It is therefore used for the PWR fuel allowable leak rate calculations. The maximum burnup of 50,000 MWD/MTU, at a minimum 1.9 wt % ^{235}U enrichment with a 5-year cool time, is conservatively used to generate the containment analysis source term. The transport cask PWR containment analysis assumes the cask holds 24 design basis PWR fuel assemblies. The PWR fuel leak rate analysis assumes the presence of control components. These components reduce the amount of cask free volume, thereby resulting in a bounding condition containment evaluation. The consolidated fuel evaluation is based on Combustion Engineering 14 x 14 fuel assembly fuel rods in a 17 x 17 array configuration. The B&W fuel assembly remains bounding for containment when the number of consolidated assemblies is assumed to be no more than four in each canister. This assumption is conservative, since only one consolidated fuel assembly may be loaded in any canister. Evaluations are performed for an assumed 3% fuel failure in normal conditions for a canister without damaged fuel and at an assumed 20% fuel failure in normal conditions for a canister containing damaged fuel. The 20% fuel failure is based on site-specific contents including intact, high burnup and damaged fuel (see Section 4.5.1.1).

The GE 9x9 (with 79 fuel rods) fuel assembly is the bounding BWR assembly and is, therefore, used in the leakage calculations for the cask transporting BWR fuel. As for the PWR fuel, a maximum design burnup of 50,000 MWD/MTU, at a minimum 1.9 wt % ^{235}U enrichment with a 5-year cool time, is also conservatively used to generate the containment analysis source term for the BWR fuel. The GE 9 x 9 assembly contains the highest fuel load and surface area of any BWR assembly analyzed. The crud concentration on the larger surface area plays a significant role in the BWR fuel assembly calculation of allowable release rate.

Activities for the fuel assemblies are determined by detailed SAS2H isotopic depletion calculations. The depletion calculation shows that enrichment and activity are inversely correlated. The lower enrichment, 1.9 wt % ^{235}U for both the PWR and BWR analysis (with a burnup of 50,000 MWD/MTU), therefore produces bounding activities for the containment analysis.

The free volume employed in the pressure and release calculation is conservatively set to the smallest free cask volume found in the UMS® canister classes (Class 1-3 PWR and 4-5 BWR). No credit is taken for the canister as a containment boundary but its mass is considered when calculating cask free volume. The Universal Transport Cask containment boundary is defined in Section 4.1. Results of package containment analyses for normal conditions of transport and hypothetical accident conditions are provided in Sections 4.2 and 4.3, respectively. These results demonstrate that the package meets the containment requirements of 10 CFR 71.51 [1] and IAEA Safety Series No. 6 (Paragraph 548) [2] for normal conditions of transport and hypothetical accident conditions.

4.1 Containment Boundary

The Universal Transport Cask containment boundary is defined by the following components: (1) inner shell; (2) bottom forging; (3) top forging; (4) cask lid and lid inner EPDM O-ring; (5) vent port coverplate and vent port coverplate inner EPDM O-ring; and (6) drain port coverplate and drain port coverplate inner EPDM O-ring.

There are three possible paths for the escape of radioactive material from the Universal Transport Cask during transport operation. These paths are past the inner EPDM O-ring seals on the lid, on the vent port coverplate and on the drain port coverplate. EPDM O-ring manufacturers data is provided in Section 4.5.2.

The cask containment integrity is verified through leak testing prior to all transport operations. A mass spectrometer leak detector is used to verify that leakage does not exceed the limits established in Section 4.2.3. These limits are in accordance with the requirements of 10 CFR 71.51 and IAEA Safety Series No. 6 (paragraph 548).

4.1.1 Containment Vessel

The primary containment vessel for the Universal Transport Cask consists of a 67.61-in. ID, 2-in.-thick inner shell; a 4.25-in.-thick bottom forging; a 8.825-in.-thick top forging; and a closure lid. The containment vessel components are fabricated from Type 304 stainless steel in accordance with the applicable requirements of the ASME Boiler and Pressure Vessel Code, [3].

4.1.2 Containment Penetrations

The Universal Transport Cask primary containment boundary is described in Section 4.1. The penetrations in the cask primary containment vessel are the vent and drain ports, and the lid. The penetrations are designed to seal the boundary and to ensure that leakage from the cavity does not exceed the established limits. 10 CFR 71.51 establishes release limits under both normal conditions of transport and hypothetical accident conditions . The quick-disconnects installed in the vent and drain openings and in the lid test port are not considered part of the containment boundary. The vent and drain port coverplates are fabricated from SA-240, Type 304 stainless steel.

4.1.3 Seals and Welds

4.1.3.1 Seals

The EPDM O-rings of the lid, vent port coverplate, and drain port coverplate are the seals that provide primary containment, as described in Section 4.1. Section 4.5.2 contains the specifications for the EPDM O-rings. The cask is leak tested before acceptance from the manufacturer and after fuel loading. These tests are described in Table 4.1-1.

4.1.3.1.1 Containment System Fabrication Verification

When fabrication is complete, containment system fabrication verification leak testing is performed on the cask containment as described in Section 8.1.3. This leak test verifies that the leak rate of the assembled containment boundary does not exceed the allowable reference air leak rate of 4.2×10^{-6} ref·cm^3/sec. Limiting leak rates are obtained from the evaluation of site-specific contents using a release fraction of 20% under normal conditions of transport. As shown in Table 4.2-4, the allowable leak rate for a PWR cask containing damaged high burnup fuel bounds the allowable leak rate for the cask containing intact PWR fuel and BWR fuel under 45,000 MWD/MTU burnup. The maximum allowable leak rates and the corresponding test sensitivities are evaluated in Section 4.2.3 for normal conditions of transport and in Section 4.3.2 for hypothetical accident conditions. Based on the analysis presented in these sections, the normal conditions allowable leak rate bounds the allowable leak rate for accident conditions.

4.1.3.1.2 Containment System Periodic Verification

The containment system periodic verification is performed on the Universal Transport Cask package containment boundary seals and components , in accordance with the leak test acceptance criteria established for the containment system fabrication verification (Section 8.1.3). This verification leak test conforms to test method A5.4 of Table A1 of ANSI N14.5-1997 [4].

Whenever a containment seal or component is replaced, the O-ring or containment component is leak tested following replacement according to the requirements of the containment system periodic verification (Section 8.1.3). This test verifies that the replacement seal or component has been properly installed and that the leak rate meets the allowable leak rate requirements established for the containment system fabrication verification specified in Section 4.2.3.

4.1.3.1.3 Containment System Verification Prior to Transport

As specified in the loading procedure (Section 7.1.3), the containment system is leak tested in accordance with Section 8.1.3 (helium leak tested), if components of the containment boundary are replaced during loading operations. If containment boundary components are not replaced, then the containment boundary is pressure tested in accordance with Paragraph 7.6.4 of ANSI N14.5-1997 to demonstrate containment boundary assembly in accordance with the operating procedures.

For unloaded (empty) transport, pressure testing is used to demonstrate containment boundary assembly.

The assembly pressure test configuration conforms to test method A5.1 of Table A1 of ANSI N14.5-1997.

4.1.3.2 Welds

Circumferential and longitudinal welds are used to fabricate the inner shell and to attach it to the top and bottom forgings. The longitudinal welds in the cylindrical sections are staggered circumferentially by 90° or 180°. Containment vessel welds are full penetration bevel or groove welds to ensure structural integrity. Upon completion of the inner shell welds, the welds are radiograph-inspected and accepted in accordance with ASME Code Section III NB-5320.

Upon completion of containment vessel fabrication, the cask containment boundary is hydrostatically tested in accordance with ASME Code requirements to ensure the integrity of the welds and containment components (Section 8.1.2.3). Following hydrostatic testing, all containment vessel welds are visually inspected by the dye penetrant examination method and evaluated in accordance with ASME Code requirements. Following fabrication, the containment boundary o-rings are leak tested in accordance with Section 8.1.3. The post-fabrication leak test is based on the bounding PWR fuel allowable leak rate of 4.2×10^{-6} ref cm^3/sec as shown in Table 4.2-4. Test equipment and methods are selected to assure a minimum test sensitivity of one half the reference leak rate, or 2.1×10^{-6} ref cm^3/sec. The equivalent allowable helium leak rate is 6.5×10^{-6} cm^3/sec at standard conditions. The required helium leak test sensitivity is 3.25×10^{-6} cm^3/sec. The helium leak rate at standard conditions is specified since the test is conducted using helium as the detector gas. Specification of standard conditions is conservative, since the actual pressure may be higher than the postulated 0 psig (1 atmosphere) pressure that is assumed.

4.1.4 Closure

The primary closure assembly for the Universal Transport Cask consists of the lid, bolts, and o-rings. The lid is recessed and bolted into the top forging of the cask body. The 6.5-in. thick, 78.17-in. diameter lid is made of ASME SA-336, Type 304 stainless steel. The lid is retained by 48 bolts that are 2-8 UN socket head cap screws fabricated from SB-637, Grade N07718 nickel alloy steel bolting material. The initial torque for installation of the lid bolts is as specified in Table 7-1. The bottom surface of the lid is sealed to the top forging of the cask body by a set of EPDM o-rings, with the inner o-ring forming the containment boundary. The second (outer) o-ring provides an annulus to test the inner o-ring seal.

The vent port is recessed into the lid and the drain port is recessed into the bottom forging. The vent and drain port coverplates are secured by four 1/2-13 UNC bolts fabricated from SA-193, Grade B6, Type 410 stainless steel.

Similar to the inner lid configuration, each of the vent and the drain coverplates is sealed by a set of o-rings, with the inner o-ring forming the containment boundary. The second (outer) o-ring provides an annulus to test the inner o-ring seal.

Table 4.1-1 Containment Verification Leak Test Requirements and Schedule

	Post-Fabrication and Annual Maintenance[1]	**Loaded Transport (O-Ring Replacement)[2]**	**Loaded Transport (No O-Ring Replacement)[2]**	**Empty Transport[2]**
Allowable Reference Leak Rate[3]	4.2×10^{-6} cm^3/sec	4.2×10^{-6} cm^3/sec	1×10^{-3} cm^3/sec	1×10^{-3} cm^3/sec
Allowable Helium Leak Rate[3]	6.5×10^{-6} cm^3/sec	6.5×10^{-6} cm^3/sec	--	--

1 All o-rings are replaced during Annual Maintenance.

2 The need for o-ring replacement is determined by inspection or by leak test results. Only the appropriate set of o-ring is replaced as necessary prior to transport.

3 The allowable leak rate is based on the bounding evaluation containing damaged high burnup PWR fuel assemblies and is the same for the transport of GTCC waste.

THIS PAGE INTENTIONALLY LEFT BLANK

4.2 Containment Requirements for Normal Conditions of Transport

The Universal Transport Cask must maintain a radioactivity release rate of not more than 10^{-6} A_2/hr under normal conditions of transport, as required by 10 CFR 71.51 and IAEA Safety Series No. 6 (paragraph 548). For the cask containing intact PWR fuel, this condition is satisfied by maintaining a maximum reference (air at standard conditions) leak rate of 5.0×10^{-5} ref·cm³/sec, or 6.6×10^{-5} cm³/sec helium at the test condition, which is conservatively considered to be the standard conditions. For the cask containing BWR fuel, the radioactivity release rate requirement is satisfied by maintaining a maximum reference leak rate from the cask of 3.3×10^{-5} ref·cm³/sec, or 4.5×10^{-5} cm³/sec helium at the test conditions. For the PWR cask containing PWR damaged high burnup fuel assemblies, the maximum reference leak rate is 4.2×10^{-6} ref cm³/sec or 6.5×10^{-6} cm³/sec helium. Consequently, the PWR high burnup fuel allowable leak rate is conservatively applied as the containment boundary test condition for post-fabrication testing, annual testing, and when containment components are replaced during cask use. Calculations of these limits are provided in this section.

The structural and thermal evaluations of the Universal Transport Cask are provided in Chapters 2.0 and 3.0, respectively. Results of these evaluations also demonstrate that cask containment is maintained during normal conditions of transport. Therefore, the package satisfies the containment requirements of 10 CFR 71.71.

4.2.1 Containment of Radioactive Material

The 10 CFR 71 limit for the release of radioactive material under normal conditions of transport is 10^{-6} A_2/hr. In this analysis, A_2 for a mixed gas is determined by using the method described in 10 CFR 71, Appendix A. The release fractions for the various radionuclides transported in the Universal Transport Cask are obtained from NUREG/CR-6487 [4] and summarized in Table 4.2-1 (located at the end of this section). The curie content per isotope for 5-year cooled PWR and BWR design basis fuel assemblies is provided in Section 4.5-3.

In addition to the radionuclides produced by the fuel material, fuel assemblies develop a coating of impurities deposited by cooling water during power generation. This coating is known as crud. Crud contains mostly nonradioactive elements but also contains a significant amount of ^{60}Co. NUREG/CR-6487 lists the maximum ^{60}Co concentrations on spent fuel assemblies to be 140 μCi/cm² for PWR assemblies and 1,254 μCi/cm² for BWR assemblies at initial discharge.

140 μCi/cm^2 for PWR assemblies and 1,254 μCi/cm^2 for BWR assemblies at initial discharge. The surface areas of the design basis PWR and BWR assemblies (B&W 15x15 and GE 9x9) are calculated to be 3.25 x 10^5 cm^2 and 1.77 x 10^5 cm^2, respectively. The total PWR crud activity, calculated by the conservative surface area and maximum activity density, envelopes assemblies with control components inserted. Fuel assembly characteristics are listed in Tables 1.2-4 and 1.2-5 for PWR and BWR fuel assemblies respectively.

4.2.1.1 Calculation of Allowable Leak Rates

The maximum permissible leak rate from the cask under normal conditions of transport is determined from the 10 CFR 71 limit of 10^{-6} A2/hr.

$$R_N = L_N C_N \leq A_2 \text{ x } \cdot 1\text{x}10^{-6} \text{hr}^{-1} \text{ or}$$
$$R_N = L_N C_N \leq A_2 \text{ x } \cdot 2.78\text{x}10^{-10} \sec^{-1}$$

where:

L_N = is the volumetric gas leakage rate [cm^3/s]
C_N = is the curies per unit volume (termed "activity density") of the radioactive material that passes through the leak path [Ci/cm^3]
R_N = Release rate for normal transport conditions [Ci/sec]

Activity Density of Radioactive Material (C_N)

The total inventory of fission product gases, volatiles fines and crud are shown in Table 4.5.3-1 through Table 4.5.3-6. These inventories are calculated by using the source terms produced by the SAS2H [6] sequence, the release fractions and the postulated crud (^{60}Co). The ^{60}Co content is decayed 5 years from discharge to the design basis fuel cool time. The PWR analysis is based on 24 design basis fuel assemblies. The BWR analysis is based on 56 design basis fuel assemblies.

$$C_n = C_{Crud} + C_{Volaties} + C_{FissionGas} + C_{Fines}$$

$$C_{Crud} = \frac{f_C M_T}{V} = \frac{f_C S_C N_A (N_R S_{AR} + S_{Ch})}{V}$$

where:

C_{crud} = activity density inside containment vessel resulting from crud spallation [Ci/cm^3]

Maximum Allowable Leak Rates

On the basis of the methodology discussed above, the maximum allowable leak rates for the casks containing standard or high burnup PWR and BWR standard fuel under normal conditions of transport are calculated to be 5.5×10^{-6} and 1.3×10^{-5} ref cm^3/sec, respectively (Table 4.2-4).

The maximum allowable release rates are more restrictive for the cask containing high burnup damaged PWR assemblies because of the higher failure rate associated with the ISG-15 specified failure rate of 50% in normal conditions in fuel with an oxide layer thickness greater than 70 microns. Per ISG-15, no more than 3% of the rods in a high burnup assembly may contain oxide layers over 70 microns. Above this level, assemblies must be placed in damaged fuel cans. The worst case containment analysis UMS® loading is, therefore, 12 intact standard assemblies failing at 3%, 8 high burnup assemblies classified as intact with 50% failure of the 3% high burnup rods, and 50% failure of rods inside the damaged fuel cans. This configuration is bounded by the 20% average release fraction applied to a full canister load of high burnup assemblies.

4.2.1.2 Correlation of Allowable Leak Rates to Air Standard

The volumetric gas leak rate, L is independent of transport cask pressure and temperature. The maximum allowable release must be correlated with air standard leak rates, which depend on gas temperatures, pressures, and leakage path length and diameter. This correlation requires calculation of the capillary opening diameter through which the flow occurs. Depending on pressure and condition of the flow, a combination of continuum and molecular flow occurs.

Continuum flow and molecular flow equations are obtained from NUREG/CR-6487, Section 2. Both continuum and molecular flow rate equations presented below are adjusted to upstream flow rate in accordance with NUREG/CR-6487 and ANSI N14.5-1997.

The continuum volumetric flow rate of the gas (cm^3/sec), L_c, is given by:

$$L_c = \frac{2.48x10^6 D^4}{a\mu}(P_u - P_d) * \frac{P_a}{P_u} = F_c * (P_u - P_d) * \frac{P_a}{P_u}$$

where:

F_c	=	coefficient for continuum flow [cm^3/atm-s]
D	=	capillary diameter [cm]
a	=	capillary length [cm]
μ	=	fluid viscosity [cP]
P_u	=	upstream pressure [atm] - pressure inside containment
P_d	=	downstream pressure [atm] - pressure outside containment

and, the molecular volumetric flow rate of the gas (cm^3/sec), L_m, is given by:

$$L_m = \frac{3.81x10^3 D^3 \sqrt{\frac{T}{M}}}{aP_a}(P_u - P_d) * \frac{P_a}{P_u} = F_m * (P_u - P_d) * \frac{P_a}{P_u}$$

where:

L_m	=	is the volumetric flow rate of gas at P_a [cm^3/sec]
F_m	=	is the coefficient for molecular flow [cm^3/atm-s]
D	=	is the capillary diameter [cm]
T	=	is the gas temperature [K]
M	=	is the gas molecular weight [g/mole]
P_a	=	is the average pressure $(P_u+P_d)/2$ [atm]
P_u	=	is the upstream pressure [atm]
P_d	=	is the downstream pressure [atm].
a	=	capillary diameter [cm]

For this analysis, the gas temperature used for molecular flow analysis is identical to the upstream temperature. Pressures and temperatures for PWR and BWR system normal operating conditions are summarized in Table 4.2-5. Based on the pressure, temperature and allowable leakage rate (L_N) the capillary diameter of the leak is determined. The calculated capillary diameter is then used to determine the air standard leak rate and helium test leak rate. Air standard condition leak rates are determined for air leaking from 1 atmosphere to 0.01 atmosphere at a temperature of 298K. The test gas is helium leaking from 1 atmosphere (0 psig) to a vacuum. Table 4.2-4 provides the standard and test leak rates for the Universal Transport Cask loaded with PWR or BWR fuel. The sensitivity for these tests is one-half the air standard leak rate as recommended by ANSI-N14.5-1997. Key PWR and BWR containment analysis parameters are summarized in Table 4.2-6.

This analysis is conservative since a higher upstream pressure, which could result from a higher average gas temperature based on decay heat, results in a higher allowable leak rate, assuming that the leak path length and the leak path diameter (calculated based on the reference air condition) are held constant. Since the test condition pressure cannot be less than 1 atmosphere, and since the average gas temperature does not have a first order effect on calculated leak rate, the helium test condition is conservative with respect to the allowable reference leak rate.

4.2.2 Pressurization of Containment Vessel

The maximum pressure in the cask during normal conditions of transport is calculated by using the methodology presented in Section 3.4.4. Assumptions underlying this calculation are that during normal conditions of transport, 3% of the fuel rods may fail and that 30% of the fission gases in the rods are releasable. The cask cavity under normal conditions of transport is backfilled to 1 atm with at least 99.9% pure helium gas.

4.2.3 Containment Criteria

The reference leak rates provided in Table 4.2-4 for PWR and BWR fuel, represent the maximum leak rate allowed if the o-rings were tested with air at 1 atm and 25°C. The maximum allowable leak rate for the containment system fabrication verification and periodic verification leak tests is described in Sections 4.1.3 and 8.1.3. This allowable leak rate is that for the BWR fuel configuration, which is more restrictive than the allowable leak rate for PWR fuel.

The sensitivity for these tests is recommended by ANSI N14.5-1997 to be one-half the allowable leak rate.

Table 4.2-1 Release Fractions: Normal and Accident Conditions

Radionuclide Origin	Fraction: Normal Conditions	Fraction: Accident Conditions
Volatiles releasable	2.00E-04	2.00E-04
Fission gas releasable	0.3	0.3
Rod mass released	3.00E-05	3.00E-05
Crud spallation factor	0.15	1.0
Fraction of fuel that fails	0.03[1]	1.0

1. PWR fuel is also evaluated at 0.20 to account for high burnup fuel failure during transport. This failure fraction envelops damaged fuel can payloads.

Table 4.2-2 Allowable Release Rate Source and A_2 Inputs for PWR Cask: Normal Conditions

B&W 15 x 15[1]	Crud	Gas	Volatiles	Fines	Total
Total Activity per Assembly (Ci)	N/C[2]	3.73E+03	1.49E+05	2.28E+05	3.81E+05
Releasable Activity per Cask (Ci)	8.48E+01	8.06E+02	2.14E+01	4.92E+00	9.17E+02
Cask Volumetric Activity (Ci/cm^3)	1.26E-05	1.20E-04	3.19E-06	7.33E-07	1.36E-04
A_2 Value (Ci)	10.80	285.50	6.39	0.114	302.81
Fraction of Activity	0.092	0.879	0.023	0.005	1.000
Fraction of Activity / A_2 (1/Ci)	0.0086	0.0031	0.0037	0.0471	0.0624
			Mixture A_2 Value (Ci)		16.03

1. Based on 3 % rod failure
2. Not explicitly calculated.

Table 4.2-3 Allowable Release Rate Source and A_2 Inputs for BWR Cask: Normal Conditions

GE 9 x 9	Crud	Gas	Volatiles	Fines	Total
Total Activity per Assembly (Ci)	N/C[1]	1.46E+03	5.76E+04	8.82E+04	1.47E+05
Releasable Activity per Cask (Ci)	9.68E+02	7.34E+02	1.94E+01	4.44E+00	1.73E+03
Cask Volumetric Activity (Ci/cm^3)	1.51E-04	1.14E-04	3.02E-06	6.93E-07	2.69E-04
A_2 Value (Ci)	10.80	285.60	6.34	0.12	302.85
Fraction of Activity	0.56	0.43	0.01	0.003	1.00
Fraction of Activity / A_2 (1/Ci)	0.052	0.001	0.002	0.022	0.078
			Mixture A_2 Value (Ci)		12.90

1 Not explicitly calculated.

Table 4.2-4 Leak Rate and Leak Test Sensitivity: Normal Conditions

Reactor Type	Assembly Type	Operating Condition	Vol. Activity Ci/cm^3	Leak Rate (cm^3/sec)		
				Volumetric (L)	Air Reference (L_R)	Test Sensitivity
PWR[1]	B&W 15x15	Normal	1.4E-04	3.3E-05	5.0E-05	2.5E-05
PWR[2]	B&W 15x15	Normal	8.4E-04	5.5E-06	4.2E-06	2.1E-06
BWR[3]	GE 9x9-2	Normal	2.7E-04	1.3E-05	3.3E-05	1.7E-05

1 The corresponding helium test leak rates and leak test sensitivities for the PWR configuration are 6.6×10^{-5} cm^3/sec and 3.3×10^{-5} cm^3/sec, respectively, at standard conditions.

2 Based on 20% fuel failure to account for high burnup fuel assemblies and damaged fuel cans. The corresponding helium test leak rates and leak test sensitivities for the PWR configuration are 6.5×10^{-6} cm^3/sec and 3.25×10^{-6} cm^3/sec, respectively, at standard conditions.

3 The corresponding helium test leak rates and leak test sensitivities for the BWR configuration are 4.5×10^{-5} cm^3/sec and 2.25×10^{-5} cm^3/sec, respectively, at standard conditions.

Table 4.2-5 Cask Free Volumes and Pressures: Normal and Accident Conditions

Reactor Type	**PWR**		**BWR**	
Cask Operating Condition	Normal	Accident[1]	Normal	Accident[1]
Free Gas Volume (liters)[2]	6,720	6,720	6,410	6,410
Pressure (atm)[2]	1.47[3]	5.72	1.25	3.91
Average Gas Temperature (K)	507.0	582.0	458.7	542.0

1 The accident condition for this analysis is 100% rod failure in combination with a fire accident raising cask temperature. This hypothetical dual failure accident conservatively maximizes both available releasable material and cask pressure.

2 Bounding values were chosen for free volume (minimum) and pressure (maximum). This conservatively minimizes free volume and capillary diameter.

3 The normal condition pressure assuming 20% fuel rod failure is 2.06 atm.

Table 4.2-6 PWR and BWR Containment Parameters - Normal Conditions

Assembly Type	**Crud Surface Activity (Ci/cm^2)**	**Containment Free Volume (cm^3)**	**Capillary Length (cm)**	**Capillary Diameter (cm)**	**Upstream Pressure (atm)**	**Gas Temperature (K)**
B&W[1] 15x15	7.3E-5	6.7E+6	0.287	6.4E-4	1.47	507
B&W[2] 15x15	7.3E-5	6.7E+6	0.287	3.3E-4	2.06	507
GE[1] 9x9-2	6.5E-4	6.4E+6	0.287	5.7E-4	1.25	459

1 Based on 3% of the fuel rods failing in normal transport conditions.

2 Based on 20% of the fuel rods failing in normal transport conditions.

4.3 Containment Requirements for Hypothetical Accident Conditions

The 10 CFR 71 requirement for the release of radioactive material under hypothetical accident conditions is met by ensuring that for the cask containing PWR fuel a reference (air) leak rate limit of 2.0×10^{-3} ref·cm³/sec is not exceeded. The corresponding air standard leak rate limit for the cask containing BWR fuel is 2.2×10^{-3} ref·cm³/sec. Calculations of these limits are provided in Section 4.3.2.

Assuming a simultaneous occurrence of a fire accident and a 100% rod failure, and on the basis of bulk average gas temperatures of 582K (PWR) and 542K (BWR) resulting from air in the cavity, the pressure within the cask cavity is calculated to be 5.7 atm (PWR) or 3.9 atm (BWR). The hypothetical presence of air in the cask provides an upper bound on the gas temperature. These pressures represent the maximum possible cask internal pressures.

The structural integrity of the cask containment during hypothetical accident conditions is demonstrated in Chapter 2.0. Therefore, the cask containment is maintained under hypothetical accident conditions.

4.3.1 Fission Gas Products

The calculated amounts of fission gases contained in the design basis PWR and BWR fuel assembly are reported in Tables 4.5.3-1 and 4.5.3-4. The accident conditions for maximum fission gas release assume 100% rod failure and also assume that 30% of the radioactive fission gases, primarily ^{85}Kr, tritium and ^{129}I, are available for release to the cask cavity. In addition, 100% of the ^{60}Co in the crud on the fuel assemblies is conservatively assumed to be available for release as an aerosol.

4.3.2 Containment of Radioactive Materials

The Universal Transport Cask is designed to maintain a release rate of less than 1 A_2/week for the hypothetical accident conditions, as required by 10 CFR 71.51. A_2 for a mixed gas is determined by using the method described in 10 CFR 71, Appendix A. The release fractions for the various radionuclides found in the cask are obtained from NUREG/CR-6487 and summarized in Table 4.2-1. The curie content per isotope for 5-year cooled PWR and BWR design basis fuel assemblies is provided in Section 4.5.3.

4.3.2.1 Calculation of Allowable Leak Rates

The allowable leak rates under hypothetical accident conditions are calculated by using the method described in Section 4.2.1.1 for normal conditions of transport. The total inventory of fission product gases, volatiles, fines, and crud are calculated by using the source terms generated by SAS2H and release fractions for the PWR and the BWR fuel. Using the A_2 values from 10 CFR 71, Appendix A (Tables 4.3-1 and 4.3-2 1), the mixture A_2 values are then determined for gas, volatile, fine, and crud mixtures. Finally, the maximum allowable release rates are calculated by using the hypothetical accident conditions allowable release limit:

$$R_A = L_A C_A \le A_2 \cdot \text{week}^{-1}$$

or

$$R_A = L_A C_A \le A_2 \cdot 1.65 \text{x} 10^{-6} \text{sec}^{-1}$$

where:

L_A	=	volumetric gas leakage rate [cm^3/s]
C_A	=	curies per unit volume (termed "activity density") of the radioactive material that passes through the leak path [Ci/cm^3]
R_A	=	release rate for accident transport conditions

Assumptions underlying the calculations for the hypothetical accident conditions are that 100% of the fuel rods fails and 100% of the crud is released (compared with the assumptions that 3% of the fuel rods fail and 15% of the crud is released in the analysis in Section 4.2.1.1 for normal conditions of transport). The mixture A_2 for gas, volatile, fine, and crud mixtures is not changed by the change in the magnitude of releasable material, but the combined A_2 changes based on the change in activity fraction in each group.

The calculated maximum permissible release rates for the casks containing design basis PWR and BWR fuel under hypothetical accident conditions are tabulated in Table 4.3-3.

4.3.2.2 Correlation of Allowable Leak Rates to Air Standard

The maximum allowable leak rates for the hypothetical accident conditions are correlated with standard leak rates by using the methodology described in Section 4.2.1.2. The results for casks containing PWR or BWR fuel as shown in Table 4.3-3.

4.3.3 Containment Criteria

The allowable leak rates calculated for the hypothetical accident conditions are much greater than those for the normal conditions of transport calculated in Section 4.2.1. Because the cask containment is demonstrated to be maintained under hypothetical accident conditions (Section 2.7), the maximum permissible leak rates for normal conditions of transport are more limiting and are therefore used for the establishment of the maximum allowable leak rates for the containment system fabrication and periodic verification leak test calculations and test acceptance criteria.

Table 4.3-1 Allowable Release Rate Source and A_2 Inputs for PWR Cask: Accident Conditions

B&W 15 x 15	**Crud**	**Gas**	**Volatiles**	**Fines**	**Total**
Total Activity per Assembly (Ci)	N/C[1]	3.73E+03	1.49E+05	2.28E+05	3.81E+05
Releasable Activity per Cask (Ci)	5.65E+02	2.69E+04	7.15E+02	1.64E+02	2.83E+04
Cask Volumetric Activity (Ci/cm^3)	8.41E-05	4.00E-03	1.06E-04	2.44E-05	4.21E-03
A_2 Value (Ci)	10.80	285.50	6.39	0.114	302.8
Fraction of Activity	0.020	0.949	0.025	0.006	1.00
Fraction of Activity / A_2 (1/Ci)	0.002	0.003	0.004	0.051	0.06
			Mixture A_2 Value (Ci)		16.68

1 Not explicitly calculated.

Table 4.3-2 Allowable Release Rate Source and A_2 Inputs for BWR Cask: Accident Conditions

GE 9 x 9	**Crud**	**Gas**	**Volatiles**	**Fines**	**Total**
Total Activity per Assembly (Ci)	N/C[1]	1.46E+03	5.76E+04	8.82E+04	1.47E+05
Releasable Activity per Cask (Ci)	6.45E+03	2.45E+04	6.45E+02	1.48E+02	3.17E+04
Cask Volumetric Activity (Ci/cm^3)	1.01E-03	3.82E-03	1.01E-04	2.31E-05	4.95E-03
A_2 Value (Ci)	10.80	285.60	6.34	0.115	302.85
Fraction of Activity	0.203	0.772	0.0204	0.005	1.00
Fraction of Activity / A_2 (1/Ci)	0.019	0.003	0.003	0.041	0.065
			Mixture A_2 Value (Ci)		15.31

1 Not explicitly calculated.

Table 4.3-3 Standard Leak Rates: Accident Conditions

Reactor Type	Assembly Type	Operating Condition	Vol. Activity (Ci/cm^3)	Leak Rates (cm^3/sec)	
				Volumetric (L)	Air Reference (L_R)
PWR	B&W 15x15	Accident	4.2E-03	6.5E-03	2.0E-03
BWR	GE 9x9-2	Accident	4.9E-03	5.1E-03	2.2E-03

Table 4.3-4 PWR and BWR Containment Parameters - Accident Conditions

Assembly Type	Crud Surface Activity (Ci/cm^2)	Containment Free Volume (cm^3)	Capillary Length (cm)	Capillary Diameter (cm)	Upstream Pressure (atm)	Gas Temperature (K)
B&W 15x15	7.3E-5	6.7E+6	0.287	1.7E-3	5.72	582
GE 9x9-2	6.5E-4	6.4E+6	0.287	1.7E-3	3.91	542

Note: 100 % of the fuel rods are postulated to fail in the accident condition.

THIS PAGE INTENTIONALLY LEFT BLANK

4.5.1 Containment Evaluation for Site Specific Contents

4.5.1.1 Containment Evaluation for Maine Yankee Contents

Pressure and radionuclide content of the Maine Yankee 14x14 fuel assemblies are bounded by the larger B&W 15x15 assembly employed in the containment evaluations presented in Sections 4.2 and 4.3. The larger fission mass of the B&W assembly produces higher fission gas inventories for a fixed burnup. The Maine Yankee fuel assemblies, with non-fuel components or in consolidated or damaged form (up to four consolidated or damaged assemblies per canister) displaces less free volume than the B&W fuel assembly forming the design basis for the containment analysis, and, therefore, results in lower pressures at a fixed decay heat.

Maine Yankee fuel with up to 50,000 MWD/MTU may be loaded in the transportable storage canister. ISG-15 requires a containment evaluation assuming 50% failure of high burnup fuel with an oxide layer thickness above 70 microns. ISG-15 also requires that fuel assemblies with more than 3% of rods with an oxide layer over 70 microns are considered as damaged and will, therefore, be placed in a damaged fuel can. High burnup fuel must be loaded in the outer fuel loading positions of the basket. The PWR basket has 24 fuel loading positions, including 12 outer positions.

The PWR containment analysis in Section 4.2.1 assumes 4 PWR (high burnup) fuel assemblies failing at 100%, 8 high burnup fuel assemblies failing at 4.5% (3% standard failure fraction plus 50% of the 3% high burnup rods), and the remaining 12 assemblies failing at 3%. This results in 20% of the fuel rods failing in normal conditions and bounds the presence of four damaged fuel cans in the basket. The PWR leak rate calculation is based on the higher failure fraction.

THIS PAGE INTENTIONALLY LEFT BLANK

enrichment fuel which may achieve this burnup, the design basis PWR source terms are calculated with an initial enrichment of 3.7 wt % ^{235}U. This assumption produces a neutron source 29% higher than that obtained by assuming 4.2 wt % ^{235}U initial enrichment. Assembly power density and cycle parameters are selected such that the assembly is activated at a power level 10% greater than a typical PWR assembly to allow for assembly power peaking during core residence. This treatment results in conservatively higher source rates due to enhanced actinide production and a shorter activation period.

Source term spectra and source region elevations are determined for the following four major PWR fuel assembly types (see Table 5.2-1):

- Westinghouse 15×15 Std — Class 1
- Westinghouse 17×17 Std — Class 1
- Babcock & Wilcox 15×15 Mark B — Class 2
- Combustion Engineering 16×16 System 80 — Class 3

These assembly types produce the limiting source terms. These assembly types are referred to in this report by the abbreviated names given in Table 5.2-1. Fuel assembly physical characteristics are given in Table 5.2-2, and hardware masses are given in Table 5.2-3. The results of the source term analysis for the fuel types given here are summarized in Table 5.2-4. Fuel assembly activated hardware source terms are shown in Table 5.2-5. These non-fuel source terms are determined on the basis of the hardware source per kilogram given in Table 5.2-4 and the hardware masses given in Table 5.2-3. The hardware activation is based on a stainless steel Type 304 composition with an assumed ^{59}Co impurity level of 1.2 g/kg.

In order to account for spectral differences in the activating neutron flux, a flux ratio of 0.2 is applied to hardware regions directly adjacent to the active core region, e.g., the lower end-fitting and upper plenum. A flux ratio of 0.1 is applied to the upper end-fitting region, except for the CE 16×16 upper end-fitting for which a 0.05 flux ratio is used. The lower end fitting region in the B&W fuel assembly model uses a 0.1 flux ratio since the model explicitly includes a lower plenum region adjacent to the fuel region. The ORIGEN-S code is used directly to calculate hardware activation spectra by activating the fuel assembly components in the SAS2H-calculated flux spectrum for each assembly type. The effects of axial flux spectrum and magnitude variation on hardware activation are estimated by flux ratios determined from empirical data [9].

5.2.4 BWR Fuel Assembly Descriptions

The Universal Transport Cask can transport up to 56 intact BWR fuel assemblies. BWR fuel is analyzed on the basis of an initial enrichment of 3.25 wt % ^{235}U, 40,000 MWD/MTU burnup, and a post irradiation cooling time of 10 years. Assembly power density and cycle parameters are selected such that the assembly is activated at a power level 10% greater than a typical BWR assembly to allow for assembly power peaking during core residence. This treatment results in conservatively higher source rates due to enhanced actinide production and a shorter activation period.

Source term spectra and source region elevations are determined for the following major BWR fuel assembly types (see Table 5.2-1):

- GE 7×7 BWR/2-3 Reactor Type, Version GE-2b — Class 4
- GE 8×8 BWR/2-3 Reactor Type, Version GE-5, 2 water holes — Class 4
- GE 8×8 BWR/2-3 Reactor Type, Version GE-10, 1 large water hole — Class 4
- GE 7×7 BWR/4-6 Reactor Type, Version GE-2 — Class 5
- GE 8×8 BWR/4-6 Reactor Type, Version GE-5, 2 water holes — Class 5
- GE 8×8 BWR/4-6 Reactor Type, Version GE-10, 1 large water hole — Class 5
- GE 9×9 BWR/4-6 Reactor Type, Version GE-11, 2 water holes, 79 fuel rods — Class 5

These assembly types are referred to in this report by the abbreviated names given in Table 5.2-1. The physical characteristics of the two classes of BWR fuel are given in Table 5.2-6 and Table 5.2-7. For fuel assemblies with a burnup of 40,000 MWD/MTU, the fuel requires a minimum of 10 years of cooling after discharge to meet the neutron and gamma source values, and the decay heat values specified in Table 5.2-8 and Table 5.2-9. The GE BWR/2-3 8x8 fuel assembly designs are analyzed on the basis of a 144 in. active fuel length in order to provide a consistent basis for comparison with the other BWR/2-3 fuel assembly designs. The GE-2b version of the GE BWR/2-3 7x7 fuel assembly is selected over the older GE-2a design since it has been discharged more recently, although the GE-2a assembly has a marginally higher (0.4%) initial heavy metal loading.

5.4.3.1 Methodology

The loading table analysis extends the applicability of the initial 10-year cooled 45,000 MWD/MTU PWR and 40,000 MWD/MTU BWR shielding design basis evaluation by providing minimum cool times for 30,000 MWD/MTU to 45,000 MWD/MTU burned fuel assemblies in increments of 5,000 MWD/MTU. In addition to the burnup range the loading table evaluation also includes minimum initial enrichment limits ranging from 1.9 to 3.7 wt % ^{235}U in 0.2 wt % ^{235}U increments. Changes in the initial enrichment can have a substantial impact on the actinide neutron source of the spent nuclear fuel and, thereby, modifies the minimum cool times required to meet the decay heat and dose rate limits imposed on the transport cask.

The fuel types analyzed in the loading table analysis include the candidate design basis fuel assemblies listed in Section 5.1.1. Note that the analysis of BWR fuel types considers only the longer BWR-4/6 type fuel, which bound the shorter BWR-2/3 type fuels.

A complete set of source spectra and decay heat values for this set of limiting assemblies is then computed using the SAS2H [4] code at various initial enrichment, burnup, and cool times representative of the fuel intended for shipment in the UMS Transport Cask.

Next, the cool time required for each fuel type, initial enrichment, and burnup combination to meet limiting values of decay heat and dose rate is determined. The decay heat limits are set based on the cool-time dependent decay heat limits established in Section 3.4.6, as shown in Table 3.4-8. The dose rate limits are established based on a one-dimensional analysis of the Transport Cask containing the design basis PWR and BWR fuels under both normal and accident conditions.

With the limiting cool times identified for each fuel combination, the results are further summarized by identifying the most limiting fuel type within each array size classification. This array size classification is intended to simplify the application of the loading tables in determining the suitability of a particular fuel for shipment without need for a detailed analysis.

The SCALE computer code system is used to evaluate radiation source terms and to perform one dimensional shielding calculations. Source terms are evaluated using the SAS2H code, which provides a simplified interface to the ORIGEN-S code, including burnup-dependent cross-section processing. Source spectra at additional cool times are evaluated by direct application of the ORIGEN-S code. The SAS1 code sequence is used to determine one-dimensional dose rates and the dose rate response functions. The SAS1 driver provides an interface to the XSDRNPM one-dimensional transport code. All SCALE analyses are conducted using the SCALE 27N18G group library.

The key analytical assumption made in this analysis is the validity of extending one-dimensional dose rate comparisons to conclusions about the dose rate field in the vicinity of the cask. This assumption is supported by the following:

1. The geometry of the cask system is essentially the same regardless of the fuel type loaded. This is particularly true when the dissipating effects on dose rate of the cask shielding materials are considered. Possible concerns about an unfavorable geometry (e.g., a fuel assembly end fitting adjacent to an area of minimal shielding) occurring for a particular fuel assembly have been considered both implicitly in the design of the system and directly in the three dimensional shielding analyses conducted for the design basis fuels.

2. The one-dimensional radial dose rates used for the comparison are themselves accurate predictions of actual dose rates. The ratio of the length of the cask to its diameter ensures that the buckling approximation implicit in a one-dimensional calculation is valid. This assumption is further justified based on the results of a three-dimensional verification study.

Furthermore, the one-dimensional dose rate comparisons are made on the basis of fuel region sources alone. This analysis is intended to consider the impact of the relationship between initial enrichment and burnup on actinide production in the active fuel region. The three-dimensional shielding calculations performed for the Transport Cask incorporate the maximum plenum and end-fitting hardware descriptions of all assemblies intended for shipment in the UMS system.

Hence, the non-fuel source regions have already been considered to the maximum extent, and it is only necessary to demonstrate that the fuel region sources are bounded by the design basis.

This argument is also applied to the suitability of considering dose rates computed only for the radial case. Since no aspect of the cask shield construction changes with varying fuel type, it is reasonable to expect the axial dose contribution from fuel sources to vary consistently with the radial contribution.

SAS2H runs are executed for each assembly type at the following combinations of burnup, initial enrichment, and cool time:

Burnup:	30, 35, 40, 45 GWD/MTU
Enrichment:	1.9, 2.1, 2.3, 2.5, 2.7, 2.9, 3.1, 3.3, 3.5, 3.7 wt % ^{235}U.
Cool Time:	5, 6, 7, 8, 9, 10, 12, 14, 16, 18, 20, 22, 24, 26, 28, 30, 35, 40 years

Final cool times are established by interpolating between results calculated for each cool time listed above. This interpolation procedure is conservative due to the exponentially decreasing behavior of decay heat and radiation source rates with time. The maximum cool time (that is, the cool time which ensures all constraints are met) is always rounded up to the next whole year.

The various combinations of enrichment and burnup shown above define a discrete mesh of possible combinations. When considering the required cool time for a particular assembly, the actual enrichment of the assembly should be rounded down to the next lower analyzed value, and the assembly burnup should be rounded up to the next higher analyzed value in order to ensure that a conservative value is obtained from the loading table.

5.4.3.2 Limiting Decay Heat and Dose Rate Values

The decay heat limits applied in the analysis are the cool-time dependent decay heat limits established in Section 3.4.6 based on clad temperature limits as a function of fuel cool time.

The maximum allowable heat load, or decay heat limit as used in the context of this chapter, is based on the more limiting of (1) cladding stress and temperature limited heat loads and (2) the overall maximum decay heat limit of 20 kW (PWR) or 16 kW (BWR). Details of this analysis are presented in Section 3.4.6.

Decay heat limits for fuel burned to less than 35 GWD/MTU are not determined in Section 3.4.6. For the minimum cooling time evaluation presented here, the 30 GWD/MTU decay heat limit is conservatively set equal to the 35 GWD/MTU decay heat limit values. Since the heat load limit is based on the rod cladding stress and pressure level, which is directly related to fission gas production, employing the 35 GWD/MTU limit for lower burnups clearly provides bounding limits.

Normal condition dose rate limits are established using the SAS1 code by computing the Transport Cask one-dimensional radial dose rate for the design basis PWR and BWR fuel descriptions. The SAS1 geometrical models are described in Section 5.3.1. The dose rate limits are established based on the computed dose rate from fuel region sources taken at a distance 2m from the edge of a 124 in. wide railcar (357.48 cm from the cask axial centerline). The resulting one-dimensional dose rate limits are 6.71 mrem/hr for PWR fuels and 4.53 mrem/hr for BWR fuels.

Since the design basis PWR and BWR fuels lead to accident condition dose rates that are much lower than regulatory limits, the approach of basing the dose rate limits on one-dimensional models of these design basis assemblies is unnecessarily conservative. Instead, a fixed one-dimensional dose rate limit of 600 mrem/hr at 1 meter from the Transport Cask is employed for the accident condition dose rate limit. This value is verified by performing three-dimensional analyses of selected fuel, burnup, and enrichment cases at the decay times resulting from the analysis. The results indicate that the 600 mrem/hr limit is sufficient to ensure that actual three-dimensional computed dose rates are below the regulatory limit of 1,000 mrem/hr at 1 meter from the cask.

It is not the intent to compare one-dimensional dose rates directly with the three-dimensional design basis values. Instead, the one-dimensional dose rates computed for each fuel combination are compared with the corresponding one-dimensional dose rates evaluated for the design basis PWR and BWR fuel descriptions. The detailed three-dimensional analysis of the design basis fuels shows that these fuels meet regulatory limits. Hence, the one-dimensional dose rates evaluated for the design basis fuels are used as the basis of comparison. This approach is verified by performing detailed three-dimensional analyses of selected fuel combinations at the cool time indicated by the loading table analysis to ensure that the design basis fuel dose rates are bounding.

5.4.3.3 Cool Time Determination

The strategy used to determine limiting cooling times for each combination of fuel type, initial enrichment, and burnup is to:

5.5.1 Site Specific Contents Shielding Evaluations

This section describes fuel assembly characteristics and configurations, or waste configurations, which are unique to specific reactor sites. These site specific content configurations result from conditions that occurred during reactor operations, participation in research and development programs, testing programs intended to improve reactor operations, and from decommissioning activities.

Site specific fuel assembly configurations are either shown to be bounded by the analysis of the standard design basis fuel assembly configuration of the same type (PWR or BWR), or are shown to be acceptable contents by specific evaluation of the configuration.

5.5.1.1 Maine Yankee Site Specific Spent Fuel

This analysis considers both assembly fuel sources and sources from activated non-fuel material such as control element assemblies (CEA), in-core instrument (ICI) thimbles, and fuel assemblies containing activated stainless steel replacement (SSR) rods. It also considers the consolidated fuel present in the Maine Yankee spent fuel inventory.

The Maine Yankee spent fuel inventory also contains fuel assemblies with hollow zirconium rods, removed fuel rods, axial blankets, poison rods, variable radial enrichment, and low enriched substitute rods. These components do not result in additional sources to be considered in shielding evaluations and are, therefore, enveloped by the standard fuel assembly evaluation. For shielding considerations of the variably enriched rods the planar-average enrichment should be employed in determining minimum cool times.

5.5.1.1.1 Fuel Source Term Description

Maine Yankee utilized 14x14 array size fuel based on designs provided by Combustion Engineering, Westinghouse, and Exxon Nuclear. The previously analyzed Combustion Engineering CE14x14 Standard fuel design is selected as the design basis for this analysis because its potential Uranium loading is the highest of the three vendor fuel types, based on a 0.3765-inch nominal fuel pellet diameter, a 137 inch active fuel length, and a 95% theoretical fuel density. This results in a fuel mass of 0.4307 MTU. This exceeds the maximum reported Maine Yankee fuel mass of 0.397 MTU, and therefore, produces bounding source terms. The

SAS2H model of the CE14x14 assembly at a nominal burnup of 45,000 MWD and initial enrichment of 3.7 wt %, based on data provided in Table 1.2-4, is shown in Figure 5.5.1.1-1.

Source terms for various combinations of burnup and initial enrichment discussed in Section 5.4.3.1 are computed by adjusting the SAS2H BURN parameter to model the desired burnup and specifying the initial enrichment in the Material Information Processor input for UO_2. For Maine Yankee CE 14 x 14 fuel, the burnup is increased to 50,000 MWD/MTU.

5.5.1.1.1.1 Control Element Assemblies (CEA)

For the CEA evaluation, the assumptions are:

1. The irradiated portion of the CEA assembly is limited to the CEA tips, as during normal operation, the elements are retracted from the core and only the tips are subject to significant neutron flux.
2. The CEA tips are defined as that portion present in the "Gas Plenum" neutron source region in the Characteristics Database (CDB) [9].
3. Material subject to activation in the CEA tips is limited to stainless steel Inconel, and the AgInCd absorber material present in the lower eight inches of the CEA.
4. All stainless steel and Inconel material is assumed to have a concentration of 1.2 g/kg ^{59}Co. The CDB indicates that a total of 2.495 kg/CEA of this material is present in the Gas Plenum region of the core during operation.
5. The mass of AgInCd present in each CEA tip is 2.767 kg/CEA [9]. The AgInCd material is modeled as 80 wt. % Ag, 15.35 wt. % In, and 5.35 wt. % Cd. Note that the composition sums to a value greater than 100%, but this only means that conservatively more mass is represented than is actually present.
6. The irradiated CEA material is assumed to be present in the bottom eight inches of the active fuel region when inserted in the assembly.
7. The decay heat generated in the most limiting CEA at a 5-year cool time is 2.16 W/kg of stainless steel or Inconel and 3.11 W/kg of AgInCd. For a cask fully loaded with fuel assemblies containing design basis CEAs, the additional heat generation due to the CEAs amounts to: [(2.16 W/kg SS or Inconel)(2.495 kg/CEA) + (3.11 W/kg AgInCd)(2.767 kg/CEA)](24 CEA/cask) = 336 W/cask.
   This value is conservatively rounded up to 350 W. Although longer cool times are considered in this analysis for the fuel source terms, this decay heat generation rate is conservatively used for all longer CEA cool times.

connected by solid steel connector rods. No explicit source term analysis is conducted for the consolidated fuel lattices themselves, instead, an analysis is presented based on the source term computed for the fuel assemblies from which the contents are derived.

5.5.1.1.2 Model Specification

The one- and three-dimensional models described in Section 5.3 are employed in this analysis. No modifications are required to the models except for the substitution of CE 14 x 14 homogenized source descriptions. These homogenizations are shown in Tables 5.5.1.1-7 through 5.5.1.1-9.

5.5.1.1.3 Shielding Evaluation

The shielding evaluation consists of a loading table analysis of the CE 14 x 14 fuel following the methodology developed in Section 5.4.3. Fuel assemblies which include non-fuel hardware are addressed explicitly. The results of the analysis are loading tables which give the required cool time for a particular fuel configuration.

No restrictions are placed on the loading locations for any of the non-fuel assembly hardware components. This implies that a canister may contain up to 24 CEAs, 24 ICI thimbles, or 24 steel substitute rod assemblies or any combination therefore as long as the most limiting cool time is selected for any of the components in the canister. The only restriction is that no two specialty hardware components may be loaded in the same basket locations. Due to physical constraints, ICI thimbles and CEAs cannot be located in the same assembly. Neither CEA's or ICI thimbles may be placed into an assembly containing steel substitute rods.

5.5.1.1.4 Standard Fuel Source Term and Loading Table Analysis

Initial results are obtained for CE 14 x 14 fuel with no additional non-fuel material included for burnups up to 50,000 MWD/MTU. The results are obtained following the loading table analysis methodology developed in Section 5.4.3. CE 14 x 14 source terms at various combinations of initial enrichment and burnup are computed using the CE 14 x 14 SAS2H model described in Section 5.5.1.1.1.

Following the methodology developed in Section 5.4.3, one-dimensional shielding calculations are performed for CE14x14 fuel region sources at various combinations of initial enrichment, burnup, and cool time. The resulting dose rate and source term data is interpolated to determine the cool time required for each combination of enrichment and burnup to decay below the design basis limiting values of dose and heat generation rate.

The resulting loading table for CE14x14 fuel with no additional non-fuel material is shown in Table 5.5.1.1-10. A three-dimensional verification study has been performed for selected fuel combinations obtained from the loading table, Table 5.4-23.

5.5.1.1.4.1 Control Element Assemblies (CEA)

The result of the CEA analysis is a set of loading tables for Maine Yankee fuel giving the cool time required for a fuel assembly with a specified burnup and enrichment combination either 1) to contain a design basis CEA with a cool time of 5, 10, 15, or 20 years or 2) to be present in a Class 2 canister with no CEA inserted. Note that this latter qualification arises because of the geometry difference between Class 1 and Class 2 canisters. Fuel assemblies containing CEAs will be loaded into Class 2 canisters, which are slightly longer than the Class 1 canisters used for bare fuel assemblies. The additional length is required to accommodate the CEA, which is inserted in the top of the fuel assembly.

The approach taken is to compute downward adjustments to the design basis one-dimensional dose rate limiting value (6.71 mrem/hr at 2m from railcar) which ensures that the fuel sources have decayed adequately to cover the effect of the additional source added as a result of CEA containment. The adjustment is determined on the basis of a conservative comparison of three-dimensional shielding analysis results for the original Class 1 canister containing CE14x14 fuel assemblies and the Class 2 canister containing either no CEA or CEAs cooled to 5, 10, 15, or 20 years. Results for CEA cool times longer than 20 years are bounded by the 20 year results.

5.5.1.1.4.1.1 Establishment of Limiting Values

Since the additional activated material in the CEA analysis is assumed to be present in the bottom eight inches of the active fuel region, the one-dimensional dose methodology developed here is not sensitive to the additional source term. The one-dimensional analysis is based on the response from fuel region sources alone. To account for the additional source, the one-dimensional normal conditions dose rate limit is adjusted by an amount which ensures that the contribution from the additional activated material is bounded.

By adjusting the one-dimensional dose rate limit, we require the fuel to cool longer to a point where the decrease in fuel region dose rate matches the increased dose rate due to the additional CEA material. Hence, it is necessary to determine the amount by which the dose rate increases as a result of the added material. A one-dimensional calculation of this additional dose rate is not reasonable due to the geometry of the CEA source region. One-dimensional buckling corrections are inaccurate for a cylindrical source where the ratio of height to diameter of the source is less than unity, as is the case here.

Instead, the additional contribution to dose rate due to the activated material is computed by a detailed three-dimensional shielding model. The model is based on the three-dimensional models described in Section 5.3. However, the fuel is modeled in a Class 2 canister since that canister will be used to ship CEA-bearing assemblies. The geometric implication of the Class 2 canister is that with a shorter canister spacer employed, the end fitting source region will be located at a lower axial position than it would be for the Class 1 canister. This moves the source region closer to a point of minimal shielding.

The three-dimensional shielding evaluation is conducted for the CE 14 x 14 fuel at a burnup of 45,000 MWD/MTU and initial enrichment of 3.7 wt % for consistency with the design basis fuel evaluated in Section 5.4.2. According to the cool time analysis conducted for CE 14 x 14 fuel with no additional non-fuel material in Section 5.5.1.1.4, this fuel will require 9 years cool time before it is acceptable for shipment in the UMS transport cask. Hence, the 9-year cooled CE 14 x 14 at 45,000 MWD/MTU and 3.7 wt % initial enrichment provides the base case for the dose rate limit adjustment calculation. This case is referred to as the Class 1 case below.

Additional three-dimensional models are defined based on the base case fuel configuration in a Class 2 canister and either containing a design basis CEA assumed to be cooled for 5, 10, 15, or 20 years or containing no CEA at all (NoCEA case below). This latter configuration is important because the slight geometry difference between Class 1 and Class 2 canisters (with respect to axial source location) is sufficient to require a modification to the cool time analysis for non-CEA containing assemblies when loaded in the Class 2 canister. Hence, the approach taken here considers the dose rate impact of both 1) the geometrical difference between Class 1 and Class 2 canisters and 2) the additional source due to activated CEA hardware.

5.5.1.1.4.1.2 CEA Source Spectra

For the Class 2 configuration with CEAs, the only difference between the cases is the combined CEA source modeled in the lower eight inches of the active fuel region. The required CEA spectra are shown in Table 5.5.1.1-2.

5.5.1.1.4.1.3 Three-Dimensional Model Results

Table 5.5.1.1-11 gives the three-dimensional UMS Transport bottom model results for each case. Only the bottom model is considered because the top model is not sensitive to changes in the CEA description. The Ratio column shown in the table gives the ratio between the base case maximum 2m+Railcar dose rate and the value computed for each remaining CEA case. This quantity is used to scale the one-dimensional design basis normal conditions dose rate limit of 6.71 mrem/hr in order to determine a modified limiting value applicable to each CEA decay case. The resulting dose rate limits are shown in the "Limit" column of the table.

5.5.1.1.4.1.4 Decay Heat Limits

As discussed in Section 5.5.1.1.1.1, the additional decay heat associated with a full cask of CEAs is conservatively taken as 0.350 kW/cask. This additional heat load is accounted for by reducing the fuel assembly decay heat limits by this amount.

5.5.1.1.4.1.5 Loading Table Analysis

With the adjusted one-dimensional dose and heat generation rate limits established above, the loading table analysis proceeds following the methodology developed in Section 5.4.3. Each combination of initial enrichment and burnup is analyzed to determine the minimum required cool time in order for an assembly to either 1) contain a design basis CEA cooled 5, 10, 15, or 20 years or 2) to be present in a Class 2 canister with no CEA inserted. The resulting cool times are shown in Table 5.5.1.1-12.

Table 5.5.1.1-9 Isotopic Compositions of Maine Yankee CE14x14 Canister Annular Region Materials (One-Dimensional Analysis Only)

Isotope	Fuel Annulus [atom/b-cm]	Upper Plenum Annulus [atom/b-cm]	Upper End Fit Annulus [atom/b-cm]	Lower End Fit Annulus [atom/b-cm]
ALUMINUM	5.96817E-03	–	–	–
CHROMIUM(SS304)	1.77895E-03	9.31065E-04	2.53529E-03	4.13797E-03
MANGANESE	1.77228E-04	9.27577E-05	2.52579E-04	4.12247E-04
IRON(SS304)	6.05870E-03	3.1710E-03	8.63463E-03	1.40930E-02
NICKEL(SS304)	7.88057E-04	4.12453E-04	1.12311E-03	1.83308E-03

Table 5.5.1.1-10 Loading Table for Maine Yankee CE14x14 Fuel with No Non-Fuel Material – Required Cool Time in Years Before Assembly is Acceptable

Loading Table for CE14x14 Fuel with No Non-Standard Fuel Material					
Enrichment	Burnup (B) [GWD/MTU]				
[wt %]	$B \leq 30$	$30 < B \leq 35$	$35 < B \leq 40$	$40 < B \leq 45$	$45 < B \leq 50$
$1.9 \leq E < 2.1$	6 years	8 years	11 years	18 years	27 years
$2.1 \leq E < 2.3$	6 years	7 years	10 years	15 years	24 years
$2.3 \leq E < 2.5$	6 years	7 years	9 years	14 years	22 years
$2.5 \leq E < 2.7$	6 years	7 years	9 years	12 years	19 years
$2.7 \leq E < 2.9$	6 years	6 years	8 years	11 years	17 years
$2.9 \leq E < 3.1$	5 years	6 years	8 years	10 years	15 years
$3.1 \leq E < 3.3$	5 years	6 years	7 years	10 years	15 years
$3.3 \leq E < 3.5$	5 years	6 years	7 years	9 years	15 years
$3.5 \leq E < 3.7$	5 years	6 years	7 years	9 years	14 years
$3.7 \leq E \leq 4.2$	5 years	6 years	7 years	9 years	14 years

Table 5.5.1.1-11 Three-Dimensional Shielding Analysis Results for Various Maine Yankee CEA Configurations Establishing One-Dimensional Dose Rate Limits for Loading Table Analysis

CEA Cool Time [y]	Dose Rate [mrem/hr]	FSD	Ratio [%]	Limit [mrem/hr]
Class 1 Result	7.70	0.72%	-	6.71
NoCea	7.92	0.63%	97.2%	6.53
5y	9.41	0.55%	81.9%	5.49
10y	8.53	0.59%	90.3%	6.06
15y	8.22	0.60%	93.6%	6.28
20y	8.08	0.61%	95.3%	6.39

Table of Contents

Table of Contents (Continued)

List of Figures

List of Figures (Continued)

List of Figures (Continued)

List of Tables

List of Tables (Continued)

List of Tables (Continued)

Table 6.2-2 BWR Fuel Assembly Characteristics (Zirc-2 Clad)

Fuel Class	Vendor	Array	Version	Max MTU	No of Fuel Rods	Pitch (in)	Rod Dia (in)	Clad Thick (in)	Pellet Dia (in)	Active Length (in)
4(5)	Ex/ANF	7 X 7	GE	0.1960	48	0.738	0.570	0.036	0.490	144
4	Ex/ANF	8 X 8	JP-3	0.1764	63	0.641	0.484	0.036	0.4045	145.2
4	Ex/ANF	9 X 9	JP-3	0.1722	79	0.572	0.424	0.03	0.3565	145.2
4	GE	7 X 7	GE-2a	0.1985	49	0.738	0.570	0.036	0.488	144
4	GE	7 X 7	GE-2b	0.1977	49	0.738	0.563	0.032	0.487	144
4	GE	7 X 7	GE-3	0.1896	49	0.738	0.563	0.037	0.477	144
4	GE	8 X 8	GE-4	0.1855	63	0.640	0.493	0.034	0.416	144
4	GE	8 X 8	GE-5	0.1788	62	0.640	0.483	0.032	0.410	145.2
4	GE	8 X 8	GE-6 (prep)	0.1788	62	0.640	0.483	0.032	0.410	145.2
4	GE	8 X 8	GE-7 (barr)	0.1788	62	0.640	0.483	0.032	0.410	145.2
4	GE	8 X 8	GE-8	0.1730	60	0.640	0.484	0.032	0.410	145.2(1)
4	GE	8 X 8	GE-10	0.1730	60	0.640	0.484	0.032	0.410	145.2(1,2)
5(6)	Ex/ANF	8 X 8	JP-4,5	0.1793	62	0.641	0.484	0.036	0.4045	150
5	Ex/ANF	9 X 9	JP-4,5	0.1779	79	0.572	0.424	0.03	0.3565	150
5	Ex/ANF	9 X 9	JP-4,5	0.1666	74	0.572	0.424	0.03	0.3565	150
5	GE	7 X 7	GE-2	0.1977	49	0.738	0.563	0.032	0.487	144
5	GE	7 X 7	GE-3a	0.1896	49	0.738	0.563	0.037	0.477	144
5	GE	7 X 7	GE-3b	0.1923	49	0.738	0.563	0.037	0.477	146
5	GE	8 X 8	GE-4a	0.1855	63	0.640	0.493	0.034	0.416	144
5	GE	8 X 8	GE-4b	0.1880	63	0.640	0.493	0.034	0.416	146
5	GE	8 X 8	GE-5	0.1847	62	0.640	0.483	0.032	0.410	150(1)
5	GE	8 X 8	GE-6 (prep)	0.1847	62	0.640	0.483	0.032	0.410	150(1)
5	GE	8 X 8	GE-7 (barr)	0.1847	62	0.640	0.483	0.032	0.410	150(1)
5	GE	8 X 8	GE-10	0.1787	60	0.640	0.484	0.032	0.410	150(1,2)
5	GE	9 X 9	GE-11	0.1854	74	0.566	0.441	0.028	0.376	150(1,3,4)
5	GE	9 X 9	GE-11	0.1979	79	0.566	0.441	0.028	0.376	150(1,3,4)

Notes
1. 6-in. natural uranium blankets on top and bottom.
2. 1 large water hole - 3.2 cm ID, 0.1 cm thickness.
3. 2 large water holes occupying 7 fuel rod locations - 2.5 cm ID, 0.07 cm thickness.
4. Shortened active fuel length in some rods.
5. Class of fuel for BWR/2-3.
6. Class of fuel for BWR/4-6.

Table 6.2-3 UMS® Transport Cask Top End Impact Bounding Fuel Dimensions

UMS® Canister Class	**1**	**2**	**3**	**4**	**5**
Vendor	WE	B&W	CE	Ex/ANF	GE
Array	15 x 15	15 x 15	16 x 16	9 x 9	8 x 8
Active Fuel Length (inch)	144	144	150	145.24	150
Fuel Rod Height (inch)	152.756	153.125	161.168	155.52	160.55
Top End-Cap Height (inch)	0.685	0[1]	0.5	0.345	0.345
Bottom End-Cap Height (inch)	0.685	0[1]	0.891	0.355	0.625
Lower Plenum Region Height (inch)	0	4.5625	0	0	0
Fuel Assembly Height (inch)	160.1	165.625	176.803	171.29	176.16
Lower Nozzle Height (inch)	2.738	2	3.812	6.94	6.76
Upper Nozzle Height (inch)	3.48	8.875	9.723	7.5	7.5
Gap Fuel Rod To Bottom Nozzle (inch)	0	0	0	0	0
Upper Plenum Region Height (inch)	5.01	4.5625	9.527	9.58	9.58
Gap Fuel Rod To Top Nozzle (inch)	1.037	1.625	2.1	1.33[2]	1.35[2]

1 A portion of this end cap is hollow. The end cap height is, therefore, conservatively set to zero.
2 This value represents the thin portion of the top end cap that normally resides below the top tie plate.

clad inner radius and increasing the clad outer radius, i.e. increasing clad thickness. Decreasing the pellet radius of the BWR fuel assembly was also determined to significantly decrease the reactivity. These results are expected, as these perturbations decrease the H/U ratio in the undermoderated fuel lattice. Additionally, varying the BWR water rod dimensions was determined to have an insignificant effect on the reactivity of the system. Therefore, these nominal dimension variations are not of concern with regard to the criticality safety of the system.

The following perturbations were determined to significantly increase the reactivity of both the PWR and BWR systems: increasing the clad inner radius and decreasing the clad outer radius, i.e., decreasing clad thickness. Increasing the guide tube inner radius or decreasing the guide tube outer radius, both decreasing tube thickness, was determined to significantly increase the reactivity of the PWR systems. The increase in reactivity is due to the fact that these perturbations increase the H/U ratio in the undermoderated fuel lattice.

A slight increase in reactivity, 0.004 Δk, is also seen in the PWR system when decreasing the pellet diameter. This is due to flooding of the pellet-to-clad gap in the accident model, which provides additional moderator to the lattice. Since 100% of clad failure is not expected during normal or accident operating conditions, no lower bound limit is placed on the fuel pellet diameter.

The effect on reactivity from perturbations in the nominal fuel dimensions requires the following limits on the fuel assembly lattice parameters in order to retain the maximum reactivity of the UMS system below existing design basis results:

PWR

a) Fuel Rod Diameter ≥ Nominal Dimension
b) Clad Thickness ≥ Nominal Dimension
c) Fuel Rod Pitch ≤ Nominal Dimension
d) Guide Tube (Instrument Tube) Thickness ≥ Nominal Dimension
e) Pellet Diameter ≤ Nominal Dimension

BWR

a) Fuel Rod Diameter $\geq$ Nominal Dimension
b) Clad Thickness $\geq$ Nominal Dimension
c) Fuel Rod Pitch $\leq$ Nominal Dimension
d) Pellet Diameter $\leq$ Nominal Dimension

6.4.5 Evaluation of Transport Cask End Impact

Evaluation of BWR System Top End Impact

Axial shifting of the contents of the Transportable Storage Canister (TSC) occurs as a result of a top end impact load condition for the transport cask containing a loaded TSC. In this scenario of contents shifting, the fuel assembly and the basket are considered to be shifted upward to contact the canister lid. The distance between the canister lid and the neutron absorber sheets, which are attached to the fuel tubes, and the distance between the top of the fuel assembly and the active fuel region are required to establish the height of active fuel exposed beyond the neutron absorber for any given assembly. Exposure of the active fuel in any specific fuel type occurs if the minimum distance between the top of the assembly and the top of the active fuel region is less than the maximum distance from the canister lid to the top of the neutron absorber sheet. The exposed fuel height evaluation is performed for each BWR fuel assembly type that is proposed to be loaded into the UMS® canister. The calculation is divided into three stages: calculation of the neutron absorber offset, determination of the active fuel offset, and calculation of the fuel exposure.

In stage one, the maximum distance between the top of the neutron absorber sheet and the canister lid is determined for each UMS® BWR canister class (Classes 4 and 5). The maximum distance provides the greatest fuel exposure, when considering a shifted fuel assembly. This distance depends on the canister class specific weldment, basket, tube and neutron absorber lengths; the relative location of the neutron absorber on the fuel tube; and tolerances associated with the basket components. The maximum distance for a BWR basket shifted to the canister lid is provided in Table 6.4-19.

In the second stage of the analysis, the minimum distances between the canister lid and the fuel assembly, and between the top of the fuel assembly and the active fuel region are determined for each BWR fuel type. Since the fuel assembly is shifted to contact the canister lid, the distance between the lid and the fuel assembly is always zero. The active fuel shifting condition in the fuel assembly assumes that:

- BWR fuel rods are either tie rods connecting the top and bottom nozzles, or are rods manufactured with an external spring between the top of the fuel rod and the top nozzle tie plate. For this evaluation, all external springs are ignored. Therefore, all BWR fuel rods are allowed to shift axially into contact with the top tie plate.
- Within BWR fuel rods, the fuel is assumed to shift upward into the plenum region. Each plenum region contains a plenum spring. Detailed structural analyses have shown that during a 60g top end impact, the BWR plenum spring will compress and rebound 1.729 inches. The fuel material in the rods is assumed to shift and remain in contact with the compressed plenum spring. A review of plenum length and spring data for various rod designs indicates a minimum of 13% of the BWR plenum space is occupied by a solid height plenum spring. The final height of the plenum spring is calculated from the sum of the solid height of the spring and a spring rebound height of 1.729 inches.
- Detailed structural analyses of the BWR assembly have also shown that during a 60g top end impact, the lifting bail will deform. The maximum BWR bail deformation was calculated to be 2.371 inches.

Therefore, spacing from the assembly top to the active fuel region is controlled by the top end-fitting height, the fuel rod end-plug height and the distance the active fuel moves into the top plenum. In the case of BWR rods, the end-plug height includes only the portion of the plug below the tie plate when the fuel rod is shifted up. The distance between the top of the fuel assembly and the active fuel region for the bounding (minimum offset) fuel types in each canister class is presented in Table 6.4-19. Also included in Table 6.4-19 is the Class 5 Exxon/ANF 9x9 assembly, since this assembly represents the maximum reactivity radial lattice geometry.

In the third stage of the evaluation, the maximum active fuel exposure (or minimum coverage) for each fuel type is determined by simply subtracting the active fuel offset from the neutron absorber offset. A positive value indicates active fuel is exposed (i.e., neutron absorber does not cover the entire active fuel region).

As shown in in Table 6.4-19, the maximum lengths of exposed BWR fuel result for the Exxon/ANF 9x9 and GE 8x8 BWR fuel assemblies at 4.312 inches. For further conservatism in the criticality analysis, the active fuel exposure length is increased to 7.625 inches for BWR fuel assemblies.

As previously mentioned, the maximum length of exposed fuel is not obtained from the BWR fuel assembly defined as having the maximum reactivity in Section 6.4. The maximum reactivity

BWR assembly documented in the SAR is the UMS® Class 5 Exxon/ANF 9x9 (79 fuel rod) assembly for BWR canisters. Therefore, rather than analyzing each fuel type with its specific exposed fuel height, the evaluated exposed fuel height of 7.625 inches (BWR) is applied to the Class 5 Exxon/ANF 9x9 BWR assembly.

To model the 7.625-inch exposed fuel length for the Class 5 Exxon/ANF 9 x 9 BWR fuel assembly criticality evaluation, a number of modifications are made to the nominal (unshifted) fuel and basket model.

- Fuel assemblies are shifted to the canister lid.
- Fuel rods are spaced from the top tie plate by the external spring.
- The active fuel is moved to the midpoint of the plenum.
- The top-nozzle height is reduced by 4.7 inches.
- The BWR neutron absorber sheet is reduced by 3.009 inches.

These model modifications produce a fuel exposure identical to that obtained by shifting the fuel in the rod until the plenum spring is compressed, by shifting the fuel rods axially against the top tie plate, by shifting the assembly and the basket axially against the canister lid, by reducing the bail height by 2.371 inches, and by reducing the neutron absorber (BORAL) height by 3.323 inches. This neutron absorber height reduction is determined based on modeling the 7.625-inch fuel exposure versus the actual 4.302-inch fuel exposure of the Class 5 Exxon/ANF 9x9 fuel assembly.

Evaluation of PWR System Top End Impact

Axial shifting of the contents of the Transportable Storage Canister (TSC) occurs as a result of a top end impact load condition for the transport cask containing a loaded TSC. In this scenario of contents shifting, the conservatively toleranced basket is assumed to remain in contact with the canister baseplate, while the fuel assembly is shifted up to contact the canister lid. The distance between the canister lid and the neutron absorber sheets, which are attached to the fuel tubes, and the distance between the top of the fuel assembly and the active fuel region are required to establish the height of active fuel exposed beyond the neutron absorber for any given assembly. Exposure of the active fuel in any specific fuel type occurs if the minimum distance between the top of the assembly and the top of the active fuel region is less than the maximum distance from the canister lid to the top of the neutron absorber sheet. The exposed fuel height evaluation is performed for each PWR fuel assembly type that is proposed to be loaded into the UMS®

canister. The calculation is divided into three stages: calculation of the neutron absorber offset, determination of the active fuel offset, and calculation of the fuel exposure.

In stage one, the maximum distance between the top of the neutron absorber sheet and the canister lid is determined for each UMS® PWR canister class (Classes 1, 2, and 3 for PWR fuel assemblies). The maximum distance provides the greatest fuel exposure, when considering a shifted fuel assembly. This distance depends on the canister class specific weldment, basket, tube and neutron absorber lengths; the relative location of the neutron absorber on the fuel tube; and tolerances associated with the basket components. The maximum distances for a PWR basket at the bottom of the canister are provided in Table 6.4-19.

In the second stage of the analysis, the minimum distances between the canister lid and the fuel assembly, and between the top of the fuel assembly and the active fuel region are determined for each PWR fuel type. Since the fuel assembly is shifted to contact the canister lid, the distance between the lid and the fuel assembly is always zero (no credit is taken for any offset produced by the PWR leaf springs). The active fuel shifting condition in the fuel assembly assumes that:

- In PWR fuel assemblies, where a space exists between the fuel rod end-cap and the end-fitting, the fuel rods are shifted within the grid until contact is made with the top end-fitting (zero gap).
- Within the PWR fuel rods, the fuel is assumed to shift upward into the plenum region. Each plenum region contains a spring, which will fully compress during an upper end impact. The fuel material in the rods is assumed to shift and remain in contact with the fully compressed (solid height) plenum spring. A review of plenum length and spring data for various rod designs indicates a minimum of 31% of the PWR plenum space is occupied by a solid height plenum spring.
- Detailed structural analyses of the PWR assembly have shown that during a 60g top end impact, no significant damage to the top end-fitting (i.e., no height reduction) occurs.

Therefore, spacing from the assembly top to the active fuel region is controlled by the end-fitting height, the fuel rod end-plug height and the distance the active fuel moves into the top plenum. The distance between the top of the fuel assembly and the active fuel region for the bounding (minimum offset) fuel types in each canister class is presented in Table 6.4-19. Also included in Table 6.4-19 is the Westinghouse 17x17 OFA assembly, since this assembly represents the maximum reactivity radial lattice geometry.

In the third stage of the evaluation, the maximum active fuel exposure (or minimum coverage) for each fuel type is determined by simply subtracting the active fuel offset from the neutron absorber offset. A positive value indicates active fuel is exposed (i.e., neutron absorber does not cover the entire active fuel region), while a negative value indicates full active fuel coverage and additional coverage to that extent.

As shown in Table 6.4-19, the maximum lengths of exposed PWR fuel result for the Westinghouse 15x15 PWR fuel assembly at 4.472 inches. For further conservatism in the criticality analysis, the active fuel exposure length is increased to 4.52 inches for PWR fuel assemblies.

As previously mentioned, the maximum length of exposed fuel is not obtained from the PWR fuel assembly defined as having the maximum reactivity in Section 6.4. The maximum reactivity PWR assembly documented in the SAR is the Westinghouse 17x17 OFA assembly for PWR canisters. Therefore, rather than analyzing each fuel type with its specific exposed fuel height, the evaluated exposed fuel height of 4.52 inches (PWR) is applied to the Westinghouse 17x17 OFA PWR assembly.

To model the 4.52-inch exposed fuel length for the Westinghouse 17x17 OFA PWR fuel assembly criticality evaluation, a number of modifications are made to the nominal (unshifted) fuel and basket model.

- Fuel assemblies are shifted to the canister lid.
- Fuel rods are shifted to the top end-fitting.
- The active fuel is moved to the midpoint of the plenum.
- The top end-fitting height is reduced by 1 inch.
- The PWR neutron absorber sheet is reduced by 0.815 inch.

These model modifications produce a fuel exposure identical to that obtained by shifting the fuel in the rod against the solid height plenum spring, by axial movement of the fuel rods and assembly, and a 0.626-inch reduction in neutron absorber (BORAL) height. This neutron absorber height reduction is determined based on modeling the 4.52-inch fuel exposure versus the actual 3.894-inch fuel exposure of the Westinghouse 17x17 OFA fuel assembly.

Fuel Assembly Minimum Intact Hardware Dimension Limits

Based on limiting the exposed height of active fuel to 4.52 inches for the PWR fuel assemblies and to 7.625 inches for the BWR fuel assemblies, intact fuel assembly hardware limits are defined to assure compliance with the safety basis of the analysis. These limits consider zero PWR top end-fitting deformation, 2.371 inches of BWR top end-fitting (lifting bail) deformation and a BWR plenum spring rebound height of 1.729 inches. The limits for each UMS® canister class containing PWR fuel are calculated by subtracting the height of exposed fuel, 4.52 inches, from the distance between the canister lid and the top of the neutron absorber. The limits for each UMS® canister class containing BWR fuel are calculated by subtracting the sum of the height of exposed fuel, 7.625 inches, and the plenum spring rebound height, 1.729 inches, from the sum of the lifting bail deformation, 2.371 inches, and the distance between the canister lid and the top of the neutron absorber. These resulting limits are provided in Table 6.4-20.

Each minimum axial assembly dimension is a generic limit that all fuel types in the respective fuel class shall meet. Compliance with these limits will ensure that the exposed fuel heights evaluated and found to result in a subcritical system will not be exceeded. For PWR fuel, the minimum intact assembly hardware dimension above the active fuel shall be calculated by summing the top end-fitting height, the top end cap height, and the solid height of the plenum spring. For BWR fuel, the minimum axial assembly dimension above the active fuel shall be calculated by summing the intact top end-fitting height, the portion of the top end-cap height below the tie plate when the fuel rod is shifted up, and the solid height of the plenum spring. Tolerances on these components shall be conservatively considered when calculating the subject dimension.

Evaluation of Bottom End Axial Fuel Shifting

Similar to the top end evaluation, a bounding hypothetical axial fuel-shifting condition is considered in which all of the fuel rods are shifted to the bottom of each assembly. For PWR fuel assemblies with a lower plenum, the fuel within every rod is assumed to shift downward to contact a fully compressed plenum spring. Each fuel assembly is assumed to remain in contact with the canister bottom plate. The basket dimensions used assume conservative tolerances, and the basket is conservatively assumed to be shifted upward to contact the canister shield lid. This bounding axial shifting scenario results in the maximum distance from the canister bottom plate to the lower end of the neutron absorber panels. For all UMS® PWR canister classes, this distance is limited to 5.22 inches. For all UMS® BWR canister classes, the distance is limited to 8.19 inches. However, all PWR and BWR fuel assembly types have rod bottom end caps, tie plates and/or components of the bottom end-fitting/nozzle that will not deform to a total height of less than 0.7 inches. Consequently, the top end axial fuel shifting condition, which considers exposed fuel lengths of 4.52 inches for PWR fuel and 7.625 inches for BWR fuel, bounds the bottom end axial fuel shifting condition.

End Impact Accident Condition Effect on System Reactivity

The bounding PWR system end impact event does not significantly affect the reactivity of the system. Therefore, poison sheet coverage is adequate for all allowed PWR fuel contents of the UMS® system. The bounding BWR end impact event increases the reactivity of the system. This increase in reactivity, a Δk_{eff} of 0.0249, is added to the most reactive accident condition system reactivity, $k_{eff} \pm 2\sigma$, of 0.9108 ± 0.0008 as determined in Section 6.4.3.3, to establish a maximum BWR system reactivity, $k_{eff} \pm 2\sigma$, of 0.9357 ± 0.0008. This value is less than the USL of 0.9361 identified in Section 6.5.4. Including code bias, code bias uncertainty, and statistical uncertainty (2σ) in accordance with Equation 6 in Section 6.5.3, the resulting system k_s of 0.9497 is less than 0.95. Thus, poison sheet coverage is adequate for all allowed BWR fuel contents of the UMS® system.

6.4.6 Regulatory Compliance

The licensing requirements for criticality analyses are provided in 10 CFR 71.55 and 10 CFR 71.59 for shipment of radioactive material.

10 CFR 71.55 and 10 CFR 71.59 require that the fissile material package be subcritical under any credible condition, e.g., optimum interior/exterior moderation and reflection and credible configuration of the material. A criticality transport index is to be assigned to the fissile material package. This transport index must be based on the number of packages (casks in this context) remaining subcritical in an array configuration.

Additional requirements imposed include the reduction in poison plate ^{10}B from 100 to 75 percent and water in the pellet-to-cladding gap.

Undamaged Cask

Compliance with the requirements of paragraphs (b) and (d) of 10 CFR 71.55 is shown by modeling an undamaged cask surrounded by water. Requirements of paragraphs (a) through (c) of 10 CFR 71.59 are satisfied by providing a value of "N" equal to infinity and a criticality transport index of 0 by imposing reflecting boundary conditions on the sides of the model simulating an infinite array of undamaged casks. Optimum interior and exterior moderation, including exterior full reflection by more than 20 cm of water, shows compliance with 10 CFR 71.55 paragraphs (b)(2), (b)(3) and (d)(3). Normal operating conditions for the transport cask include a dry canister cavity. The canister is loaded, dried, and seal welded inside a transfer cask. Only after the canister is dried and sealed is it placed into the transport cask. A set of exterior moderator density and cask pitch analyses show compliance with 10 CFR 71 under dry cavity conditions.

Damaged Cask

Compliance with the requirements of paragraph (e) of 10 CFR 71.55 is shown by modeling a damaged cask surrounded by water. Compliance with 10 CFR 71.59 is automatically demonstrated by imposing reflection boundary conditions on the sides of the model to simulate an infinite array of damaged casks, thereby resulting in a criticality transport index of 0. Optimum interior and exterior moderation, including exterior full reflection by more than 20 cm of water, shows compliance with 10 CFR 55 paragraphs (e)(2) and (e)(3) and 10 CFR 71.59 paragraph (a)(2).

A damaged transport cask is defined as having been subjected to the hypothetical accident conditions specified in 10 CFR 71. Under these conditions the cask containment is maintained, and the cavity therefore remains dry. However, to show the cask's capability to remain subcritical under optimum internal and external moderation, an internally wet cask is analyzed. During the accident, the radial neutron shield is assumed to be lost as a result of fire and is replaced by the external moderator. Even though the fuel is assumed to remain intact following the cask drop, the pellet-to-clad gap is assumed to be filled by the internal-to-cask moderator. Introducing additional moderator into the normally under-moderated fuel assembly lattice increases reactivity.

Figure 6.4-1 Visage Slice - Hypothetical Shifting of PWR Fuel

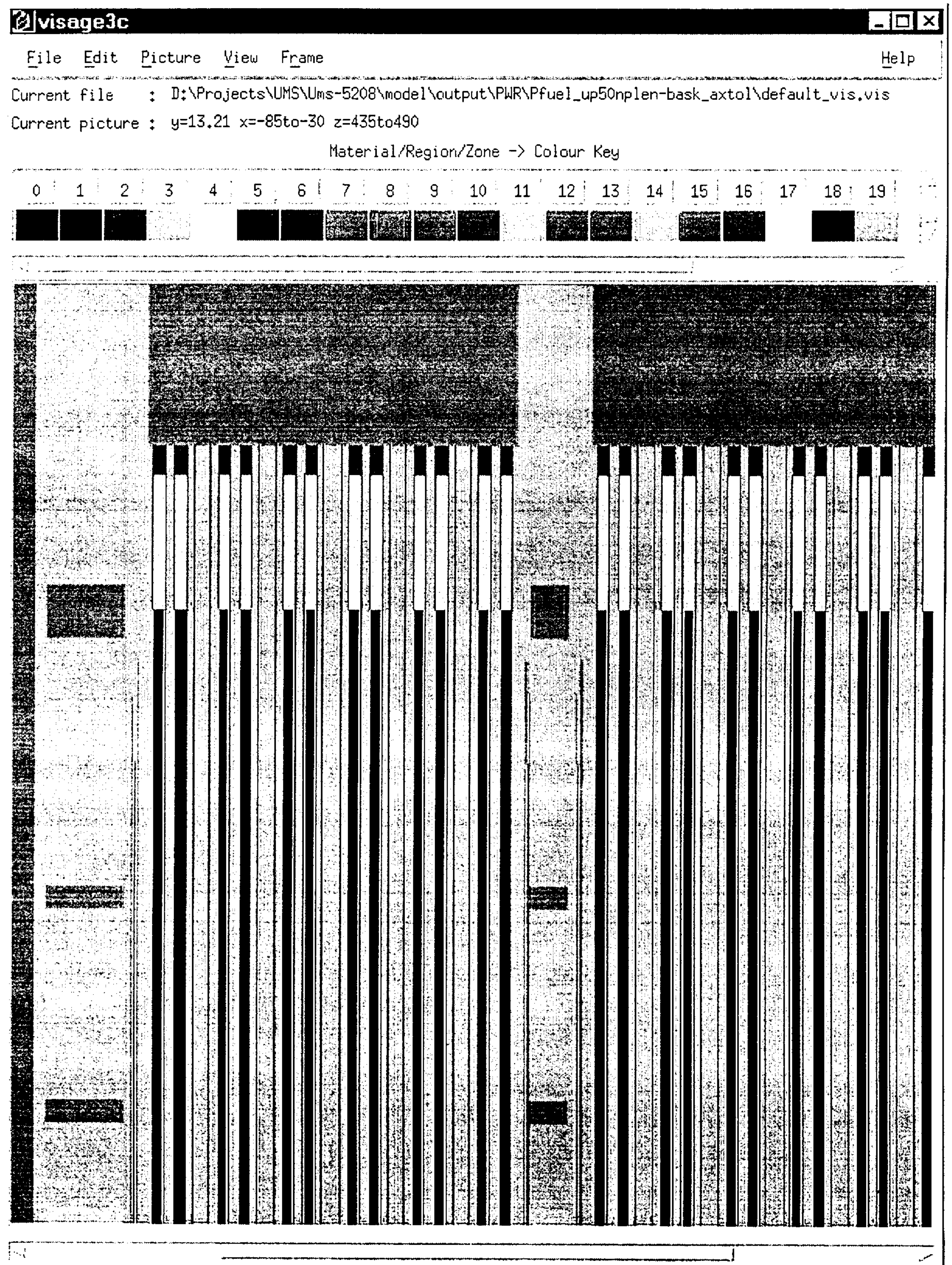

Figure 6.4-2 Visage Slice - Hypothetical Shifting of BWR Fuel

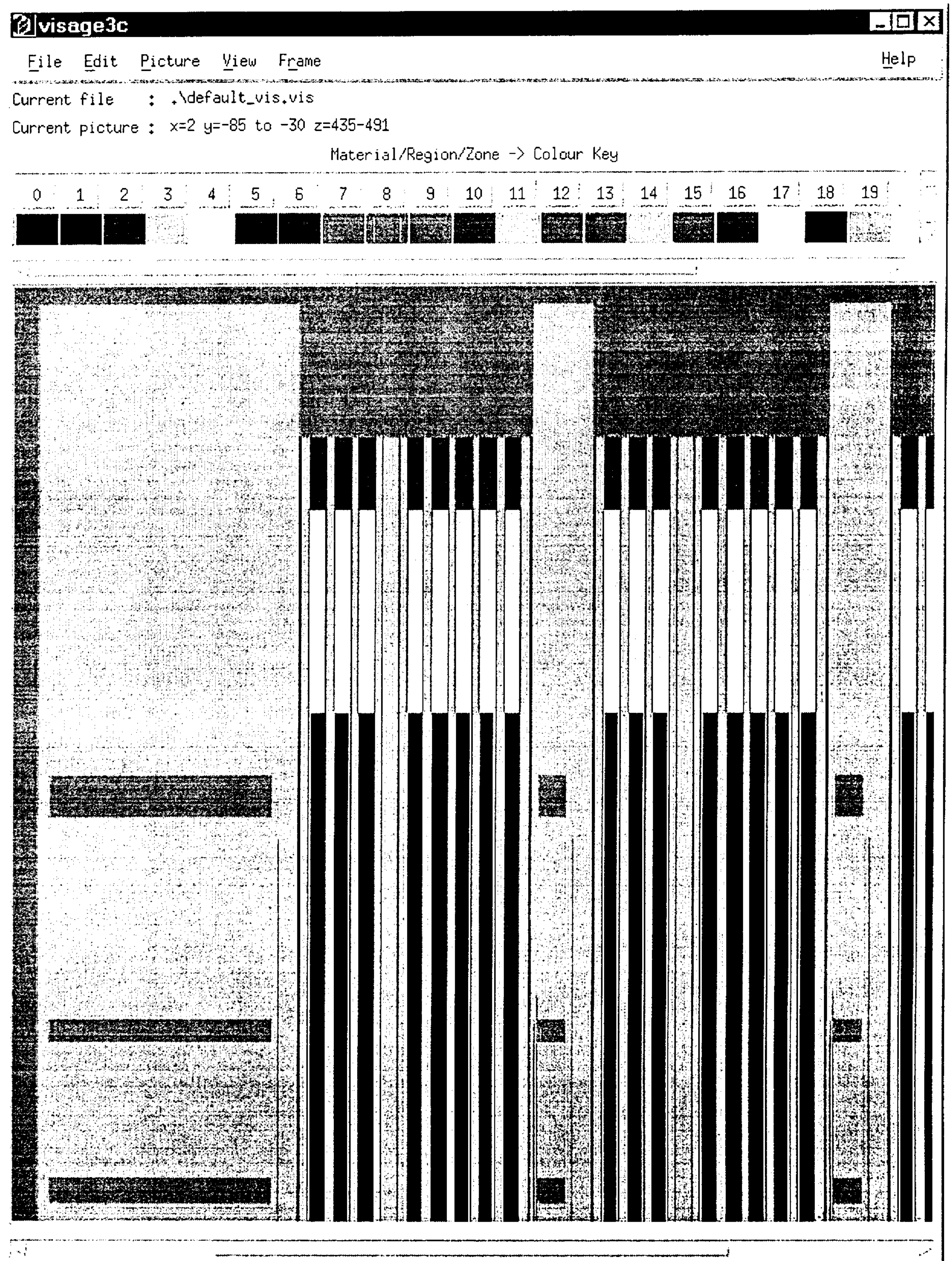

Table 6.4-1 k_{eff} for Most Reactive PWR Fuel Assembly Determination (1.0-in. Web)

Assembly Type	Dry Gap		Wet Gap		Δk_{eff} Wet - Dry
	k_{eff}	σ	k_{eff}	σ	
B&W 15x15 Mark B4	0.9613	0.0011	0.9692	0.0012	0.0079
B&W 17x17 Mark C	0.9621	0.0012	0.9705	0.0011	0.0084
CE 14x14	0.9295	0.0013	0.9381	0.0011	0.0085
CE 16x16 SYS 80	0.9356	0.0012	0.9372	0.0012	0.0016
West 14x14	0.9177	0.0013	0.9264	0.0012	0.0086
West 14x14 OFA	0.9238	0.0012	0.9326	0.0012	0.0088
West 15x15	0.9662	0.0011	0.9712	0.0012	0.0050
West 17x17	0.9596	0.0012	0.9673	0.0012	0.0077
West 17x17 OFA	0.9656	0.0013	0.9727	0.0012	0.0070
Ex/ANF 14x14 CE	0.9309	0.0012	0.9362	0.0011	0.0053
Ex/ANF 14x14 WE	0.9065	0.0012	0.9176	0.0011	0.0111
Ex/ANF 15x15 WE	0.9559	0.0012	0.9634	0.0013	0.0074
Ex/ANF 17x17 WE	0.9631	0.0012	0.9704	0.0012	0.0073

Table 6.4-2 k_{eff} for Highest Reactivity Assemblies in 1.5-in. Web (Dry Gap)

Assembly Type	k_{eff}	σ
B&W 15x15 Mark B4	0.9119	0.0011
B&W 17x17 Mark C	0.9141	0.0011
West 15x15	0.9147	0.0013
West 17x17	0.9116	0.0012
West 17x17 OFA	0.9196	0.0012
Ex/ANF 17x17 WE	0.9172	0.0011

Table 6.4-3 k_{eff} for Most Reactive BWR Fuel Assembly Determination

Assembly Type	Number Rods		Channel Thickness	Dry Gap		$\Delta k_{eff}^{(1)}/\sigma$
	Fuel	Water		k_{eff}	σ	
GE 7x7	49	0	80 mil	0.8807	0.0012	-6.678
GE 8x8	63	1	80 mil	0.8765	0.0012	-9.992
GE 8x8	63	1	100 mil	0.8755	0.0012	-10.760
GE 8x8	63	1	120 mil	0.8784	0.0011	-9.098
GE 8x8	62	2	80 mil	0.8821	0.0011	-5.708
GE 8x8	62	2	100 mil	0.8823	0.0011	-5.513
GE 8x8	60	4	2 mm	0.8772	0.0012	-9.644
GE 9x9	79	2	2 mm	0.8796	0.0011	-8.434
GE 9x9	74	$2^{(2)}$	2 mm	0.8778	0.0011	-9.558
GE 9x9	74	$2^{(2)}$	80 mil	0.8847	0.0012	-3.342
Ex/ANF 7x7	49	0	80 mil	0.8792	0.0012	-7.634
Ex/ANF 8x8	63	1	80 mil	0.8778	0.0012	-8.861
Ex/ANF 8x8	62	2	80 mil	0.8787	0.0012	-8.517
Ex/ANF 9x9	79	2	2 mm	0.8886	0.0009	0.000
Ex/ANF 9x9	79	2	80 mil	0.8873	0.0008	-1.464
Ex/ANF 9x9	74	$2^{(2)}$	80 mil	0.8862	0.0012	-2.034

Note:

(1) $\Delta k_{eff} = k_{eff} - k_{eff}$(Ex/ANF 9x9 79 Fuel rod 80 mil channel)

(2) Two large water rods occupying the space of seven fuel rods.

Table 6.4-4 PWR Fuel Tube in Basket Model KENO-Va Results for Geometric Tolerances and Mechanical Perturbations

	k_{eff}	σ	Δk_{eff}	$\Delta k_{eff}/\sigma$
Reference case	0.9582	0.0006		
Dimensions Tolerance on Disk Opening Center Location				
Minimum web	0.9598	0.0006	0.0015	2.6
Maximum web	0.9575	0.0006	-0.0008	-1.3
Dimensions tolerance on tube opening				
Minimum tube	0.9546	0.0006	-0.0036	-6.2
Maximum tube	0.9627	0.0006	0.0045	7.6
Dimension tolerance on disk opening				
Minimum opening	0.9594	0.0006	0.0012	2.0
Maximum opening	0.9591	0.0006	0.0008	1.4
Fuel movement in tube - tube centered in disk opening				
Mirrored boundary	0.9572	0.0006	-0.0011	-1.8
Periodic boundary	0.9566	0.0006	-0.0016	-2.8
Tube movement in disk opening - fuel assembly centered in tube				
Mirrored boundary	0.9606	0.0006	0.0024	4.0
Periodic boundary	0.9591	0.0006	0.0009	1.5
Move fuel tube in opening and assembly in tube				
Mirrored boundary	0.9595	0.0006	0.0012	2.1
Periodic boundary	0.9567	0.0006	-0.0015	-2.5

Table 6.4-5 PWR Basket in Cask KENO-Va Results for Geometric Tolerances and Tube Movement

Analysis	k_{eff}	σ	Δk_{eff}	$\Delta k_{eff}/\sigma$
Nominal	0.9192	0.0009	----	----
Geometric Tolerance	0.9227	0.0009	0.0035	4.0
Geo. Tol.+Tube In	0.9286	0.0009	0.0094	11.1
Geo. Tol.+Tube Out	0.9176	0.0009	-0.0017	-1.9
Geo. Tol.+Corner	0.9240	0.0009	0.0048	5.3
Geo. Tol.+Tube Side	0.9235	0.0009	0.0043	4.8

Table 6.4-6 BWR Basket in Cask KENO-Va Results for Geometric Tolerances and Mechanical Perturbations

Analysis	k_{eff}	σ	Δk_{eff}	$\Delta k_{eff}/\sigma$
Nominal basket	0.8873	0.0008	N/A	N/A
Geometric tolerances				
Min tube	0.8860	0.0008	-0.0013	-1.607
Max tube	0.8864	0.0008	-0.0010	-1.169
Min disk opening	0.8861	0.0008	-0.0012	-1.577
Max disk opening	0.8855	0.0008	-0.0018	-2.244
Shift openings in	0.8879	0.0008	0.0006	0.702
Shift openings out	0.8891	0.0008	0.0018	2.173
Mechanical perturbations				
Assembly shift top right	0.8685	0.0008	-0.0189	-23.886
Assembly shift top	0.8780	0.0008	-0.0093	-11.402
Assembly shift top left	0.8820	0.0008	-0.0053	-6.386
Assembly shift left	0.8915	0.0008	0.0042	4.940
Assembly shift bottom left	0.8942	0.0008	0.0069	8.747
Assembly shift bottom	0.8918	0.0008	0.0045	5.531
Assembly shift bottom right	0.8801	0.0008	-0.0073	-8.667
Assembly shift right	0.8749	0.0008	-0.0124	-14.988
Assembly shift radial in	0.8990	0.0008	0.0116	14.195
Assembly shift radial out	0.8710	0.0008	-0.0163	-19.927
Fuel tube shift top right	0.8873	0.0008	0.0000	-0.048
Fuel tube shift top	0.8856	0.0008	-0.0017	-2.175
Fuel tube shift top left	0.8854	0.0009	-0.0020	-2.329
Fuel tube shift left	0.8873	0.0008	-0.0001	-0.072
Fuel tube shift bottom left	0.8858	0.0008	-0.0015	-1.795
Fuel tube shift bottom	0.8882	0.0008	0.0008	0.976
Fuel tube shift bottom right	0.8868	0.0008	-0.0005	-0.607
Fuel tube shift right	0.8878	0.0008	0.0005	0.563
Fuel tube shift radial in	0.8932	0.0008	0.0058	6.952
Fuel tube shift radial out	0.8827	0.0008	-0.0046	-5.750
Combined analysis				
Tube + assembly radial in	0.9050	0.0008	0.0177	22.075

Table 6.4-7 PWR Single Cask Analysis Criticality Results

Water Density (g/cm^3)		Neutron Shield	Water in Gap	^{10}B	k_{eff}	σ	k_s
Inside	Outside						
1.0	1.0	Yes	No	100%	0.9135	0.0009	0.9276
1.0	1.0	Yes	No	75%	0.9222	0.0009	0.9362
0.0001	1.0	Yes	No	75%	0.3774	0.0006	0.3914
1.0	1.0	No	Yes	100%	0.9210	0.0009	0.9350
1.0	1.0	No	Yes	75%	0.9295	0.0009	0.9436
0.0001	1.0	No	Yes	75%	0.3782	0.0006	0.3922

Table 6.4-8 PWR Cask Array Analysis Criticality Results - Normal Condition-Dry Interior

Cask Pitch	Water Density (g/cm^3)		Neutron Shield	Water in Gap	^{10}B	k_{eff}	σ	k_s
	Inside	Outside						
Touching	0.0001	1.0	Yes	No	75%	0.3775	0.0006	0.3914
270 cm	0.0001	1.0	Yes	No	75%	0.3774	0.0006	0.3914
300 cm	0.0001	1.0	Yes	No	75%	0.3770	0.0007	0.3910
Touching	0.0001	0.8	Yes	No	75%	0.3814	0.0006	0.3954
270 cm	0.0001	0.8	Yes	No	75%	0.3820	0.0007	0.3960
300 cm	0.0001	0.8	Yes	No	75%	0.3825	0.0006	0.3965
Touching	0.0001	0.6	Yes	No	75%	0.3874	0.0006	0.4014
270 cm	0.0001	0.6	Yes	No	75%	0.3873	0.0006	0.4013
300 cm	0.0001	0.6	Yes	No	75%	0.3864	0.0006	0.4004
Touching	0.0001	0.4	Yes	No	75%	0.3913	0.0006	0.4052
270 cm	0.0001	0.4	Yes	No	75%	0.3928	0.0006	0.4068
300 cm	0.0001	0.4	Yes	No	75%	0.3915	0.0006	0.4055
Touching	0.0001	0.2	Yes	No	75%	0.3936	0.0007	0.4076
270 cm	0.0001	0.2	Yes	No	75%	0.3941	0.0006	0.4080
300 cm	0.0001	0.2	Yes	No	75%	0.3938	0.0006	0.4078
Touching	0.0001	0.1	Yes	No	75%	0.3960	0.0006	0.4100
270 cm	0.0001	0.1	Yes	No	75%	0.3963	0.0007	0.4103
300 cm	0.0001	0.1	Yes	No	75%	0.3962	0.0006	0.4101

Table 6.4-9 PWR Cask Array Analysis Criticality Results - Accident Condition - Wet Interior

Cask Pitch	Water Density (g/cm^3) Inside	Outside	Neutron Shield	Water in Gap	^{10}B	k_{eff}	σ	k_s
Touching	1.0	1.0	No	Yes	75%	0.9286	0.0009	0.9427
270 cm	1.0	1.0	No	Yes	75%	0.9308	0.0009	0.9448
300 cm	1.0	1.0	No	Yes	75%	0.9295	0.0009	0.9436
Touching	0.8	0.8	No	Yes	75%	0.8645	0.0008	0.8785
270 cm	0.8	0.8	No	Yes	75%	0.8649	0.0009	0.8790
300 cm	0.8	0.8	No	Yes	75%	0.8634	0.0009	0.8775
Touching	0.6	0.6	No	Yes	75%	0.7832	0.0012	0.7974
270 cm	0.6	0.6	No	Yes	75%	0.7840	0.0012	0.7982
300 cm	0.6	0.6	No	Yes	75%	0.7826	0.0011	0.7967
Touching	0.4	0.4	No	Yes	75%	0.6808	0.0010	0.6950
270 cm	0.4	0.4	No	Yes	75%	0.6800	0.0010	0.6941
300 cm	0.4	0.4	No	Yes	75%	0.6814	0.0011	0.6956
Touching	0.2	0.2	No	Yes	75%	0.5478	0.0013	0.5620
270 cm	0.2	0.2	No	Yes	75%	0.5472	0.0012	0.5614
300 cm	0.2	0.2	No	Yes	75%	0.5445	0.0011	0.5587
Touching	0.1	0.1	No	Yes	75%	0.4762	0.0009	0.4903
270 cm	0.1	0.1	No	Yes	75%	0.4769	0.0009	0.4910
300 cm	0.1	0.1	No	Yes	75%	0.4758	0.0009	0.4899

Table 6.4-10 PWR Cask Array Analysis Criticality Results—Mist Exterior

Cask Pitch	Water Density (g/cm^3) Inside	Outside	Neutron Shield	Water in Gap	^{10}B	k_{eff}	σ	k_s
Touching	1.0	0.005	No	Yes	75%	0.9285	0.0009	0.9426
300 cm	1.0	0.005	No	Yes	75%	0.9291	0.0009	0.9432
Touching	0.8	0.005	No	Yes	75%	0.8645	0.0009	0.8785
300 cm	0.8	0.005	No	Yes	75%	0.8654	0.0009	0.8795
Touching	0.5	0.005	No	Yes	75%	0.7359	0.0012	0.7501
300 cm	0.5	0.005	No	Yes	75%	0.7363	0.0011	0.7505
Touching	0.2	0.005	No	Yes	75%	0.5508	0.0012	0.5650
300 cm	0.2	0.005	No	Yes	75%	0.5488	0.0012	0.5630

Table 6.4-11 BWR Single Cask Analysis Criticality Results

Water Density (g/cm^3) Inside	Water Density (g/cm^3) Outside	Neutron Shield	Water in Gap	^{10}B	k_{eff}	σ	k_s
1.0	1.0	Yes	No	100%	0.8897	0.0008	0.9037
1.0	1.0	Yes	No	75%	0.9055	0.0008	0.9196
0.0001	1.0	Yes	No	75%	0.3924	0.0007	0.4064
1.0	1.0	No	Yes	100%	0.8949	0.0008	0.9090
1.0	1.0	No	Yes	75%	0.9077	0.0008	0.9217
0.0001	1.0	No	Yes	75%	0.3931	0.0007	0.4071

Table 6.4-12 BWR Cask Array Analysis Criticality Results - Normal Condition - Dry Interior

Cask Pitch	Water Density (gm/cm^3) Inside	Water Density (gm/cm^3) Outside	Neutron Shield	Water in Gap	^{10}B	k_{eff}	σ	k_s
Touching	0.0001	1.0	Yes	No	75%	0.3948	0.0010	0.4089
270 cm	0.0001	1.0	Yes	No	75%	0.3935	0.0010	0.4076
300 cm	0.0001	1.0	Yes	No	75%	0.3919	0.0009	0.4060
Touching	0.0001	0.8	Yes	No	75%	0.3951	0.0010	0.4092
270 cm	0.0001	0.8	Yes	No	75%	0.3971	0.0009	0.4111
300 cm	0.0001	0.8	Yes	No	75%	0.3950	0.0009	0.4091
Touching	0.0001	0.6	Yes	No	75%	0.3983	0.0011	0.4125
270 cm	0.0001	0.6	Yes	No	75%	0.3972	0.0011	0.4114
300 cm	0.0001	0.6	Yes	No	75%	0.3966	0.0008	0.4107
Touching	0.0001	0.4	Yes	No	75%	0.3985	0.0009	0.4125
270 cm	0.0001	0.4	Yes	No	75%	0.3988	0.0009	0.4129
300 cm	0.0001	0.4	Yes	No	75%	0.3989	0.0009	0.4130
Touching	0.0001	0.2	Yes	No	75%	0.3991	0.0010	0.4132
270 cm	0.0001	0.2	Yes	No	75%	0.4005	0.0008	0.4146
300 cm	0.0001	0.2	Yes	No	75%	0.3997	0.0009	0.4138
Touching	0.0001	0.1	Yes	No	75%	0.3985	0.0009	0.4125
270 cm	0.0001	0.1	Yes	No	75%	0.3995	0.0009	0.4136
300 cm	0.0001	0.1	Yes	No	75%	0.3971	0.0010	0.4112

Table 6.4-13 BWR Cask Array Analysis Criticality Results - Accident Condition - Wet Interior

Cask Pitch	Water Density (gm/cm^3) Inside	Water Density (gm/cm^3) Outside	Neutron Shield	Water in Gap	^{10}B	k_{eff}	σ	k_s
Touching	1.0	1.0	No	Yes	75%	0.9086	0.0008	0.9226
270 cm	1.0	1.0	No	Yes	75%	0.9084	0.0008	0.9224
300 cm	1.0	1.0	No	Yes	75%	0.9075	0.0008	0.9215
Touching	0.8	0.8	No	Yes	75%	0.8810	0.0008	0.8950
270 cm	0.8	0.8	No	Yes	75%	0.8785	0.0008	0.8926
300 cm	0.8	0.8	No	Yes	75%	0.8779	0.0008	0.8919
Touching	0.6	0.6	No	Yes	75%	0.8370	0.0011	0.8511
270 cm	0.6	0.6	No	Yes	75%	0.8366	0.0012	0.8508
300 cm	0.6	0.6	No	Yes	75%	0.8378	0.0011	0.8519
Touching	0.4	0.4	No	Yes	75%	0.7653	0.0015	0.7797
270 cm	0.4	0.4	No	Yes	75%	0.7698	0.0014	0.7842
300 cm	0.4	0.4	No	Yes	75%	0.7680	0.0014	0.7824
Touching	0.2	0.2	No	Yes	75%	0.6524	0.0012	0.6666
270 cm	0.2	0.2	No	Yes	75%	0.6562	0.0012	0.6704
300 cm	0.2	0.2	No	Yes	75%	0.6560	0.0012	0.6702
Touching	0.1	0.1	No	Yes	75%	0.5662	0.0013	0.5805
270 cm	0.1	0.1	No	Yes	75%	0.5708	0.0014	0.5851
300 cm	0.1	0.1	No	Yes	75%	0.5668	0.0013	0.5810

Table 6.4-14 BWR Cask Array Analysis Criticality Results —Mist Exterior

Cask Pitch	Water Density (g/cm^3) Inside	Water Density (g/cm^3) Outside	Neutron Shield	Water in Gap	^{10}B	k_{eff}	σ	k_s
Touching	1.0	0.005	No	Yes	75%	0.9098	0.0008	0.9239
300 cm	1.0	0.005	No	Yes	75%	0.9095	0.0008	0.9235
Touching	0.8	0.005	No	Yes	75%	0.8795	0.0008	0.8935
300 cm	0.8	0.005	No	Yes	75%	0.8793	0.0008	0.8933
Touching	0.5	0.005	No	Yes	75%	0.8078	0.0010	0.8219
300 cm	0.5	0.005	No	Yes	75%	0.8091	0.0011	0.8233
Touching	0.2	0.005	No	Yes	75%	0.6628	0.0012	0.6770
300 cm	0.2	0.005	No	Yes	75%	0.6604	0.0012	0.6746

Table 6.4-15 BWR Cask Array Analysis Criticality Results—Variable Exterior

Cask Pitch	Water Density (g/cm^3) Inside	Outside	Neutron Shield	Water in Gap	^{10}B	k_{eff}	σ	k_s
300 cm	1.0	1.0	No	Yes	75%	0.9075	0.0008	0.9215
300 cm	1.0	0.8	No	Yes	75%	0.9081	0.0008	0.9221
300 cm	1.0	0.6	No	Yes	75%	0.9108	0.0008	0.9248
300 cm	1.0	0.4	No	Yes	75%	0.9092	0.0008	0.9233
300 cm	1.0	0.2	No	Yes	75%	0.9094	0.0008	0.9234
300 cm	1.0	0.0	No	Yes	75%	0.9091	0.0008	0.9231

Table 6.4-16 Heterogeneous vs. Homogeneous Enrichment Analysis Results (GE)

Case		Enrichment (% ^{235}U)			Loading Pattern				
Array	Fuel Rods	Average	Min	Max	Heterog.	Homog.	k_{eff}	σ	Δk/σ
8x8	62	2.824	N/A	N/A		X	0.8024	0.0011	---
8x8	62	2.824	1.30	3.80	X		0.7894	0.0011	-12.28
8x8	62	3.750	N/A	N/A		X	0.8683	0.0011	---
8x8	62	3.750	1.73	3.98	X		0.8501	0.0011	-15.93
8x8	60	3.404	N/A	N/A		X	0.8418	0.0012	---
8x8	60	3.404	1.60	3.90	X		0.8364	0.0011	-4.53
8x8	60	3.750	N/A	N/A		X	0.8648	0.0012	---
8x8	60	3.750	1.76	4.35	X		0.8547	0.0011	-8.22
9x9	74	4.085	N/A	N/A		X	0.8884	0.0012	---
9x9	74	4.085	2.00	4.90	X		0.8785	0.0012	-8.37
9x9(1)	74	4.085	2.00	4.90	X		0.8809	0.0012	-6.31
9x9	74	3.750	N/A	N/A		X	0.8707	0.0011	---
9x9	74	3.750	1.84	4.50	X		0.8608	0.0011	-8.84
9x9(1)	74	3.750	1.84	4.50	X		0.8672	0.0011	-7.13
9x9	74	4.000	N/A	N/A		X	0.8839	0.0011	N/A
9x9	74	4.000	1.96	4.80	X		0.8759	0.0012	-7.06
9x9(2)	74	4.000	N/A	N/A		X	0.8890	0.0012	N/A
9x9(2)	74	4.000	1.96	4.80	X		0.8805	0.0012	-7.08
9x9(3)	74	4.000	3.68	5.00	X		0.8821	0.0012	-5.77

Notes:

(1) Rotated water holes.
(2) Exxon Assembly.
(3) Eighteen 5 wt% ^{235}U enriched rods near center of assembly

Table 6.4-17 PWR Lattice Parameter Study Criticality Analysis Results

Description	k_{eff}	σ	Δk	2σ	$\Delta k / 2\sigma$
Base Case - Westinghouse 17x16 OFA	0.9732	0.0008	----	0.0016	----
decreases clad inner radius by 0.005 cm	0.9697	0.0008	-0.0035	----	-2.1875
increases clad inner radius by 0.005 cm	0.9784	0.0008	0.0052	----	3.2500
decreases clad outer radius by 0.005 cm	0.9782	0.0009	0.0050	----	3.1250
increases clad outer radius by 0.005 cm	0.9702	0.0009	-0.0030	----	-1.8750
decreases pellet radius by 0.005 cm	0.9744	0.0008	0.0012	----	0.7500
decreases pellet radius by 0.010 cm	0.9742	0.0008	0.0010	----	0.6250
decreases pellet radius by 0.015 cm	0.9773	0.0008	0.0041	----	2.5625
decreases pellet radius by 0.020 cm	0.9758	0.0008	0.0026	----	1.6250
decreases pellet radius by 0.025 cm	0.9761	0.0008	0.0029	----	1.8125
decreases pellet radius by 0.030 cm	0.9754	0.0008	0.0022	----	1.3750
decreases pellet radius by 0.035 cm	0.9750	0.0008	0.0018	----	1.1250
decreases pellet radius by 0.040 cm	0.9750	0.0008	0.0018	----	1.1250
increases pellet radius by 0.005 cm	0.9714	0.0009	-0.0018	----	-1.1250
decreases pellet & clad inner radii by 0.015 cm	0.9637	0.0008	-0.0095	----	-5.9375
decreases guide tube inner radius by 0.010 cm	0.9710	0.0008	-0.0022	----	-1.3750
increases guide tube inner radius by 0.015 cm	0.9753	0.0008	0.0021	----	1.3125
increases guide tube inner radius by 0.010 cm	0.9740	0.0009	0.0008	----	0.5000
decreases guide tube outer radius by 0.010 cm	0.9755	0.0008	0.0023	----	1.4375
increases guide tube outer radius by 0.015 cm	0.9712	0.0008	-0.0020	----	-1.2500
increases guide tube outer radius by 0.010 cm	0.9720	0.0008	-0.0012	----	-0.7500

Table 6.4-18 BWR Lattice Parameter Study Criticality Analysis Results

Description	k_{eff}	σ	Δk	2σ	Δk/2σ
Base Case - Exxon\ANF 9x9	0.8904	0.0008	----	0.0016	----
decreases clad inner radius by 0.005 cm	0.8889	0.0008	-0.0015	----	-0.9375
decreases clad inner radius by 0.008 cm	0.8874	0.0008	-0.0030	----	-1.8750
increases clad inner radius by 0.005 cm	0.8930	0.0008	0.0026	----	1.6250
decreases clad outer radius by 0.005 cm	0.8919	0.0008	0.0015	----	0.9375
decreases clad outer radius by 0.010 cm	0.8957	0.0008	0.0053	----	3.3125
increases clad outer radius by 0.005 cm	0.8885	0.0009	-0.0019	----	-1.1875
increases clad outer radius by 0.010 cm	0.8830	0.0009	-0.0074	----	-4.6250
decreases pellet radius by 0.005 cm	0.8896	0.0008	-0.0008	----	-0.5000
decreases pellet radius by 0.010 cm	0.8909	0.0008	0.0005	----	0.3125
decreases pellet radius by 0.015 cm	0.8881	0.0008	-0.0023	----	-1.4375
decreases pellet radius by 0.020 cm	0.8832	0.0008	-0.0072	----	-4.5000
decreases pellet radius by 0.025 cm	0.8867	0.0008	-0.0037	----	-2.3125
decreases pellet radius by 0.030 cm	0.8835	0.0008	-0.0069	----	-4.3125
decreases pellet radius by 0.035 cm	0.8837	0.0008	-0.0067	----	-4.1875
decreases pellet radius by 0.040 cm	0.8807	0.0008	-0.0097	----	-6.0625
increases pellet radius by 0.005 cm	0.8908	0.0008	0.0004	----	0.2500
increases pellet radius by 0.008 cm	0.8907	0.0009	0.0003	----	0.1875
decreases water rod inner radius by 0.010 cm	0.8908	0.0008	0.0004	----	0.2500
decreases water rod inner radius by 0.015 cm	0.8916	0.0008	0.0012	----	0.7500
increases water rod inner radius by 0.010 cm	0.8919	0.0008	0.0015	----	0.9375
increases water rod inner radius by 0.015 cm	0.8911	0.0008	0.0007	----	0.4375
decreases water rod outer radius by 0.010 cm	0.8901	0.0008	-0.0003	----	-0.1875
decreases water rod outer radius by 0.015 cm	0.8913	0.0008	0.0009	----	0.5625
increases water rod outer radius by 0.010 cm	0.8916	0.0008	0.0012	----	0.7500
increases water rod outer radius by 0.015 cm	0.8892	0.0009	-0.0012	----	-0.7500
replaces water rod with water	0.8926	0.0008	0.0022	----	1.3750

Table 6.4-19 Transport Cask Top End Impact Bounding Exposed Fuel Heights

Fuel Type	Canister Class	Neutron Absorber Offset (in)	Fuel Offset (in)	Calculated Exposed Fuel Height (in)	Evaluated Exposed Fuel Height (in)
WE 15x15	1	10.19 [1]	5.718	4.472	4.52 [3]
WE 17x17 OFA	1	10.19 [1]	6.296	3.894	4.52
B&W 15x15	2	12.29 [1]	10.289	2.001	4.52 [3]
CE16x16 (SYS 80)	3	8.69 [1]	13.176	-4.486	4.52 [3]
Ex/ANF 9x9	4	12.76 [2]	8.448	4.312	7.625 [4]
Ex/ANF 9x9	5	12.76 [2]	8.458	4.302	7.625
GE 8x8	5	12.76 [2]	8.448	4.312	7.625 [4]

1 Conservatively assumes the PWR basket remains in contact with canister bottom plate.
2 Takes credit for the BWR basket shifting up to contact the lid.
3 Evaluated using maximum reactivity UMS® Class 1 WE 17x17 OFA fuel.
4 Evaluated using maximum reactivity UMS® Class 5 Ex/ANF 9x9 fuel.

Table 6.4-20 Fuel Assembly Minimum Intact Hardware Dimension Limits

UMS® Fuel Class	1	2	3	4	5
Neutron Absorber Offset (in)	10.19	12.29	8.69	12.76	12.76
Evaluated Exposed Fuel Height (in)	4.52	4.52	4.52	7.625	7.625
Top End Fitting Deformation (in)	0	0	0	2.371	2.371
Plenum Spring Rebound Height (in)	Not Analyzed			1.729	1.729
Minimum Intact Hardware Dimension Limit (in) [1]	5.67	7.77	4.17	5.777	5.777

1 Each minium dimension is a generic limit that all fuel types in the respective fuel class shall meet. See Section 6.4.5 for details on how these minium dimensions are calculated

THIS PAGE INTENTIONALLY LEFT BLANK

NUREG/CR-6361. However, if no strong correlation can be determined, then a constant bias adjustment can be made. This is typically done with a one-side tolerance factor that guarantees 95% confidence in the uncertainty in the bias. This is the approach taken in the UMS criticality analysis.

Both NUREG/CR-6361 and the NAC evaluation perform regression analysis on key system parameters. For all of the major system parameters, the evaluation found no strong correlation. This is based on the observation that the correlation coefficients are all much less than ± 1. Thus a constant bias with a 95/95 confidence factor is applied to the system k_{eff}. NAC's statistical analysis of the k_{eff} results produced a bias of 0.0052 and a 95/95 uncertainty of 0.0087. Adding the two together and subtracting from 0.95 yields an effective constant USL of 0.9361.

To assure compliance with NUREG/CR-6361, an upper safety limit is generated using USLSTATS and is compared to the constant NAC bias and bias uncertainty used in Section 6.5.2.

To evaluate the relative importance of the trend analysis to the upper safety limits, correlation coefficients are required for all independent parameters. Table 6.5-2 contains the correlation coefficient, R, for each linear fit of k_{eff} versus experimental parameter (data is extracted from Figure 6.5-2 through Figure 6.5-7 by taking the square root of the R^2 value). Based on the highest correlation coefficient and the method presented in NUREG/CR-6361, a USL is established based on the variation of k_{eff} with enrichment. Note that even the enrichment function shows a low statistical correlation coefficient (an |R| equal or near 1 would indicate a good fit). The output generated by USLSTATS is shown in Figure 6.5-8.

The NAC applied USL of 0.9361 bounds the calculated upper safety limits for all enrichment values above 3.0 wt % ^{235}U. Since the maximum reactivities in the UMS® are calculated at enrichments well above this level, the existing bias bounds the NUREG calculated USL. The parameters of the most reactive configurations for the UMS® design basis PWR and BWR fuels and for the Maine Yankee fuel are presented in Table 6.5-3. This table also compares the most reactive fuel parameters to the minimum and maximum benchmark values to demonstrate the applicability of the critical benchmarks.

6.5.5 MONK Validation in Accordance with NUREG/CR-6361

NUREG/CR-6361, "Criticality Benchmark Guide for Light-Water-Reactor Fuel in Transportation and Storage Packages" (NUREG), provides a guide to LWR criticality benchmark calculations and the determination of bias and subcritical limits in critical safety evaluations. Section 6.5.1 contains detail on the implementation of the NUREG in subcritical limit evaluations for the UMS Transport Cask. This section implements the ULSTATS method of the NUREG for MONK8A application with JEF 2.2 point energy libraries in LWR transport and storage applications.

AEA Technologies has performed an extensive benchmarking of MONK8A. Critical benchmarks relevant to LWR fuel evaluations were extracted from the total benchmark set and listed in Table 6.5-6. The range of the parameters to be benchmarked is summarized in Table 6.5-4. Trending in k_{eff} was evaluated for the following independent variables: enrichment, rod pitch, fuel pellet diameter, fuel rod diameter, H/U ratio, average neutron group causing fission, ^{10}B loading for flux trap cases, and flux trap gap thickness. The data is plotted in Figures 6.5-9 through 6.5-16.

To evaluate the relative importance of the trend analysis to the upper safety limits, correlation coefficients are required for all independent parameters. Table 6.5-5 contains the correlation coefficient, R, for each linear fit of k_{eff} versus experimental parameter (data is extracted from Figure 6.5-9 through Figure 6.5-16 by taking the square root of the R^2 value). Based on the highest correlation coefficient and the method presented in NUREG/CR-6361, a USL is established based on the variation of k_{eff} with flux trap thickness. Note that even the flux trap function shows a low statistical correlation coefficient (an $|R|$ equal or near 1 would indicate a good fit). The output generated by USLSTATS is shown in Figure 6.5-17.

The NAC applied USL is 0.9425, and bounds the calculated upper safety limits for the typical flux trap spacing found in multi-purpose casks. The parameters of the most reactive CY-MPC payload are included in Table 6.5-4.

Table 6.5-2 Scale 4.3 Correlation Coefficient for Linear Curve-Fit of Critical Benchmarks

Correlation Studied	Correlation Coefficient (R)
k_{eff} versus enrichment	0.361
k_{eff} versus rod pitch	0.328
k_{eff} versus H/U volume ratio	0.246
k_{eff} versus ^{10}B loading	0.069
k_{eff} versus average group causing fission	0.133
k_{eff} versus flux gap thickness	0.137

Table 6.5-3 Scale 4.3 Range of Correlated Parameters of the Most Reactive Configuration

	Benchmark Value		Design Basis Models		
Parameter	Minimum	Maximum	WE 17x17 OFA	Ex/ANF 9x9	Maine Yankee Fuel
Enrichment (wt. % ^{235}U)	2.35	4.74	4.2	4.0	4.2
Rod pitch (cm)	1.26	2.54	1.26	1.45	1.50
H/U volume ratio	1.6	11.5	2.28	1.99	2.68
^{10}B areal density (g/cm^2)	0.00	0.45	0.025	0.011	0.025
Average energy group causing fission	21.7	24.2	22.3	22.4	22.5
Flux gap thickness (cm)	0.64	5.16	2.22 to 3.81	1.65	2.22 to 3.81

Table 6.5-4 MONK8A Range of Correlated Parameters for Design Basis Fuel

Parameter	Benchmark Value		Design Basis Models	
	Minimum	Maximum	WE 17x17 OFA	Ex/ANF 9x9
Enrichment (wt % ^{235}U)	2.35	7.00	4.20	4.00
Rod pitch (cm)	1.26	2.54	1.26	1.45
H/U (fissile) atomic ratio	97.08	453.84	154.02	140.98
^{10}B loading (g/cm^2)	0.000	0.072	0.025	0.011
Log energy causing fission	7.31E-08	3.33E-07	2.39E-07	1.82E-07
Cluster gap thickness (cm)	0.0	11.92	2.22-3.81	1.65
Fuel diameter (cm)	0.743	1.265	0.7844	0.9055
Clad diameter (cm)	0.8324	1.4150	0.9144	1.0770

Table 6.5-5 MONK8A – Correlation Coefficient for Linear Curve-Fit of Critical Benchmarks

Correlation Studied	Correlation Coefficient (R)
k_{eff} versus enrichment	0.390
k_{eff} versus rod pitch	0.140
k_{eff} versus H/U (fissile) atomic ratio	0.369
k_{eff} versus ^{10}B loading	0.273
k_{eff} versus log energy causing fission	0.127
k_{eff} versus cluster gap thickness	0.532
k_{eff} versus fuel diameter	0.236
k_{eff} versus clad diameter	0.185

Table of Contents

List of Tables

Table 7-2 Containment Verification Leak Test Requirements

	Post-Fabrication and Annual Maintenance[3]	Loaded Transport (O-Ring Replacement)[2,3]	Loaded Transport (No O-Ring Replacement)[2]	Empty Transport
Allowable Reference Leak Rate[1]	4.2×10^{-6} cm³/sec	4.2×10^{-6} cm³/sec	1×10^{-3} cm³/sec	1×10^{-3} cm³/sec
Allowable Helium Leak Rate[1]	6.5×10^{-6} cm³/sec	6.5×10^{-6} cm³/sec	--	--

1 The allowable leak rate is based on the bounding high burnup Maine Yankee fuel and is the same for the transport of GTCC waste.
2 The need for o-ring replacement is determined by inspection or by leak test results.
3 All o-rings are replaced during Annual Maintenance. Only the appropriate set of o-rings is replaced as necessary during use.

THIS PAGE INTENTIONALLY LEFT BLANK

5. Lower the canister into the Universal Transport Cask.
6. Disengage the lift sling hooks from the hoist rings and close the Transfer Cask doors.
7. Remove the Transfer Cask and store it in the designated location.
8. Remove the hoist rings from the top of the canister structural lid and install threaded plugs.
9. Attach the adapter plate lifting sling to the adapter plate.
10. Remove the four bolts attaching the adapter plate to the Universal Transport Cask.
11. Remove the adapter plate and store it in the designated location.
12. Remove the cask adapter ring and clean the sealing surface.
13.
14. Install the cask lid alignment pins.
15. Attach the lid-lifting device to the lid and to the overhead crane.
16. Install the lid, using the alignment pins to assist in proper seating.
17. Install 10 cask lid bolts equally spaced and torque hand-tight.
18. Remove the lid alignment pins.
19. Install the remaining cask lid bolts and torque all of the bolts to the value specified in Table 7-1.
20. If previously removed, re-install the drain port coverplate.
21. Connect a pressure test fixture to the drain port coverplate o-ring test port and pressurize to 15 (+2, -0) psig and hold for a minimum of 10 minutes. There must be no pressure drop in the test period.

    Note: If the test condition is not met, remove the drain port coverplate and inspect and clean the o-rings and o-ring sealing surfaces and re-perform the test. If the test condition is not met on the second attempt, replace the o-rings, cleaning the o-ring grooves and sealing surface. A small amount of vacuum grease may be used to lubricate new o-rings.

    Caution: If the drain port o-rings are replaced as a result of the inspection, then a helium leak test of the new o-rings must be performed at Step 29. Using a helium leak detector with a sensitivity of 3.25×10^{-6} cm^3/sec, establish a vacuum in the o-ring annulus and test for helium leakage. The leak rate must be less than 6.5×10^{-6} cm^3/sec (helium) in accordance with Table 7-2.
22. Connect the Vacuum Drying System vacuum pump to the cask vent port and evacuate the cask cavity to a stable vacuum pressure of 3 mm Hg for 10 minutes.
23. Backfill the cask with high purity helium (99.9%) to 1 atm (absolute) pressure.
24. Operate the vacuum system to obtain a vacuum pressure of 3 mm Hg. When the vacuum pressure is obtained, backfill the cask with high purity helium (99.9% minimum) to 1 atm (absolute) pressure.

25. Disconnect the vacuum system and helium supply.
26. Install the vent port coverplate and torque the bolts as specified in Table 7-1.
27. Connect a pressure test fixture to the lid o-ring test port (marked "Seal Test" on cask lid) and pressurize to 15 (+2, -0) psig and hold for a minimum of 10 minutes. There must be no pressure drop in the test period.

    Note: If the test condition is not met, replace the o-rings, cleaning the o-ring grooves and sealing surface. A small amount of vacuum grease may be used to lubricate new o-rings.

    Caution: If the lid o-rings are replaced as a result of the inspection in Step 12 of Section 7.1.2, then a helium leak test of the new o-rings must be performed. Using a helium leak detector with a sensitivity of 3.25×10^{-6} cm^3/sec, establish a vacuum in the o-ring annulus and test for helium leakage. The leak rate must be less than 6.5×10^{-6} cm^3/sec in accordance with Table 7-2.
28. Install the plug in the lid Seal Test port, verifying that the test plug o-ring is in place, and torque the plug to the value specified in Table 7-1.
29. Connect a pressure test fixture to the vent coverplate o-ring test port and pressurize to 15 (+2, -0) psig and hold for a minimum of 10 minutes. There must be no pressure drop in the test period.

    Note: If the test condition is not met, remove the vent port coverplate and inspect and clean the o-rings and o-ring sealing surfaces and re-perform the test. If the test condition is not met on the second attempt, replace the o-rings, cleaning the o-ring grooves and sealing surface. A small amount of vacuum grease may be used to lubricate new o-rings.

    Caution: If the vent and/or drain port o-rings are replaced as a result of the inspection, then a helium leak test of the new o-rings must be performed. Using a helium leak detector with a sensitivity of 3.25×10^{-6} cm^3/sec, establish a vacuum in the o-ring annulus and test for helium leakage. The leak rate must be less than 6.5×10^{-6} cm^3/sec in accordance with Table 7-2.
30. Install the vent port o-ring test plug, verifying that the test plug o-ring is in place and torque the test plug to the value specified in Table 7-1.
31. Perform external decontamination activities and radiation surveys to verify that contamination is within acceptable levels (2,200 dpm/100 cm^2 β, γ, and 220 dpm/100 cm^2 α) as identified in 10 CFR 71.87 [2].

7.5 Appendix

7.5.1 References

1. Code of Federal Regulations Title 10, Part 20 (10CFR20), "Standards for Protection Against Radiation," April 1996.

2. Code of Federal Regulations Title 10, Part 71 (10CFR71), "Packaging and Transportation of Radioactive Materials," April 1996.

3. Code of Federal Regulations Title 49, Part 173 (49CFR173), "Shippers - General Requirements for Shipments and Packaging," October 1995.

4. IAEA Safety Series No. 6, "Regulations for the Safe Transport of Radioactive Materials," International Atomic Energy Agency, Vienna, Austria, 1985 Edition, as amended 1990.

5. Peckner, D., and Bernstein, R.M., Handbook of Stainless Steels, McGraw-Hill Book Company, 1977.

6. Code of Federal Regulations Title 49, Part 172 (49CFR172), "Hazardous Materials Table, Special Provisions, Hazardous Materials Communications, Emergency Response Information, and Training Requirements," October 1995.

7. Title 10 of the Code of Federal Regulations, Part 61 (10 CFR 61), "Licensing Requirements for Land Disposal of Radioactive Waste," January, 1996.

THIS PAGE INTENTIONALLY LEFT BLANK

Table of Contents

Table of Contents (Continued)

List of Figures

List of Tables

THIS PAGE INTENTIONALLY LEFT BLANK

8.1.3 Leak Tests

Acceptance leak testing is performed on the containment weldment during fabrication and on the containment boundary having replaceable components, when fabrication is complete. The purpose of this leak testing is to confirm that the leak rate from any sealed containment penetration does not exceed the allowable leak rates, calculated in Chapter 4.0, and to confirm that the 10 CFR 71.85(a) [1] requirements are satisfied. Leak tests are performed in accordance with the methodologies and requirements of ANSI N14.5-1997 [11], using approved written procedures. Personnel performing tests shall be qualified in accordance with Section 8.5 of ANSI N14.5-1977.

Containment Weldment Testing

Following the hydrostatic testing of the containment weldment in accordance with Section 8.1.2.3, the containment cavity is drained and cleaned. A helium leak test of the containment weldment is performed in accordance with the requirements of Section V, Article 10 of the ASME Code. The containment weldment shall be leak tested to demonstrate a leak rate of 2×10^{-7} cm^3/sec (helium), or less, using a minimum detector sensitivity of 1×10^{-7} cm^3/sec (helium), to qualify the weldment as leak tight as defined in ANSI N14.5-1997.

If a leak is detected exceeding the acceptance criteria, the affected weld shall be rejected. Rejected welds shall be repaired in accordance with the requirements of Article NB-4450 of the ASME Code. The repaired weld area shall be retested and reinspected using the same procedure and acceptance criteria.

Containment Fabrication Acceptance Testing

Once cask fabrication is complete, helium leak tests are performed on the o-rings sealing the mechanical joints at the containment boundary.

Containment fabrication acceptance testing is performed with the cask assembled in accordance with the cask handling procedure except that the quick disconnects at the vent and drain ports are not installed. This ensures that when the cask cavity is backfilled with helium, helium is present on the containment side of the port coverplate containment o-rings. The leak test is then conducted by establishing a vacuum in the o-ring annulus of the lid and port coverplates using the seal test ports and testing for helium.

Leak tests are performed on the cask lid and the vent and drain port coverplate o-rings. Containment o-ring testing is performed to demonstrate a leak rate of 6.5×10^{-6} cm^3/sec (helium), or less. The helium leak detector sensitivity shall be 3.25×10^{-6} cm^3/sec or less. The allowable leak rate is based on the calculated allowable leak rate for BWR fuel (Table 4.2-4).

A leak rate that exceeds the allowable leak rate limit is cause for rejection of the component being tested. Seal replacement or other corrective actions are taken to correct any leak. The component is then retested and inspected in accordance with the test requirements and acceptance criteria. On successful completion of the leak tests, the quick disconnects are re-installed in the vent and drain ports.

8.1.4 Component Tests

Individual cask components are tested as applicable to ensure that the component meets the design requirements for its intended function during operation of the cask system. Test acceptance criteria are established on the basis of the component function, the corresponding graded quality category and design requirements of the component being tested.

8.1.4.1 Transportable Storage Canister

The Transportable Storage Canister is not considered to be a containment boundary when transported in the Universal Transport Cask. However, all of the longitudinal and girth welds are radiographically inspected in accordance with ASME Code, Section V, Article 2. Radiographic acceptance is in accordance with ASME Code Section III, NB-5320. The weld between the canister baseplate and the canister shell is ultrasonically examined in accordance with ASME Code Section V, Article 5. Acceptance criteria are in accordance with ASME Code Section III, NB-5330.

The welds made in the field to attach the shield lid to the canister shell are subjected to dye-penetrant testing on the root weld and final weld surface in accordance with the requirements of the ASME Code, Section V, Article 6. Following welding of the shield lid, a helium leak test is performed as described in the operating procedures. The root weld, intermediate, and final weld surface of the structural lid weld to the canister shell are also dye penetrant examined in accordance with ASME Code, Section V, Article 6 to ensure the quality of the weld. The liquid penetrant test acceptance criteria are as described in ASME Code Section III, Article NB-5350.

acceptable if the measured heat rejection rate is equal to, or greater than, the design basis heat rejection rate.

The nominal test conditions are 70°F ambient and initial cask body temperature, no solar insolation, still air, no external radiant heat sources, and dry steam at 212°F. At these test conditions, the neutron shield shell temperature is within 2°F of the calculated steady state equilibrium temperature of 174°F within 48 hours. The thermal test procedure shall provide a thermal transient heatup curve to show the time at which equilibrium is expected to be established, and a table or set of curves which correlates equilibrium neutron shield shell temperature with a range of ambient temperatures. For purposes of the thermal test, equilibrium temperature is assumed to be established when the change in neutron shell temperature no longer exceeds 2°F in a two (2) hour period.

8.1.6.2 Thermal Test Acceptance Criteria

The purpose of the thermal test is to confirm that the heat rejection capabilities of the as-built Universal Transport Cask are acceptable by showing that the measured temperature gradients correspond to those calculated in the thermal analyses.

Cask thermal test acceptance is based on demonstration that the measured temperature gradients are less than, or equal to, the thermal gradients calculated in the thermal analyses and that the total heat rejection rate is equal to, or greater than, the cask design basis heat rejection rate.

8.1.7 Neutron Absorber Verification Tests

Neutron-absorbing material, BORAL, is used as a poison in the BWR and PWR fuel tubes. BORAL is manufactured by AAR Manufacturing, Inc. (AAR) of Livonia, Michigan, under a Quality Assurance/Quality Control program in conformance with the requirements of 10 CFR 50, Appendix B. The computer-aided manufacturing process consists of several steps - the first being the mixing of the aluminum and boron-carbide powders that form the core of the finished material, with the amount of each powder a function of the desired ^{10}B areal density. The methods used to control the weight and blend the powders are patented and proprietary processes of AAR.

After manufacturing, test samples from each batch of BORAL® neutron absorber (poison) sheets are tested using wet chemistry or neutron absorption to verify the presence, proper distribution, and minimum weight percent of ^{10}B. The tests are performed in accordance with approved written procedures.

8.1.7.1 Neutron Absorber Material Sampling Plan

The neutron absorber material sampling plan is selected to demonstrate a 95/95 statistical confidence level in the neutron absorber sheet material compliance with the specification. In addition to the specified sampling plan, each sheet of material is visually and dimensionally inspected using at least 6 measurements on each sheet. No rejected neutron absorber sheet is used. The sampling plan is supported by written and approved procedures.

The sampling plan requires that a coupon sample be taken from each of the first 100 sheets of absorber material. Thereafter, coupon samples are taken from 20 randomly selected sheets from each set of 100 sheets. This 1 in 5 sampling plan continues until there is a change in lot or batch of constituent materials of the sheet (i.e., boron carbide powder, aluminum powder, or aluminum extrusion) or a process change. The sheet samples are indelibly marked and recorded for identification. This identification is used to document neutron absorber test results, which become part of the quality record documentation package.

8.1.7.2 Wet Chemistry Test Performance

An approved facility with chemical analysis capability is selected to perform the wet chemistry tests. The tests ensures the presence of boron and enable the calculation of the ^{10}B areal density.

The most common method of verifying the acceptability of neutron absorber material is the wet chemistry method—a chemical analysis where the aluminum is separated from a sample with known thickness and volume. The remaining boron-carbide material is weighed and the areal density of ^{10}B is computed. A statistical conclusion about the BORAL® sheet from which the sample was taken and that batch of BORAL® sheets may then be drawn based on the test results and the established manufacturing processes previously noted.

8.1.7.3 Neutron Absorption Test Performance

An approved facility with a neutron source and neutron detection capability is selected to perform the described tests, if the neutron absorption test method is used. The tests will ensure that the neutron absorption capacity of the material tested is equal to, or higher than, the given reference value and will verify the uniformity of boron distribution. The principle of measurement of neutron absorption is that the presence of boron results in a reduction of neutron flux between the thermalized neutron source and the neutron detector—depending on the material thickness and boron content.

Typical test equipment consists of thermal neutron source equipment, a neutron detector and a counting instrument. The test equipment is calibrated using BORAL standards, whose ^{10}B content has been checked and verified by an independent method such as chemical analysis. The highest permissible counting rate is determined from the neutron counting rates of the reference sheet(s), which should be ground to the minimum allowable plate thickness. This calibration process is repeated daily (every 24 hours) while tests are being performed.

8.1.7.4 Acceptance Criteria

The wet chemistry test results are considered acceptable if the minimum ^{10}B areal density is determined to be equal to, or greater than, that specified on the fuel tube drawings.

When used, the neutron absorption test shall be considered acceptable if the neutron count determined for each test specimen is less than, or equal to, the highest permissible neutron count rate determined from the BORAL standard, which is based on the ^{10}B areal density specified on the fuel tube drawings. Any specimen not meeting the acceptance criteria for either test method shall be rejected and all of the sheets from that batch shall be similarly rejected.

Figure 8.1-1 Thermal Test Arrangement

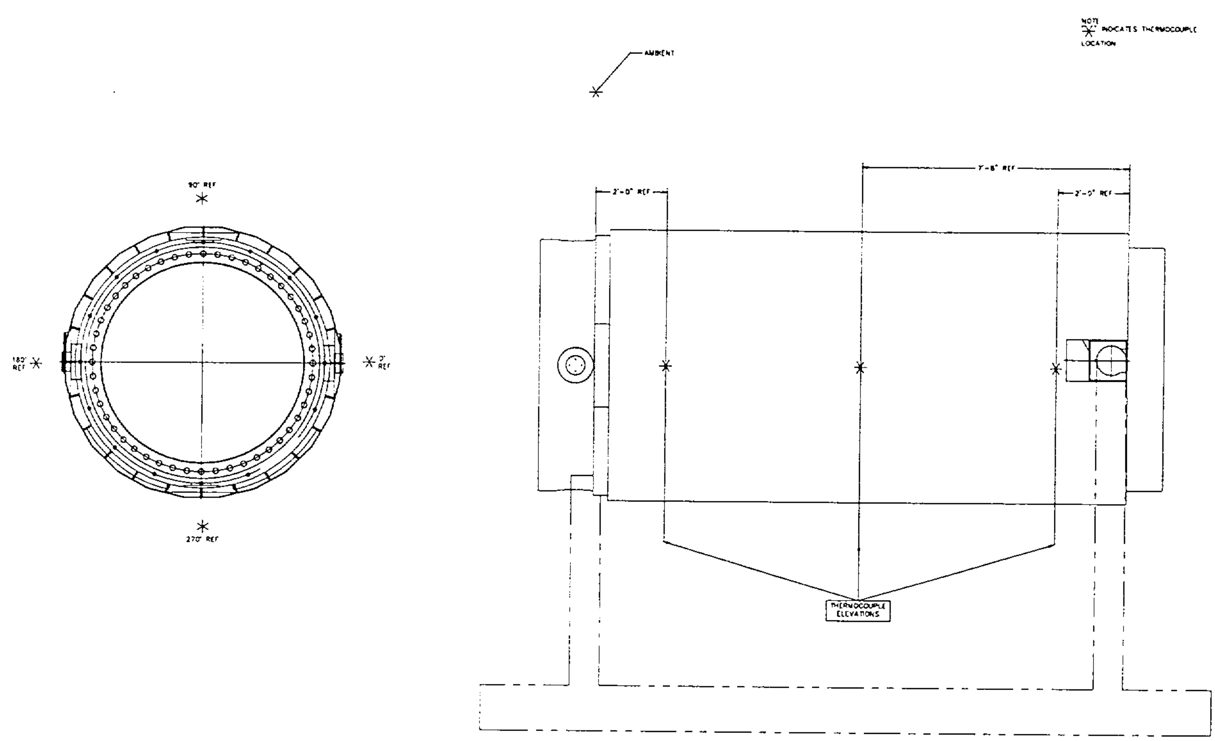

8.2 Maintenance Program

A maintenance program for the Universal Transport Cask is established to ensure continued performance and use of the package. The cask maintenance program specifies the inspections, tests, and replacement of components to be performed and the frequency and schedule for these activities. This section describes the overall requirements of the maintenance program and establishes the frequency and schedule for the maintenance activities. The detailed, written inspection, test, component replacement, and repair procedures will be included in the Universal Transport Cask Operations Manual. The Operations Manual is issued to users of the packaging prior to their use of the cask.

The welded Transportable Storage Canister containing fuel does not require any maintenance.

8.2.1 Structural and Pressure Tests

The four lifting trunnions or two trunnions if the secondary trunnions are not attached and the two rotation pockets are visually inspected prior to each shipment. The visual inspections are performed in accordance with approved written procedures, and the results are evaluated against established acceptance criteria.

Evidence of cracking on the load-bearing surfaces is cause for rejection of the affected trunnion until an approved repair is completed and the surfaces are reinspected and accepted. Such repairs are implemented and documented in accordance with an approved quality assurance program. Any identified damage to the bolted trunnions and the rotation pockets, such as cracking and wear, must be evaluated to determine if replacement of the affected components is necessary.

The lifting trunnions are also inspected annually in accordance with Paragraph 6.3.1(b) of ANSI N14.6 [7]. All trunnion welds, trunnion bolts, trunnion bolt load-bearing surfaces, and welds that are part of the load path are visually inspected for permanent deformation, galling, or cracking. Liquid penetrant examinations of welds and load bearing surfaces are performed in accordance with the ASME Code, Section V, Articles 6 [3]. Liquid penetrant acceptance standards are those of Paragraph NF-5350 of the ASME Boiler and Pressure Vessel Code, Section III, Division 1 [9].

During periods of nonuse of the transport cask, the inspection of the trunnions may be omitted provided that the trunnions are inspected in accordance with this section prior to the next use.

8.2.2 Leak Tests

8.2.2.1 Containment Periodic Verification Leak Testing

As shown in Table 8.2-1, the periodic verification leak test is performed in accordance with approved written test procedures and the test requirements and acceptance criteria established in Section 8.1.3 for the containment fabrication verification leak test.

The periodic verification leak test is performed on each cask after the third use (prior to fourth cask loading sequence), and every 12 months thereafter to verify the containment capability, and whenever a replaceable containment component (containment o-ring set or port coverplate) is replaced.

When the cask is not in use , the periodic verification leak test need not be performed annually but must be re-performed before returning the cask to service .

Leak tests are performed in accordance with the methodologies and requirements of ANSN14.5-1997, using approved written procedures. Personnel performing tests shall be qualified in accordance with Section 8.5 of ANSI N14.5-1997.

8.2.2.2 Periodic Verification Leak Test Acceptance Criteria

The maximum allowable leak rate requirements and the minimum required test sensitivity for the containment fabrication verification and periodic verification leak tests are provided in Section 8.1.3. Unacceptable leak test results are cause for rejection of the component tested. Corrective actions, including repair or replacement of the o-rings or closure component, are taken and documented as appropriate. Before the cask is returned to service, the leak test and corrective actions are repeated until acceptable results are achieved.

8.2.3 Subsystems Maintenance

The Universal Transport Cask has no subsystem maintenance requirements.

Table 8.2-1 Maintenance Program Schedule

Task/Activity	**Frequency**
Visual inspection of cavity	Prior to loading
Visual inspection of o-rings	Prior to loading
Visual inspection of cask lid and port coverplate bolts	Prior to installation (each use)
Visual and Proper Function Inspection of Cask	Prior to each shipment
Visual inspection of lifting trunnions and rotation pockets	Prior to each shipment
Liquid penetrant inspection of lifting trunnion surfaces	Annually during use
Containment system periodic verification leak test of cask lid and o-rings	After the third use of a transport cask. Annually during use. After each o-ring or port coverplate replacement
Containment system leak test of cask lid and o-rings	Prior to each shipment
Containment system periodic verification leak test of vent and drain port coverplates and o-rings	After the third use of a transport cask. Annually during use. After each o-ring or port coverplate replacement
Containment system leak test of vent and drain port coverplates and o-rings	Prior to each shipment
Visual inspection of impact limiter	Prior to each shipment
Inspection of quick disconnects for proper function	Each cask loading/unloading operation
Replacement of quick disconnects	Every two years of service
Replacement of O-ring	As required by inspection during operations and at each annual maintenance
Replacement of lid bolts	Every 20 years

THIS PAGE INTENTIONALLY LEFT BLANK

8.3 Appendices

8.3.1 References

1. Title 10 of the Code of Federal Regulations, Part 71 (10 CFR 71), "Packaging and Transportation of Radioactive Materials," April 1996.

2. IAEA Safety Series No. 6, "Regulations for the Safe Transport of Radioactive Materials," International Atomic Energy Agency, Vienna, Austria, 1985 Edition, as amended 1990.

3. ASME Boiler and Pressure Vessel Code, Section V, "Nondestructive Examination," 1995 Edition with 1995 Addenda.

4. ASME Boiler and Pressure Vessel Code, Section VIII, "Rules for Construction of Pressure Vessels," 1995 Edition with 1995 Addenda.

5. Recommended Practice No. SNT-TC-1A, "Personnel Qualification and Certification in Nondestructive Testing," The American Society for Nondestructive Testing, Inc., edition as invoked by the applicable ASME Code.

6. ASME Boiler and Pressure Vessel Code, Division I, Section III, Subsection NB, "Class 1 Components," 1995 Edition with 1995 Addenda.

7. ANSI N14.6, "American National Standard for Special Lifting Devices for Shipping Containers Weighing 10,000 Pounds (4,500 kg) or More for Nuclear Materials," American National Standards Institute, February 1993.

8. Field Manual of the Interchange Rules as Adopted by the Association of American Railroads, Rule 88, "Mechanical Requirements for Acceptance," Washington, D.C., 1986.

9. ASME Boiler and Pressure Vessel Code, Division 1, Section III, Subsection NF, "Component Supports," 1995 Edition with 1995 Addenda.

10. ASTM B-29-92, "Standard Specification for Refined Lead," American Society for Testing and Materials, 1992 (Reapproved 1997).

11. ANSI N14.5-1997, "American National Standard for Leakage Tests on Packages for Shipment of Radioactive Materials," American National Standards Institute, December 1997.

8.3.2 Cask Body Fabrication

The Universal Transport Cask is a welded structure of stainless steel plates and forgings. The major chronological steps involved in the fabrication of the cask body are:

- Welding of plate sections to form the inner shell.
- Welding of inner shell to top and bottom forging to form cask containment.
- Perform hydrostatic and helium leak testing of the containment weldment.
- Welding of plate sections to form outer shell.
- Welding of outer shell to cask containment to form cask body.
- Welding of backing bars and supports in preparation for lead pour.
- Lead pour.
- Installation of NS-4-FR shielding material between cask bottom and bottom forging.
- Welding of cask bottom to outer shell.
- Welding of primary trunnions to top forging.
- Installation of NS-4-FR outside cask outer shell.
- Perform load testing of the primary and secondary lifting trunnions.
- Perform containment boundary o-ring leak testing.

Welding on the cask is performed in accordance with the requirements of the ASME Boiler and Pressure Vessel Code as specified on the cask license drawings (Section 1.3.4). The type and location of the major welds on the cask body and the type of inspection required on the welds are shown in Figure 8.3-1. Pouring of chemical copper lead between the cask inner and outer shells to provide gamma shielding is addressed in Section 8.3.3. Installation of the NS-4-FR shielding material between the neutron shield top and bottom plates in the annulus formed by the cask outer shell and the neutron shield shell is discussed in the following paragraphs.

The methods and process for installation of the NS-4-FR shielding material will be qualified by means of a full-scale mockup test prior to actual installation in a cask or by methods and process that have already demonstrated successful and proper installation. The mockup test will establish that appropriate procedures are followed in the NS-4-FR installation process and that critical NS-4-FR material properties and characteristics are in accordance with the manufacturer's specification. The mockup structure will consist of a minimum of two cavities separated by three heat transfer fins. The NS-4-FR will be installed according to an approved procedure into two adjacent cavities of the mockup. After mixing but prior to installation, the wet material density will be measured and compared with the manufacturer's specification. Upon curing, the mockup will undergo destructive examination and testing. The destructive examination and tests will